Charles University
Faculty of Mathematics and Physics
Prague

Three-dimensional Euler Equations and Their Numerical Solution, Moving Particle Scheme for Grid Generation

Pavel Šolín

Supervisor: **Dr. Jiří Felcman, CSc.**
Consultant: **Prof. Dr. Miloslav Feistauer, DrSc.**
Branch: Mathematical and Computer Modelling

Declaration

I declare setting up this thesis by myself using the mentioned sources only.
This work can be lent at will.

Prague, April 15, 1996

Pavel Šolín

Acknowledgments

I am very grateful to all people who supported my work by their help, advice or just by their interest.

My thanks belong especially to Dr. Jiří Felcman and Prof. Miloslav Feistauer who introduced me to the problems of fluid dynamics. Their friendly approach, advises, suggestions, motivation and great flexibility in helping me to solve problems were (and still are) inestimable for me.

I thank also Prof. Gerald Warnecke for his support during my stay at the Otto-von-Guericke University in Magdeburg where a notable part of this work has been developed and Dr. Oldřich Ulrych for his great help with Unix, computer network and Tex.

Further I wish to thank PhD students Petr Knobloch for telling me his experience with writing fluid solvers, Vít Dolejší who supported by help and advice my numerical experiments and student Petr Vojtěchovský for his remarks to the second part of this work.

Part I
Euler equations

Introduction

Nowadays people in many different domains of their activity meet the problem how to describe or predict behavior of physical quantities in flowing mediums. Due to the development of highly efficient computers the Computational Fluid Dynamics plays an important role in searching answers. Its application does not only lie in the design of turbines, in construction of planes, ships or cars but also in medicine, dealing with flow of blood.

Part I of this thesis is devoted to the three-dimensional Euler equations. First, we introduce some basic notation and physical quantities describing motion of fluids. We will formulate the system of conservation laws which govern compressible inviscid flow. After having introduced the Finite Volume Method, prepared some basic theoretical tools and discussed the boundary conditions, we will develop four methods for solving it. These methods will be compared and then some more interesting numerical experiments performed.

There is a wide class of literature concerning the study of numerical solution of the Euler equations which we think it is useful to mention here shortly – e.g. [13], [26], [31] [37], [36], [35], [7], [14], [33], [3], [5], [6], [11], [24], [27], [28], [23], [32] etc.

In the second part we will deal with grid generation. We will set up a method based on computer simulation of a real physical process – interaction of elementary particles with charge.

Notations

Throughout this contribution we endeavour to stick to the common notation. To support openness and comprehensibility of our explanations, in our conception vectors will always be columns and we will use bold-faced symbols for them. Here is a short list of symbols we will use:

t ... time variable,
$\mathbf{x} = (x, y, z)^T$ ... space variable,
$\mathbf{v} = \mathbf{v}(\mathbf{x}, t)$ ... velocity vector,
$u(\mathbf{x}, t), v(\mathbf{x}, t), w(\mathbf{x}, t)$ ... its components,
$\mathbf{v}^2$ ... square of its Euclidean norm,
$\varrho(\mathbf{x}, t)$ ... density,
$p(\mathbf{x}, t)$ ... pressure,
$T(\mathbf{x}, t)$ ... absolute temperature,
$e(\mathbf{x}, t) = c_v T$ ... intern specific energy,
$E(\mathbf{x}, t) = \varrho(e + \frac{1}{2}\mathbf{v}^2)$ ... total specific energy,
$S(\mathbf{x}, t)$ ... entropy,
$c(\mathbf{x}, t) = \sqrt{\kappa \frac{p}{\varrho}}$ ... sound speed,
$\mathbf{f}(\mathbf{x}, t) = (f_1, f_2, f_3)^T(\mathbf{x}, t)$ ... external body forces per unit of mass,
$\tau(\mathbf{x}, t)$ ... stress tensor,
$q(\mathbf{x}, t)$ ... density of external heat sources,
$\underline{q}(\mathbf{x}, t)$ ... heat flux vector,
c_p, c_v ... specific heats,
$R = c_p - c_v$ ... the universal gas constant and
$\kappa = \frac{c_p}{c_v}$ ... the Poisson adiabatic constant.

We denote further

$\mathbb{R}$ ... real numbers,
$\mathbb{R}^+$ ... open interval $(0, \infty)$,
$\mathbb{R}^i$ ... i-dimensional geometrical space generated by $\mathbb{R}$,
$exp(\mathbb{R}^i)$ ... the set of all subsets of $\mathbb{R}^i$,
μ_i ... the Lebesgue measure in $\mathbb{R}^i$, $i = 1, 2, 3$.
$\mathbf{I}$ ... the canonical matrix,
$\mathrm{diag}(\dots)$ ... diagonal matrix $\mathbf{I}(\dots)^T$,
∇_i ... gradient operator in $\mathbb{R}^i$ where $i = 1, 2, \dots, 5$.

Except this, from time to time we will have to use the index-notation for vector components, especially in sums, enumerations etc. We won't be using the Einstein convention.

1 Basic equations describing flow

At first we are going to mention the famous Transport theorem and derive some basic equations describing flow. Then we put them together and formulate the problem.

1.1 Transport theorem

Assumptions:
$i)$ (T_1, T_2) is a finite time interval.
$ii)$ $\Omega : (T_1, T_2) \to exp(\mathbb{R}^3)$ is a time-dependent domain, $\Omega(t)$ is bounded and has Lipschitz-continuous boundary for $t \in (T_1, T_2)$.
We denote $\mathcal{M} = \{(\mathbf{x}, t), \mathbf{x} \in \Omega(t), t \in (T_1, T_2)\}$.
$iii)$ the velocity vector $\mathbf{v}$ is defined in $\mathcal{M}$, $\mathbf{v} \in [\mathrm{C}^1(\mathcal{M})]^3$.
$iv)$ t_0 is an arbitrary time instant, $t_0 \in (T_1, T_2)$, $\sigma(t_0) = \sigma \subset \overline{\sigma} \subset \Omega(t_0)$ is a bounded domain with Lipschitz-continuous boundary (so-called *control volume*).
$v)$ F is an arbitrary scalar function defined in $\mathcal{M}$, $F \in \mathrm{C}^1(\mathcal{M})$.
Further, we denote $\varphi(\mathbf{X}, t)$ the trajectory of the particle which at the time instant t_0 occured at the position $\mathbf{X} \in \Omega(t_0)$.

Theorem:
Under assumptions $i), ii), \ldots, v)$ there is a finite time interval $t_0 \in (t_1, t_2) \subset (T_1, T_2)$ for every time instant t of which the equation

$$\frac{\mathrm{d}}{\mathrm{d}t} \int_{\sigma(t)} F(\mathbf{x}, t) \mathrm{d}\mathbf{x} = \int_{\sigma(t)} \frac{\partial F}{\partial t}(\mathbf{x}, t) + \mathrm{div} F(\mathbf{x}, t)\mathbf{v}(\mathbf{x}, t) \mathrm{d}\mathbf{x} \tag{1}$$

is valid.

Proof: see [13].

1.2 Conservation laws

1.2.1 Law of conservation of mass

"*The mass of a piece of fluid formed by the same particles at any time instant is constant in time*", i.e.

$$\frac{\mathrm{d}}{\mathrm{d}t} \int_{\sigma(t)} \varrho(\mathbf{x}, t) \mathrm{d}\mathbf{x} = 0.$$

Using the Transport theorem (the relation (1)), we can write

$$\int_{\sigma(t)} \frac{\partial \varrho}{\partial t}(\mathbf{x}, t) + \mathrm{div} \varrho(\mathbf{x}, t)\mathbf{v}(\mathbf{x}, t) \mathrm{d}\mathbf{x} = 0.$$

The control volume $\sigma(t_0)$ is arbitrary, hence

(2) $$\frac{\partial \varrho}{\partial t}(\mathbf{x},t) + \mathrm{div}\varrho(\mathbf{x},t)\mathbf{v}(\mathbf{x},t) = 0.$$

1.2.2 Balance of momentum

"*The rate of change of total momentum of a piece of fluid formed by the same particles at any time instant is equal to the forces acting on this piece of fluid*", i.e.

$$\frac{\mathrm{d}}{\mathrm{d}t}\int_{\sigma(t)} \varrho\mathbf{v}\mathrm{d}\mathbf{x} = \int_{\sigma(t)} \varrho\mathbf{f}\mathrm{d}\mathbf{x} + \int_{\partial\sigma(t)} \tau.\nu\mathrm{d}S.$$

Here the external body forces $\mathbf{f}$ and the stress tensor τ are given, by ν we denote the outside normal vector. Using the Transport theorem, we have

$$\int_{\sigma(t)} \frac{\partial \varrho v_i}{\partial t} + \mathrm{div}\varrho v_i\mathbf{v}\mathrm{d}\mathbf{x} = \int_{\sigma(t)} \varrho f_i\mathrm{d}\mathbf{x} + \int_{\sigma(t)} \mathrm{div}(\tau)_i\mathrm{d}\mathbf{x}$$

for every vector component, respectively. Once more, the control volume $\sigma(t_0)$ is arbitrary, hence

(3) $$\frac{\partial \varrho v_i}{\partial t} + \mathrm{div}\varrho v_i\mathbf{v} = \varrho f_i + \mathrm{div}(\tau)_i.$$

Since $\tau : \mathbb{R}^3 \to \mathbb{R}^3$, it is

$$\mathrm{div}\tau = \left(\sum_{j=1}^{3}\frac{\partial \tau_{j1}}{\partial x_j}, \sum_{j=1}^{3}\frac{\partial \tau_{j2}}{\partial x_j}, \sum_{j=1}^{3}\frac{\partial \tau_{j3}}{\partial x_j}\right)^T.$$

1.2.3 Law of conservation of energy

"*The rate of change of the total energy of a piece of fluid formed by the same particles at any time instant is equal to the sum of the powers of the volume and surface forces acting on this piece of fluid and to the amount of heat transmitted to this piece of fluid*", i.e.

$$\frac{\mathrm{d}}{\mathrm{d}t}\int_{\sigma(t)} E\mathrm{d}\mathbf{x} = \int_{\sigma(t)} \varrho\mathbf{f}.\mathbf{v}\mathrm{d}\mathbf{x} + \int_{\partial\sigma(t)} \tau\nu.\mathbf{v}\mathrm{d}S + \int_{\sigma(t)} \varrho q\mathrm{d}\mathbf{x} - \int_{\partial\sigma(t)} \underline{q}.\nu\mathrm{d}S.$$

In the end, we obtain

(4) $$\frac{\partial E}{\partial t} + \mathrm{div}E\mathbf{v} = \varrho\mathbf{f}.\mathbf{v} + \sum_{i=1}^{3}\sum_{j=1}^{3}\frac{\partial \tau_{ji}v_i}{\partial x_j} + \varrho q - \mathrm{div}\underline{q}$$

in the same way as before.

1.3 Formulation of the problem

In case of the Euler equations we neglect external body forces, heat flux and external heat sources. We consider the stress tensor in the Newtonian form $\tau = -p\mathbf{I}$ (where p is the pressure). In our conception, the domain $\Omega \subset \mathbb{R}^3$ will be constant in time, with piecewise linear continuous boundary. Further, let $\mathcal{T} > 0$ be a real number and let e, ϱ, p, $\mathbf{v}$ be defined and piecewise smooth in $\overline{\Omega} \times (0, \mathcal{T})$.

To settle number of equations and number of unknowns, we must set additional assumptions. Thus, let us consider a perfect gas, which means $p = p(\varrho, e)$ and the state equation

$$p = \varrho RT \tag{5}$$

is valid. After having replaced T and R, we get the wanted dependence

$$p = \varrho RT = \varrho R\left(\frac{e}{c_v}\right) = \varrho\left(\frac{c_p - c_v}{c_v}\right)e = (\kappa - 1)\varrho e = (\kappa - 1)\left(E - \frac{1}{2}\varrho\mathbf{v}^2\right). \tag{6}$$

Now we can put equations (2), (3) ... (6) together, present the system of the Euler equations in its conservative form

$$\frac{\partial}{\partial t}\begin{pmatrix} \varrho \\ \varrho u \\ \varrho v \\ \varrho w \\ E \end{pmatrix} + \frac{\partial}{\partial x}\begin{pmatrix} \varrho u \\ \varrho u^2 + p \\ \varrho uv \\ \varrho uw \\ (E+p)u \end{pmatrix} + \frac{\partial}{\partial y}\begin{pmatrix} \varrho v \\ \varrho uv \\ \varrho v^2 + p \\ \varrho vw \\ (E+p)v \end{pmatrix} + \frac{\partial}{\partial z}\begin{pmatrix} \varrho w \\ \varrho uw \\ \varrho vw \\ \varrho w^2 + p \\ (E+p)w \end{pmatrix} = 0 \tag{7}$$

and formulate the problem:
We search for piecewise smooth scalar functions ϱ, u, v, w, E and p defined in $\overline{\Omega} \times (0, \mathcal{T})$ meeting for almost all $(\mathbf{x}, t) \in \overline{\Omega} \times (0, \mathcal{T})$ the system (7) with the initial condition

$$\mathbf{q}(\mathbf{x}, 0) = \mathbf{q}_0(\mathbf{x}) \qquad \mathbf{x} \in \Omega \tag{8}$$

and the boundary condition

$$B(\mathbf{q}(\mathbf{x}, t)) = 0 \qquad (\mathbf{x}, t) \in \partial\Omega \times (0, \mathcal{T}), \tag{9}$$

where $\mathbf{q}(\mathbf{x}, t) = (\varrho, \varrho u, \varrho v, \varrho w, E)^T(\mathbf{x}, t)$, B is a boundary operator (the form of which has not been found out until now) and $\mathbf{q}_0(\mathbf{x})$ is a given piecewise smooth function defined almost everywhere in $\overline{\Omega}$.

Using the new notation, we have

$$\varrho = q_1, \quad u = q_2/q_1, \quad v = q_3/q_1, \quad w = q_4/q_1, \quad E = q_5 \tag{10}$$

and according to (6)

$$p = (\kappa - 1)\left(q_5 - \frac{{q_2}^2 + {q_3}^2 + {q_4}^2}{2q_1}\right), \qquad \kappa > 1. \tag{11}$$

Conditions $\varrho > 0$ and $p > 0$ call for a definition of physical admissible state set

$$\mathcal{Q} = \left\{ \mathbf{q} \in \mathbb{R}^5; \quad q_1 > 0 \ \ \& \ \ q_5 > \left(\frac{{q_2}^2 + {q_3}^2 + {q_4}^2}{2q_1}\right)\right\}. \tag{12}$$

Now let us transform the system (7) into the new variables:

$$\frac{\partial}{\partial t}\mathbf{q}(\mathbf{x},t) + \frac{\partial}{\partial x}\mathbf{f}(\mathbf{q}(\mathbf{x},t)) + \frac{\partial}{\partial y}\mathbf{g}(\mathbf{q}(\mathbf{x},t)) + \frac{\partial}{\partial z}\mathbf{h}(\mathbf{q}(\mathbf{x},t)) = 0, \tag{13}$$

where $\mathbf{f}, \mathbf{g}, \mathbf{h} : \mathcal{Q} \to \mathbb{R}^5$. According to (7), (10) and (11) it is

$$\mathbf{f}(\mathbf{q}) = \begin{pmatrix} q_2 \\ \frac{{q_2}^2}{q_1} + (\kappa - 1)\left(q_5 - \frac{{q_2}^2+{q_3}^2+{q_4}^2}{2q_1}\right) \\ \frac{q_2 q_3}{q_1} \\ \frac{q_2 q_4}{q_1} \\ \frac{q_2}{q_1}\left(\kappa q_5 - (\kappa - 1)\frac{{q_2}^2+{q_3}^2+{q_4}^2}{2q_1}\right) \end{pmatrix}. \tag{14}$$

The remaining two functions $\mathbf{g}(\mathbf{q})$, $\mathbf{h}(\mathbf{q})$ look similar.

2 Numerical solution

2.1 Finite volume method

Let us divide the domain Ω into a finite number of subdomains Ω_i, $i = 1, 2, \ldots, N$ in the following manner:

1. Ω_i open, convex with a piecewise linear boundary (polyhedra), $i = 1, 2, \ldots, N$
2. $\overline{\Omega} = \bigcup_{i=1}^{N} \overline{\Omega}_i$
3. $\Omega_i \cap \Omega_j = \emptyset$, $i = 1, 2, \ldots, N$
4. in case $\partial\Omega_i \cap \partial\Omega_j \neq \emptyset$ $i, j \in \{1, 2, \ldots, N\}$, exactly one of the following options is valid:

   a) $\partial\Omega_i$ and $\partial\Omega_j$ share just one vertex
   b) $\partial\Omega_i$ and $\partial\Omega_j$ share just one edge
   c) $\partial\Omega_i$ and $\partial\Omega_j$ share just one side,

The expression '$\partial\Omega_i$ and $\partial\Omega_j$ share a vertex' means that this point is a vertex in $\partial\Omega_i$ and is a vertex in $\partial\Omega_j$ etc.

These subdomains are so-called *finite volumes (elements)*. In case $\mu_2(\partial\Omega_i \cap \partial\Omega) \neq 0$, Ω_i is a *boundary finite volume*. In case $\mu_2(\partial\Omega_i \cap \partial\Omega_j) \neq 0$ and 4c) is valid, we call these finite volumes *neighbours*. Let us n_b denote the boundary finite element number. Because of the discretization of the Euler equations we need that every finite volume has just so many neighbours how many sides it has. That is why we define so-called *fictive finite volumes*:

Let Ω_i, $i \in \{1, 2, \ldots, N\}$, be a boundary finite volume. To its side $D \subset \partial\Omega_i \cap \partial\Omega$ we define the fictive finite volume Ω_{iD} as an arbitrary representative of the class

$$\mathcal{B} = \{\tilde{\Omega}_{iD};\ \ \tilde{\Omega}_{iD} \text{ open convex polyhedron},\ \ \tilde{\Omega}_{iD} \cap \Omega_i = \emptyset,\ \ \partial\tilde{\Omega}_{iD} \cap \partial\Omega_i = \partial\Omega_i \cap \partial\Omega\}.$$

Finite volumes which are not fictive we call *real*. The set of all fictive finite volumes has $M \geq n_b$ members which we can denote $\Omega_{N+1}, \Omega_{N+2}, \ldots, \Omega_{N+M}$. Let us define the index set

$$\mathcal{K}(i) = \{j \in \{1, 2, \ldots, N + M\} \setminus \{j\};\ \ \mu_2(\partial\Omega_i \cap \partial\Omega_j) > 0\} \qquad i \in \{1, 2, \ldots, N\}. \tag{2.1.15}$$

Let Ω_i and Ω_j be two neighbouring finite volumes, $i \in \{1, 2, \ldots, N\}$, $j \in \{1, 2, \ldots, N + M\}$, we denote $\partial\Omega_{ij} = \partial\Omega_i \cap \partial\Omega_j$. For the boundary of every finite volume it holds

$$\partial\Omega_i = \bigcup_{j \in \mathcal{K}(i)} \partial\Omega_{ij} \qquad i = 1, 2, \ldots, N. \tag{2.1.16}$$

Number of members of any index set $\mathcal{K}(i)$ is at least four, is not limited and it needs not to be the same for $i \in \{1, 2, \ldots, N\}$. Now we define the set

$$\mathcal{V} = \left\{f \in L^1(\Omega);\ \ f(\mathbf{x}) \text{ is constant for } \mathbf{x} \in \Omega_i,\ \ i = 1, 2, \ldots, N\right\}. \tag{2.1.17}$$

An arbitrary function $f \in L^1(\Omega)$ will be approximated with the function (or with the class of L^1 - equivalent functions) $\tilde{f} \in \mathcal{V}$ meeting

$$\tilde{f}(\mathbf{x}) = \left\{ \begin{array}{ccc} \frac{1}{\mu_3(\Omega_i)} \int\limits_{\Omega_i} f(\xi) \ \mathrm{d}\xi & \text{for } \ \mathbf{x} \in \Omega_i & i = 1, 2, \ldots, N \\ & & \\ 0 & \text{elsewhere in } \ \Omega & \end{array} \right\}. \tag{2.1.18}$$

The value $\tilde{f}(\mathbf{x})$ we usually identify with the value in the center of gravity of Ω_i. For more detail explanation about the error estimate see [26]. Let us now proceed to the discretization of the system (7):

Having integrated the system (13) over finite volumes Ω_i, $i = 1, 2, \ldots, N$ and having used the Gauss theorem we obtain

$$\frac{\mathrm{d}}{\mathrm{d}t} \int_{\Omega_i} \mathbf{q}(\mathbf{x}, t) \mathrm{d}\mathbf{x} + \int_{\partial\Omega_i} \mathbf{f}(\mathbf{q}(\mathbf{x}, t)) \nu_{ij\,1}(\mathbf{x}) + \mathbf{g}(\mathbf{q}(\mathbf{x}, t)) \nu_{ij\,2}(\mathbf{x}) + \mathbf{h}(\mathbf{q}(\mathbf{x}, t)) \nu_{ij\,3}(\mathbf{x}) \mathrm{d}S = 0, \tag{2.1.19}$$

where $i = 1, 2, \ldots, N$, $t \in (0, \mathcal{T})$ and ν_{ij} is the unit outside normal vector to $\partial\Omega_i$ at $\mathbf{x} \in \partial\Omega_i$ defined almost everywhere in Ω.

Using (2.1.16) we can transform (2.1.19) to

$$\frac{\mathrm{d}}{\mathrm{d}t} \int_{\Omega_i} \mathbf{q}(\mathbf{x}, t) \mathrm{d}\mathbf{x} + \sum_{j \in \mathcal{K}(i)} \int_{\partial\Omega_{ij}} \mathbf{f}(\mathbf{q}(\mathbf{x}, t)) \nu_{ij\,1}(\mathbf{x}) + \mathbf{g}(\mathbf{q}(\mathbf{x}, t)) \nu_{ij\,2}(\mathbf{x}) + \mathbf{h}(\mathbf{q}(\mathbf{x}, t)) \nu_{ij\,3}(\mathbf{x}) \mathrm{d}S = 0,$$

where $i = 1, 2, \ldots, N$, $t \in (0, \mathcal{T})$. We replace the function $\mathbf{q}(\cdot, t)$ by the piecewise constant function $\tilde{\mathbf{q}}(\cdot, t)$ defined by (2.1.18):

$$\mu_3(\Omega_i) \frac{\mathrm{d}}{\mathrm{d}t} \tilde{\mathbf{q}}_\mathbf{i}(t) + \sum_{j \in \mathcal{K}(i)} \Phi(\tilde{\mathbf{q}}_\mathbf{i}(t), \tilde{\mathbf{q}}_\mathbf{j}(t), \nu_{ij}, \mu_2(\partial\Omega_{ij})) = 0 \quad i = 1, 2, \ldots, N, \tag{2.1.20}$$

where $\tilde{\mathbf{q}}_\mathbf{i}(t)$ denotes $\tilde{\mathbf{q}}(\mathbf{x}, t)$ for $\mathbf{x} \in \Omega_i$ etc. The function $\Phi(\tilde{\mathbf{q}}_\mathbf{i}(t), \tilde{\mathbf{q}}_\mathbf{j}(t), \nu_{ij}, \mu_2(\partial\Omega_{ij}))$ (or simply $\Phi_{ij}(\tilde{\mathbf{q}}_\mathbf{i}(t), \tilde{\mathbf{q}}_\mathbf{j}(t))$) approximates the integral

$$\int_{\partial\Omega_{ij}} \mathbf{f}(\mathbf{q}(\mathbf{x}, t)) \nu_{ij\,1} + \mathbf{g}(\mathbf{q}(\mathbf{x}, t)) \nu_{ij\,2} + \mathbf{h}(\mathbf{q}(\mathbf{x}, t)) \nu_{ij\,3} \mathrm{d}S \tag{2.1.21}$$

which expresses the flux of $\mathbf{q}(\mathbf{x}, t)$ through the side $\partial\Omega_{ij}$ of the finite volume Ω_i. The function Φ (so-called *numerical flux*) must satisfy the following two conditions:

$$\Phi(\mathbf{q}, \mathbf{q}, \nu, a) = a(\mathbf{f}(\mathbf{q})\nu_1 + \mathbf{g}(\mathbf{q})\nu_2 + \mathbf{h}(\mathbf{q})\nu_3) \tag{2.1.22}$$
$$\Phi(\mathbf{q_1}, \mathbf{q_2}, \nu, a) = -\Phi(\mathbf{q_2}, \mathbf{q_1}, -\nu, a) \tag{2.1.23}$$

for every $\mathbf{q}, \mathbf{q_1}, \mathbf{q_2} \in \mathcal{Q}$, $\nu \in \mathbb{R}^3$ $|\nu| = 1$ and for every $a \in \mathbb{R}^+$.

The relation (2.1.22) is so-called *consistence condition*, the other one secures the numerical flux is conservative.

Let us consider a finite division of the time interval $(0, \mathcal{T})$: $0 = t_0 < t_1 < \ldots < t_L = \mathcal{T}$ and denote $\mathbf{q_i}^k = \mathbf{q_i}(t_k)$, $k = 0, 1, \ldots, L$. We consider the equation (2.1.20) only at this discrete times and approximate

$$\frac{\mathrm{d}\mathbf{q_i}}{\mathrm{d}t} \approx \frac{\mathbf{q_i}^{k+1} - \mathbf{q_i}^k}{t_{k+1} - t_k},$$

where $k = 0, 1, \ldots, L-1$ and $i = 0, 1, \ldots, N$. The equation (2.1.20) has now the form

$$\mathbf{q_i}^{k+1} = \mathbf{q_i}^k - \frac{\Delta t_k}{\mu_3(\Omega_i)} \sum_{j \in \mathcal{K}(i)} \Phi_{ij}(\mathbf{q_i}^k, \mathbf{q_j}^k), \tag{2.1.24}$$

where $\Delta t_k = t_{k+1} - t_k$, $k = 0, 1, \ldots, L-1$ and $i = 0, 1, \ldots, N$.

The scheme (2.1.24) is explicit, conservative and its properties are given notably by choice of the numerical flux Φ. Later, in sections **2.4** and **2.5**, we will construct the Osher-Solomon numerical flux. Before this, after having prepared some necessary theoretical tools, we will mention the Riemann problem, the approximate solution to which is for the flux construction very important.

2.2 Theoretical tools

2.2.1 Matrix A

Let us denote by the symbol $\mathbf{A}(\mathbf{q})$ the Jacobi matrix of $\mathbf{f}(\mathbf{q})$. We express $\mathbf{f}(\mathbf{q})$ in the conservation variables, calculate its gradient and present it in its physical form:

$$\mathbf{A}(\mathbf{q}) = \begin{pmatrix} 0 & 1 & 0 & 0 & 0 \\ \frac{\kappa-1}{2}\mathbf{v}^2 - u^2 & (3-\kappa)u & (1-\kappa)v & (1-\kappa)w & \kappa - 1 \\ -uv & v & u & 0 & 0 \\ -uw & w & 0 & u & 0 \\ u\left((\kappa-1)\mathbf{v}^2 - \kappa\frac{E}{\varrho}\right) & \kappa\frac{E}{\varrho} - (\kappa-1)u^2 - \frac{\kappa-1}{2}\mathbf{v}^2 & (1-\kappa)uv & (1-\kappa)uw & \kappa u \end{pmatrix}. \tag{2.2.25}$$

2.2.2 Eigenvalues

In this paragraph we will calculate eigenvalues of the matrix $\mathbf{A}(\mathbf{q})$. Let us denote $\mathbf{M}(\mathbf{q}, \lambda) = \mathbf{A}(\mathbf{q}) - \lambda\mathbf{I}$. Its determinant can be computed quite easily using reduction of the first row.

We denote $\mathbf{M_1}$ the matrix formed by omitting the first row and the first column of $\mathbf{M}$ and $\mathbf{M_2}$ the matrix formed by omitting the first row and second column of $\mathbf{M}$.

It follows

$$\det\mathbf{M} = -\lambda\det\mathbf{M_1} - \det\mathbf{M_2}. \tag{2.2.26}$$

Both the determinants we will obtain in a similar way. We denote

$\mathbf{M_{11}}$ the matrix formed by omitting the second row and the first column of $\mathbf{M_1}$,
$\mathbf{M_{12}}$ the matrix formed by omitting the second row and the second column of $\mathbf{M_1}$,
$\mathbf{M_{21}}$ the matrix formed by omitting the second row and the first column of $\mathbf{M_2}$
$\mathbf{M_{22}}$ the matrix formed by omitting the second row and the second column of $\mathbf{M_2}$.

and start to calculate:

$$\det\mathbf{M_{11}} = -v(u-\lambda)^2(\kappa-1) \tag{2.2.27}$$

$$\det\mathbf{M_{12}} = -\frac{1}{2}(u-\lambda)((v^2-w^2)(\kappa-1) - u^2(3+\kappa) + 6u\lambda - 2(\lambda^2+c^2)) \tag{2.2.28}$$

$$\det\mathbf{M_{21}} = \det\mathbf{M_{11}} \tag{2.2.29}$$

$$\det\mathbf{M_{22}} = \frac{1}{2}(u-\lambda)\left(-2u^3 - u^2\lambda(\kappa-3) - 2v^2u(1-\kappa) - w\lambda(\kappa-1) + 2c^2u - v^2\lambda(\kappa-1)\right). \tag{2.2.30}$$

According to the reduction theorem we further have

$$\det\mathbf{M_1} = -v\det\mathbf{M_{11}} - (\lambda-u)\det\mathbf{M_{12}} \tag{2.2.31}$$

$$\det\mathbf{M_2} = uv\det\mathbf{M_{21}} - (\lambda-u)\det\mathbf{M_{22}}. \tag{2.2.32}$$

By substituting into (2.2.26) we get

$$\det\mathbf{M}(\mathbf{q},\lambda) = (\lambda-u)^3(\lambda-u-c)(\lambda-u+c). \tag{2.2.33}$$

Thus, $\mathrm{Sp}(\mathbf{A}(\mathbf{q})) = \{c-u, u, c+u\}$. As you will see later, at this moment it is suitable to arrange the eigenvalues according to the magnitude $\lambda_1(\mathbf{q}) = c-u$, $\lambda_2(\mathbf{q}) = \lambda_3(\mathbf{q}) = \lambda_4(\mathbf{q}) = u$ and $\lambda_5(\mathbf{q}) = u+c$.

2.2.3 Eigenvectors

In this paragraph we will calculate the matrix $\mathbf{A}(\mathbf{q})$ eigenvectors. First, let us deal with the eigenvalue $\lambda_2(\mathbf{q}) = \lambda_3(\mathbf{q}) = \lambda_4(\mathbf{q}) = u$:

$$\mathbf{A}-u\mathbf{I} = \begin{pmatrix} -u & 1 & 0 & 0 & 0 \\ \frac{\kappa-1}{2}\mathbf{v}^2 - u^2 & (2-\kappa)u & (1-\kappa)v & (1-\kappa)w & (\kappa-1) \\ -uv & v & 0 & 0 & 0 \\ -uw & w & 0 & 0 & 0 \\ u\left((\kappa-1)\mathbf{v}^2 - \kappa\frac{E}{\varrho}\right) & \kappa\frac{E}{\varrho} - (\kappa-1)u^2 - \frac{(\kappa-1)}{2}\mathbf{v}^2 & (1-\kappa)uv & (1-\kappa)uw & \kappa-1u \end{pmatrix}. \tag{2.2.34}$$

The second row of (2.2.34) multiplied by $(-u)$ and added to the last row equals to the first row multiplied by $(\kappa\frac{E}{\varrho} - u^2 - \frac{\kappa-1}{2}\mathbf{v}^2)$. The rank of (2.2.34) is equal to two, which means we can neglect the last three rows and take care of the first two only.

We are looking for three linear independent vectors (denoted $\mathbf{z_1}(\mathbf{q})$, $\mathbf{z_2}(\mathbf{q})$ and $\mathbf{z_3}(\mathbf{q})$) which are orthogonal to the following two rows:

$$(-u, 1, 0, 0, 0) \tag{2.2.35}$$

$$\left(\frac{\kappa-1}{2}\mathbf{v}^2 - u^2, (2-\kappa)u, (1-\kappa)v, (1-\kappa)w, (\kappa-1)\right). \tag{2.2.36}$$

When we set the two first components of two sought vectors equal to zero, it is sufficient to look for them in the orthogonal supplement of

$$(0, 0, v, w, -1). \tag{2.2.37}$$

Thus, we obtain easily

$$\mathbf{z_1}(\mathbf{q}) = (0, 0, 1, 0, v)^T \tag{2.2.38}$$

$$\mathbf{z_2}(\mathbf{q}) = (0, 0, 0, 1, w)^T. \tag{2.2.39}$$

Let us note that these vectors are not unique - for every $\mathbf{q} \in \mathcal{Q}$ they can be multiplied by an arbitrary nonzero constant. In general they can be multiplied by an arbitrary nonzero function of $\mathbf{q}$. In our case, these functions are set identically to one.

The first two components of $\mathbf{z_3}(\mathbf{q})$ are (from the orthogonality to (2.2.35)) $z_{31} = 1$ and $z_{32} = u$. Further, orthogonality to (2.2.36) gives

$$(1-\kappa)vz_{33} + (1-\kappa)wz_{34} + (\kappa-1)z_{35} = (\kappa-1)\left(u^2 - \frac{\mathbf{v}^2}{2}\right) \tag{2.2.40}$$

and

$$vz_{33} + wz_{34} + u^2 = \frac{\mathbf{v}^2}{2} + z_{35}. \tag{2.2.41}$$

Setting $z_{33} = v$ and $z_{24} = w$ we get

$$\mathbf{z_3}(\mathbf{q}) = \left(1, u, v, w, \frac{\mathbf{v}^2}{2}\right)^T. \tag{2.2.42}$$

With these vectors, there would be some troubles in further explanation. As you see later, we will need all the eigenvectors to have a nonzero first component. We use that eigenvectors of $\mathbf{A}$ corresponding to the eigenvalue u generate for every $\mathbf{q} \in \mathcal{Q}$ a linear subspace in $\mathbb{R}^5$. It is easy to see that vectors $\mathbf{r_2}(\mathbf{q})$, $\mathbf{r_3}(\mathbf{q})$ and $\mathbf{r_4}(\mathbf{q})$ generate for every $\mathbf{q} \in \mathcal{Q}$ the same subspace.

$$\mathbf{r_2}(\mathbf{q}) = \left(1, u, v, w, \frac{\mathbf{v}^2}{2}\right)^T \tag{2.2.43}$$

$$\mathbf{r_3}(\mathbf{q}) = \left(1, u, v-c, w, \frac{\mathbf{v}^2}{2} - vc\right)^T \tag{2.2.44}$$

$$\mathbf{r_4}(\mathbf{q}) = \left(1, u, v, w-c, \frac{\mathbf{v}^2}{2} - wc\right)^T . \tag{2.2.45}$$

Analogously to $\lambda_1(\mathbf{q}) = u - c$ we find the eigenvector

$$\mathbf{r_1}(\mathbf{q}) = \left(1, u-c, v, w, \frac{\mathbf{v}^2}{2} + \frac{c^2}{\kappa - 1} - uc\right)^T \tag{2.2.46}$$

and to the last eigenvalue $\lambda_5(\mathbf{q}) = u + c$ the eigenvector

$$\mathbf{r_5}(\mathbf{q}) = \left(1, u+c, v, w, \frac{\mathbf{v}^2}{2} + \frac{c^2}{\kappa - 1} + uc\right)^T . \tag{2.2.47}$$

Vectors $\mathbf{r_1}(\mathbf{q})$, $\mathbf{z_2}(\mathbf{q})$, $\mathbf{z_3}(\mathbf{q})$, $\mathbf{z_4}(\mathbf{q})$ and $\mathbf{r_5}(\mathbf{q})$ are linearly independent for every $\mathbf{q} \in \mathcal{Q}$, therefore also $\mathbf{r_1}(\mathbf{q})$, $\mathbf{r_2}(\mathbf{q})$, $\mathbf{r_3}(\mathbf{q})$, $\mathbf{r_4}(\mathbf{q})$ and $\mathbf{r_5}(\mathbf{q})$ are linearly independent for every $\mathbf{q} \in \mathcal{Q}$.

2.2.4 Eigenvector basis

Eigenvectors of the matrix $\mathbf{A}(\mathbf{q})$ are for every $\mathbf{q} \in \mathcal{Q}$ linearly independent which means they generate the whole $\mathbb{R}^5$. For every $\mathbf{q} \in \mathcal{Q}$ we can construct a transition matrix from the eigenvector basis to the canonical basis. This matrix, denoted by $\mathbf{R}(\mathbf{q})$, has the eigenvectors $\mathbf{r_1}(\mathbf{q})$, $\mathbf{r_2}(\mathbf{q})$, $\mathbf{r_3}(\mathbf{q})$, $\mathbf{r_4}(\mathbf{q})$ and $\mathbf{r_5}(\mathbf{q})$ as its columns:

$$\mathbf{R}(\mathbf{q}) = \begin{pmatrix} 1 & 1 & 1 & 1 & 1 \\ u-c & u & u & u & u+c \\ v & v & v-c & v & v \\ w & w & w & w-c & w \\ \frac{\mathbf{v}^2}{2} + \frac{c^2}{\kappa-1} - uc & \frac{\mathbf{v}^2}{2} & \frac{\mathbf{v}^2}{2} - vc & \frac{\mathbf{v}^2}{2} - wc & \frac{\mathbf{v}^2}{2} + \frac{c^2}{\kappa-1} + uc \end{pmatrix} . \tag{2.2.48}$$

Its inverse has the form

$$\mathbf{R}^{-1}(\mathbf{q}) = \frac{1}{c^2} \begin{pmatrix} \frac{1}{2}\left(\frac{(\kappa-1)\mathbf{v}^2}{2} + uc\right) & -\frac{c+u(\kappa-1)}{2} & -\frac{v(\kappa-1)}{2} & -\frac{w(\kappa-1)}{2} & \frac{\kappa-1}{2} \\ c^2 - c(v+w) - (\kappa-1)\frac{\mathbf{v}^2}{2} & u(\kappa-1) & c + v(\kappa-1) & c + w(\kappa-1) & 1-\kappa \\ vc & 0 & -c & 0 & 0 \\ wc & 0 & 0 & -c & 0 \\ \frac{1}{2}\left(\frac{(\kappa-1)\mathbf{v}^2}{2} - uc\right) & \frac{c-u(\kappa-1)}{2} & -\frac{v(\kappa-1)}{2} & -\frac{w(\kappa-1)}{2} & \frac{\kappa-1}{2} \end{pmatrix} . \tag{2.2.49}$$

Let us denote $\mathbf{\Lambda}(\mathbf{q}) = \mathbf{R}^{-1}(\mathbf{q})\mathbf{A}(\mathbf{q})\mathbf{R}(\mathbf{q})$ and present it:

$$\mathbf{\Lambda}(\mathbf{q}) = \begin{pmatrix} u-c & 0 & 0 & 0 & 0 \\ 0 & u & 0 & 0 & 0 \\ 0 & 0 & u & 0 & 0 \\ 0 & 0 & 0 & u & 0 \\ 0 & 0 & 0 & 0 & u+c \end{pmatrix}. \tag{2.2.50}$$

2.2.5 Rotational invariance of the Euler equations

Theorem 2.2.1
Let $\alpha, \beta \in \langle 0, 2\pi)$,

$$\mathbf{T}(\alpha,\beta) = \begin{pmatrix} 1 & 0 & 0 & 0 & 0 \\ 0 & \cos(\alpha)\cos(\beta) & \sin(\alpha)\cos(\beta) & \sin(\beta) & 0 \\ 0 & -\sin(\alpha) & \cos(\alpha) & 0 & 0 \\ 0 & -\cos(\alpha)\sin(\beta) & -\sin(\alpha)\sin(\beta) & \cos(\beta) & 0 \\ 0 & 0 & 0 & 0 & 1 \end{pmatrix} \tag{2.2.51}$$

and let $\mathbf{f}$, $\mathbf{g}$, $\mathbf{h} : \mathcal{Q} \to \mathbb{R}^5$ be the functions defined in section **1** Then it holds

$$\cos(\alpha)\cos(\beta)\mathbf{f}(\mathbf{q}) + \sin(\alpha)\cos(\beta)\mathbf{g}(\mathbf{q}) + \sin(\beta)\mathbf{h}(\mathbf{q}) = \mathbf{T}^{-1}(\alpha,\beta)\mathbf{f}\left(\mathbf{T}(\alpha,\beta)\mathbf{q}\right) \tag{2.2.52}$$

$$-\sin(\alpha)\mathbf{f}(\mathbf{q}) + \cos(\alpha)\mathbf{g}(\mathbf{q}) = \mathbf{T}^{-1}(\alpha,\beta)\mathbf{g}\left(\mathbf{T}(\alpha,\beta)\mathbf{q}\right) \tag{2.2.53}$$

$$-\cos(\alpha)\sin(\beta)\mathbf{f}(\mathbf{q}) - \sin(\alpha)\sin(\beta)\mathbf{g}(\mathbf{q}) + \cos(\beta)\mathbf{h}(\mathbf{q}) = \mathbf{T}^{-1}(\alpha,\beta)\mathbf{h}\left(\mathbf{T}(\alpha,\beta)\mathbf{q}\right). \tag{2.2.54}$$

Under the notation $\frac{D\mathbf{g}}{D\mathbf{q}} = \mathbf{B}(\mathbf{q})$ and $\frac{D\mathbf{h}}{D\mathbf{q}} = \mathbf{C}(\mathbf{q})$ it holds further

$$\cos(\alpha)\cos(\beta)\mathbf{A}(\mathbf{q}) + \sin(\alpha)\cos(\beta)\mathbf{B}(\mathbf{q}) + \sin(\beta)\mathbf{C}(\mathbf{q}) = \mathbf{T}^{-1}(\alpha,\beta)\mathbf{A}\left(\mathbf{T}(\alpha,\beta)\mathbf{q}\right)\mathbf{T}(\alpha,\beta) \tag{2.2.55}$$

$$\sin(\alpha)\mathbf{A}(\mathbf{q}) + \cos(\alpha)\mathbf{B}(\mathbf{q}) = \mathbf{T}^{-1}(\alpha,\beta)\mathbf{B}\left(\mathbf{T}(\alpha,\beta)\mathbf{q}\right)\mathbf{T}(\alpha,\beta) \tag{2.2.56}$$

$$-\cos(\alpha)\sin(\beta)\mathbf{A}(\mathbf{q}) - \sin(\alpha)\sin(\beta)\mathbf{B}(\mathbf{q}) + \cos(\beta)\mathbf{C}(\mathbf{q}) = \mathbf{T}^{-1}(\alpha,\beta)\mathbf{C}\left(\mathbf{T}(\alpha,\beta)\mathbf{q}\right)\mathbf{T}(\alpha,\beta). \tag{2.2.57}$$

where the matrix **A** was defined in **2.2.1**.

Proof: The matrix

$$\mathbf{T}_0(\alpha,\beta) = \begin{pmatrix} \cos(\alpha)\cos(\beta) & \sin(\alpha)\cos(\beta) & \sin(\beta) \\ -\sin(\alpha) & \cos(\alpha) & 0 \\ -\cos(\alpha)\sin(\beta) & -\sin(\alpha)\sin(\beta) & \cos(\beta) \end{pmatrix} \tag{2.2.58}$$

is a rotational matrix in $\mathbb{R}^3$, ${\mathbf{T}_0}^{-1}(\alpha,\beta) = {\mathbf{T}_0}^T(\alpha,\beta)$, which means $\mathbf{T}^{-1}(\alpha,\beta) = \mathbf{T}^T(\alpha,\beta)$. Now it is easy to verify the validity of (2.2.52), (2.2.53), (2.2.54) and consequently the validity of (2.2.55), (2.2.56) and (2.2.57).

2.2.6 Hyperbolicity of the Euler equations

Definition 2.2.2
The system of the Euler equations is *hyperbolic* if for every $\mathbf{q} \in \mathcal{Q}$, $\nu = (\nu_1, \nu_2, \nu_3)^T \in \mathbb{R}^3$ the eigenvalues of the matrix

$$\mathbf{P}(\mathbf{q}, \nu) = \frac{D\mathbf{f}}{D\mathbf{q}}(\mathbf{q})\nu_1 + \frac{D\mathbf{g}}{D\mathbf{q}}(\mathbf{q})\nu_2 + \frac{D\mathbf{h}}{D\mathbf{q}}(\mathbf{q})\nu_3 \tag{2.2.59}$$

are real and this matrix is diagonalizable.

Theorem 2.2.3
The system of the Euler equation is hyperbolic according to the previous definition.

Proof: If $\nu \in \mathbb{R}^3$ was equal to the zero vector, the previous definition would be satisfied. In the opposite case let us express ν in its polar coordinates: $r(\cos(\alpha)\cos(\beta), \sin(\alpha)\cos(\beta), \sin(\beta))^T$, where $r \neq 0$ and $\alpha, \beta \in \langle 0, 2\pi)$. According to (2.2.55),

$$\mathbf{P}(\mathbf{q}, \nu) = r\mathbf{T}^{-1}(\alpha, \beta)\mathbf{A}\left(\mathbf{T}(\alpha, \beta)\mathbf{q}\right)\mathbf{T}(\alpha, \beta)$$

and consequently

$$\begin{aligned} &\det\left(\mathbf{P}(\mathbf{q}, \nu) - \mu\mathbf{I}\right) = \det\left(r\mathbf{T}^{-1}(\alpha, \beta)\mathbf{A}\left(\mathbf{T}(\alpha, \beta)\mathbf{q}\right)\mathbf{T}(\alpha, \beta) - \mu\mathbf{I}\right) = \\ &= \det\left(r\mathbf{T}^{-1}(\alpha, \beta)\left(\mathbf{A}(\mathbf{T}(\alpha, \beta)\mathbf{q}) - \frac{\mu}{r}\mathbf{I}\right)\mathbf{T}(\alpha, \beta)\right) = r^5 \det\left(\mathbf{A}(\mathbf{T}(\alpha, \beta)\mathbf{q}) - \frac{\mu}{r}\mathbf{I}\right). \end{aligned}$$

According to (2.2.33), the eigenvalues of $\mathbf{A}(\mathbf{q})$ are real for all $\mathbf{q} \in \mathcal{Q}$. Hence, the eigenvalues of $\mathbf{P}(\mathbf{q}, \nu)$ are real for all $\mathbf{q} \in \mathcal{Q}$ and for all $\nu \in \mathbb{R}^3$. It remains to verify the diagonalisability of $\mathbf{P}(\mathbf{q}, \nu)$.

Let us set $\mathbf{Q}(\mathbf{q}, \nu) = \mathbf{T}^{-1}(\alpha, \beta)\mathbf{R}(\mathbf{T}(\alpha, \beta)\mathbf{q})$, where $\mathbf{R}(\mathbf{q})$ was defined by (2.2.48). Then

$$\mathbf{Q}^{-1}(\mathbf{q}, \nu)\mathbf{P}(\mathbf{q}, \nu)\mathbf{Q}(\mathbf{q}, \nu) = r\mathrm{diag}\left(\lambda_1(\mathbf{T}(\alpha, \beta)\mathbf{q}), \lambda_2(\mathbf{T}(\alpha, \beta)\mathbf{q}), \ldots, \lambda_5(\mathbf{T}(\alpha, \beta)\mathbf{q})\right),$$

where $\lambda_1(\mathbf{T}(\alpha, \beta)\mathbf{q}), \lambda_2(\mathbf{T}(\alpha, \beta)\mathbf{q}), \ldots, \lambda_5(\mathbf{T}(\alpha, \beta)\mathbf{q})$ are eigenvalues of the matrix $\mathbf{A}(\mathbf{T}(\alpha, \beta)\mathbf{q})$. Hence, the matrix $\mathbf{P}(\mathbf{q}, \nu)$ is diagonalizable.

2.2.7 Riemann invariants

Definition 2.2.4
Let us suppose that the matrix $\mathbf{A}(\mathbf{q})$ from (2.2.25) is an element of $\mathrm{C}(\mathcal{Q}, \mathrm{Lin}(\mathbb{R}^5))$ and that its eigenvectors from (2.2.43) ... (2.2.47) $\mathbf{r_1}(\mathbf{q}), \mathbf{r_2}(\mathbf{q}), \ldots, \mathbf{r_5}(\mathbf{q})$ are elements of $\mathrm{C}(\mathcal{Q}, \mathbb{R}^5)$. *Riemann invariants* are functions $\psi^{(k)} \in \mathrm{C}^1(\mathcal{Q}, \mathbb{R})$ satisfying

$$\nabla_5 \psi^{(k)}(\mathbf{q}) \cdot \mathbf{r_k}(\mathbf{q}) = 0 \qquad k = 1, 2, \ldots, 5 \tag{2.2.60}$$

for every $\mathbf{q} \in \mathcal{Q}$. For every $\mathbf{q} \in \mathcal{Q}$, the condition (2.2.60) can be satisfied by at most four functions ${\psi_1}^{(k)}(\mathbf{q}), \psi_2^{(k)}(\mathbf{q}), {\psi_3}^{(k)}(\mathbf{q}), \psi_4^{(k)}(\mathbf{q})$, gradients of which are linear independent for every $\mathbf{q} \in \mathcal{Q}$. Now it will be our aim to find them.

To search for the Riemann invariants means to solve a first order partial differential equation. In our case we succeed using the First Integral Method. Let us show the technique at the simplest eigenvector of $\mathbf{A}(\mathbf{q})$.

We are solving the equation

$$\nabla_5 \psi^{(2)}(\mathbf{q}) \cdot \mathbf{r_2}(\mathbf{q}) = 0 \qquad (k=2) \tag{2.2.61}$$

i.e.

$$\frac{\partial \psi^{(2)}}{\partial q_1}(\mathbf{q}) q_1 + \frac{\partial \psi^{(2)}}{\partial q_2}(\mathbf{q}) q_2 + \frac{\partial \psi^{(2)}}{\partial q_3}(\mathbf{q}) q_3 + \frac{\partial \psi^{(2)}}{\partial q_4}(\mathbf{q}) q_4 + \frac{\partial \psi^{(2)}}{\partial q_5}(\mathbf{q}) \frac{{q_2}^2 + {q_3}^2 + {q_4}^2}{2q_1} = 0. \tag{2.2.62}$$

We want to find a smooth function $\xi : \mathcal{Q} \times (0, \infty) \to \mathcal{Q}$ in order that

$$\frac{\partial \xi_1}{\partial t}(\mathbf{q}, t) = q_1, \quad \frac{\partial \xi_2}{\partial t}(\mathbf{q}, t) = q_2, \quad \frac{\partial \xi_3}{\partial t}(\mathbf{q}, t) = q_3, \quad \frac{\partial \xi_4}{\partial t}(\mathbf{q}, t) = q_4 \;\text{ and }\; \frac{\partial \xi_5}{\partial t}(\mathbf{q}, t) = \frac{{q_2}^2 + {q_3}^2 + {q_4}^2}{2q_1}.$$

The solution is

$$\begin{aligned} \xi_1(\mathbf{q}, t) &= q_1 t + \vartheta_1(\mathbf{q}) \\ \xi_2(\mathbf{q}, t) &= q_2 t + \vartheta_2(\mathbf{q}) \\ \xi_3(\mathbf{q}, t) &= q_3 t + \vartheta_3(\mathbf{q}) \\ \xi_4(\mathbf{q}, t) &= q_4 t + \vartheta_4(\mathbf{q}) \\ \xi_5(\mathbf{q}, t) &= \frac{{q_2}^2 + {q_3}^2 + {q_4}^2}{2q_1} t + \vartheta_5(\mathbf{q}), \end{aligned}$$

where $\vartheta \in \mathrm{C}^1(\mathcal{Q}, \mathbb{R})$ is an arbitrary function respecting the condition $\xi(\mathbf{q}, t) \in \mathcal{Q}$ for $(\mathbf{q}, t) \in \mathcal{Q} \times (0, \infty)$.
It is easy to show that any function $\varphi \in \mathrm{C}^1(\mathcal{Q}, \mathbb{R})$, which satisfies $\frac{\mathrm{d}}{\mathrm{d}t}(\varphi \circ \xi)(\mathbf{q}, t) = 0$, is a solution to (2.2.61):

$$\begin{aligned} 0 &= \frac{\mathrm{d}}{\mathrm{d}t}(\varphi \circ \xi)(\mathbf{q}, t) = \sum_{i=1}^{5} \frac{\partial \varphi}{\partial q_i}(\xi(\mathbf{q}, t)) \frac{\mathrm{d}\xi_i}{\mathrm{d}t}(\mathbf{q}, t) = \sum_{i=1}^{5} \frac{\partial \varphi}{\partial q_i}(\xi(\mathbf{q}, t)) \left(\frac{\partial \xi_i}{\partial \mathbf{q}}(\mathbf{q}, t) \frac{\mathrm{d}\mathbf{q}}{\mathrm{d}t} + \frac{\partial \xi_i}{\partial t}(\mathbf{q}, t) \right) = \\ &= \sum_{i=1}^{5} \frac{\partial \varphi}{\partial q_i}(\xi(\mathbf{q}, t)) \frac{\partial \xi_i}{\partial t}(\mathbf{q}, t) = \frac{\partial \varphi}{\partial q_1}(\xi(\mathbf{q}, t)) q_1 + \frac{\partial \varphi}{\partial q_2}(\xi(\mathbf{q}, t)) q_2 + \ldots + \frac{\partial \varphi}{\partial q_5}(\xi(\mathbf{q}, t)) \frac{{q_2}^2 + {q_3}^2 + {q_4}^2}{2q_1}. \end{aligned}$$

Now let us give some examples. Setting $\vartheta(\mathbf{q})$ to be identically zero, we have

$$\xi(\mathbf{q}, t) = t \left(q_1, \;\; q_2, \;\; q_3, \;\; q_4, \;\; \frac{{q_2}^2 + {q_3}^2 + {q_4}^2}{2} \right)^T.$$

Having chosen $\varphi(\mathbf{q}) = \frac{q_2}{q_1}$, we have $\varphi(\xi(\mathbf{q}, t)) = \frac{q_2}{q_1} = u$. Having chosen $\varphi(\mathbf{q}) = \frac{q_5}{q_1}$ we get $\varphi(\xi(\mathbf{q}, t)) = \frac{{q_2}^2 + {q_3}^2 + {q_4}^2}{2q_1^2} = \frac{1}{2}\mathbf{v}^2$ and so on.

Now let us present all obtained Riemann invariants. The reader can verify them and find the appropriated functions $\varphi(\mathbf{q})$ and $\vartheta(\mathbf{q})$.

1. eigenvalue $\lambda_1(\mathbf{q}) = u - c$

   eigenvector $\mathbf{r_1}(\mathbf{q}) = \left(1, u - c, v, w, \frac{\mathbf{v}^2}{2} + \frac{c^2}{\kappa - 1} - uc\right)^T$

   $\psi_1^{(1)}(\mathbf{q}) = v$

   $\psi_2^{(1)}(\mathbf{q}) = w$

   $\psi_3^{(1)}(\mathbf{q}) = p/\varrho^\kappa$

   $\psi_4^{(1)}(\mathbf{q}) = u + \frac{2c}{\kappa - 1}$

2. eigenvalue $\lambda_2(\mathbf{q}) = u$

   eigenvector $\mathbf{r_2}(\mathbf{q}) = \left(1, u, v, w, \frac{\mathbf{v}^2}{2}\right)^T$

   $\psi_1^{(2)}(\mathbf{q}) = p$

   $\psi_2^{(2)}(\mathbf{q}) = u$

   $\psi_3^{(2)}(\mathbf{q}) = v$

   $\psi_4^{(2)}(\mathbf{q}) = w$

3. eigenvalue $\lambda_3(\mathbf{q}) = u$

   eigenvector $\mathbf{r_3}(\mathbf{q}) = \left(1, u, v - c, w, \frac{\mathbf{v}^2}{2} - vc\right)^T$

   $\psi_1^{(3)}(\mathbf{q}) = p$

   $\psi_2^{(3)}(\mathbf{q}) = u$

   $\psi_3^{(3)}(\mathbf{q}) = v - 2c$

   $\psi_4^{(3)}(\mathbf{q}) = w$

4. eigenvalue $\lambda_4(\mathbf{q}) = u$

   eigenvector $\mathbf{r_4}(\mathbf{q}) = \left(1, u, v, w - c, \frac{\mathbf{v}^2}{2} - wc\right)^T$

   $\psi_1^{(4)}(\mathbf{q}) = p$

   $\psi_2^{(4)}(\mathbf{q}) = u$

   $\psi_3^{(4)}(\mathbf{q}) = v$

   $\psi_4^{(4)}(\mathbf{q}) = w - 2c$

5. eigenvalue $\lambda_5(\mathbf{q}) = u + c$

   eigenvector $\mathbf{r_5}(\mathbf{q}) = \left(1, u + c, v, w, \frac{\mathbf{v}^2}{2} + \frac{c^2}{\kappa - 1} + uc\right)^T$

   $\psi_1^{(5)}(\mathbf{q}) = v$

   $\psi_2^{(5)}(\mathbf{q}) = w$

   $\psi_3^{(5)}(\mathbf{q}) = p/\varrho^\kappa$

   $\psi_4^{(5)}(\mathbf{q}) = u - \frac{2c}{\kappa - 1}$

You can easily make sure that the corresponding gradients are linear independent for all $\mathbf{q} \in \mathcal{Q}$.

2.2.8 Integration of the matrix A eigenvectors

A very useful property of the Riemann invariants is that they stay constant along every smooth curve in $\mathcal{Q}$, to which the corresponding eigenvector of $\mathbf{A}(\mathbf{q})$ is tangential at every its point.

Theorem 2.2.5
Let $\tilde{\mathbf{q}} = \tilde{\mathbf{q}}(\xi)$, $\xi \in \langle a, b\rangle$, where $a, b \in \mathbb{R}$ and $a < b$, be a smooth curve in $\mathcal{Q}$ such that

$$\frac{\mathrm{d}\tilde{\mathbf{q}}}{\mathrm{d}\xi}(\xi) = \mathbf{r_k}(\tilde{\mathbf{q}}(\xi)) \tag{2.2.63}$$

for all $\xi \in (a, b)$ where $\mathbf{r_k}(\mathbf{q})$ is one of the matrix $\mathbf{A}(\mathbf{q})$ eigenvectors, $k \in \{1, 2, \ldots, 5\}$. Then any of the Riemann invariants $\psi^{(k)}$ is constant along this curve, i.e.

$$\psi^{(k)}(\tilde{\mathbf{q}}(\xi)) = \psi^{(k)}(\tilde{\mathbf{q}}(a)) \tag{2.2.64}$$

for all $\xi \in \langle a, b\rangle$.

Proof: It is very easy to see that

$$\frac{\mathrm{d}}{\mathrm{d}\xi}(\tilde{\mathbf{q}}(\xi)) = \nabla_5 \psi^{(k)}(\tilde{\mathbf{q}}(\xi)) \cdot \frac{\mathrm{d}\tilde{\mathbf{q}}}{\mathrm{d}\xi}(\xi) = \nabla_5 \psi^{(k)}(\tilde{\mathbf{q}}(\xi)) \cdot \mathbf{r_k}(\tilde{\mathbf{q}}(\xi)) = 0.$$

Remark 2.2.6
These curves are very important because informations about physical quantities in the form of the Riemann invariants propagate along them into the domain. We will see later that direction of the propagation depends on the sign of the corresponding matrix $\mathbf{A}$ eigenvalue. At this moment we will not dwell on this interesting subject – we will wait until the section where the boundary conditions are treated.

Our recently found Riemann invariants and the matrix $\mathbf{A}$ eigenvectors are so simple that we are able to express the above curves explicitly.

Let $\mathbf{p} \in \mathcal{Q}$. We prove the existence of such unique curves $\mathbf{q}^{(1)}, \mathbf{q}^{(2)}, \ldots, \mathbf{q}^{(5)} \in \mathrm{C}^\infty(\mathbb{R}^+, \mathcal{Q})$ that

$$\frac{\mathrm{d}\mathbf{q}^{(k)}}{\mathrm{d}\xi}(\xi) = \mathbf{r_k}(\mathbf{q}^{(k)}(\xi)) \qquad \xi \in \mathbb{R}^+ \tag{2.2.65}$$

$$\mathbf{q}^{(k)}(p_1) = \mathbf{p}, \tag{2.2.66}$$

where $k = 1, 2, \ldots, 5$. Let us consider the simplest case again, i.e. the eigenvector $\mathbf{r_2}(\mathbf{q}) = \left(1, u, v, w, \frac{\mathbf{v}^2}{2}\right)^T$. Equation (2.2.65) gives the following system of five partial differential equations

$$\frac{\mathrm{d}q_1^{(k)}}{\mathrm{d}\xi}(\xi) = 1, \quad \frac{\mathrm{d}q_2^{(k)}}{\mathrm{d}\xi}(\xi) = \frac{q_2^{(k)}(\xi)}{q_1^{(k)}(\xi)}, \quad \frac{\mathrm{d}q_3^{(k)}}{\mathrm{d}\xi}(\xi) = \frac{q_3^{(k)}(\xi)}{q_2^{(k)}(\xi)}, \quad \frac{\mathrm{d}q_4^{(k)}}{\mathrm{d}\xi}(\xi) = \frac{q_4^{(k)}(\xi)}{q_3^{(k)}(\xi)} \quad \text{and}$$

$$\frac{\mathrm{d}q_5^{(k)}}{\mathrm{d}\xi}(\xi) = \frac{\left(q_2^{(k)}(\xi)\right)^2 + \left(q_3^{(k)}(\xi)\right)^2 + \left(q_4^{(k)}(\xi)\right)^2}{2q_1^{(k)}(\xi)}.$$

Its solution is

$$\mathbf{q}^{(2)}(\xi) = \left(\xi + C_1,\ \ C_2(\xi + C_1),\ \ C_3(\xi + C_1),\ \ C_4(\xi + C_1),\ \ C_5 + \xi\frac{C_2^2 + C_3^2 + C_4^2}{2}\right)^T.$$

According to (2.2.66) we find that

$$C_1 = 0,\ \ C_2 = \psi_2^{(2)}(\mathbf{p}),\ \ C_3 = \psi_3^{(2)}(\mathbf{p}),\ \ C_4 = \psi_4^{(2)}(\mathbf{p})\ \text{ and }\ C_5 = \frac{\psi_1^{(2)}(\mathbf{p})}{\kappa - 1}.$$

When we try to construct a similar system to another eigenvector, we see that it is too complicated. Therefore we must take use of having no necessity to know the general solution.

Let us present this technique at the case of the eigenvector $\mathbf{r_5}(\mathbf{q}) = \left(1, u + c, v, w, \frac{\mathbf{v}^2}{2} + \frac{c^2}{\kappa-1} + uc\right)^T$.

We denote $s_1^{(5)} = \psi_1^{(5)}(\mathbf{p}),\ \ s_2^{(5)} = \psi_2^{(5)}(\mathbf{p}), \ldots,\ \ s_5^{(5)} = \psi_5^{(5)}(\mathbf{p})$.

It holds $\frac{\mathrm{d}q_1^{(5)}}{\mathrm{d}\xi}(\xi) = 1$ and according to (2.2.66) we obtain $q_1^{(5)}(\xi) = \xi$.

The corresponding Riemann invariant must stay constant along it, i.e.

$$\begin{aligned} s_3^{(5)} &= \psi_3^{(5)}(\mathbf{q}^{(5)}(\xi)),\ \ \psi_3^{(5)} = \frac{p}{\varrho^\kappa}\ \text{ and }\ c(\mathbf{q}^{(5)}(\xi)) = \sqrt{\kappa s_3^{(5)}}\,\varrho(\mathbf{q}^{(5)}(\xi))^{\frac{\kappa-1}{2}} \\ u(\mathbf{q}^{(5)}(\xi)) &= s_4^{(5)} + \frac{2}{\kappa - 1}c(\mathbf{q}^{(5)}(\xi)) = s_4^{(5)} + \frac{2}{\kappa - 1}\sqrt{\kappa s_3^{(5)}}\,\varrho(\mathbf{q}^{(5)}(\xi))^{\frac{\kappa-1}{2}}. \end{aligned}$$

Using correspondence between physical and conservation variables we obtain

$$\begin{aligned} q_2^{(5)}(\xi) &= \xi u(\mathbf{q}^{(5)}(\xi)) = \xi s_4^{(5)} + \frac{2}{\kappa - 1}\sqrt{\kappa s_3^{(5)}}\,\xi^{\frac{\kappa+1}{2}} \\ q_3^{(5)}(\xi) &= \xi v(\mathbf{q}^{(5)}(\xi)) = \xi s_1^{(5)} \\ q_4^{(5)}(\xi) &= \xi w(\mathbf{q}^{(5)}(\xi)) = \xi s_2^{(5)}. \end{aligned}$$

For the last component it holds

$$q_5^{(5)}(\xi) = E(\mathbf{q}^{(5)}(\xi)) = \frac{p(\mathbf{q}^{(5)}(\xi))}{\kappa - 1} + \varrho(\mathbf{q}^{(5)}(\xi))\frac{u(\mathbf{q}^{(5)}(\xi))^2 + v(\mathbf{q}^{(5)}(\xi))^2 + w(\mathbf{q}^{(5)}(\xi))^2}{2} =$$

$$\frac{s_3^{(5)}\varrho(\mathbf{q}^{(5)}(\xi))^\kappa}{\kappa - 1} + \frac{2s_3^{(5)}\varrho(\mathbf{q}^{(5)}(\xi))^\kappa}{(\kappa - 1)^2} + \xi\frac{\left(s_4^{(5)}\right)^2 + \left(s_1^{(5)}\right)^2 + \left(s_2^{(5)}\right)^2}{2} + \frac{2}{\kappa - 1}s_4^{(5)}\sqrt{\kappa s_3^{(5)}}\,\varrho(\mathbf{q}^{(5)}(\xi))^{\frac{\kappa+1}{2}}$$

and finally

$$q_5^{(5)}(\xi) = \frac{3\kappa-1}{(\kappa-1)^2} s_3^{(5)} \xi^{\kappa} + \frac{2}{\kappa-1} s_4^{(5)} \sqrt{\kappa s_3^{(5)}}\, \xi^{\frac{\kappa+1}{2}} + \xi \frac{\left(s_4^{(5)}\right)^2 + \left(s_1^{(5)}\right)^2 + \left(s_2^{(5)}\right)^2}{2}.$$

In the remaining cases we proceed in the same way. Let us now present all obtained curves in their explicit form:

Curve corresponding to $\mathbf{r_1}(\mathbf{q}) = \left(1, u-c, v, w, \frac{\mathbf{v}^2}{2} + \frac{c^2}{\kappa-1} - uc\right)^T$:

$$\begin{aligned}
q_1^{(1)}(\xi) &= \xi \\
q_2^{(1)}(\xi) &= \xi s_4^{(1)} - \frac{2}{\kappa-1}\sqrt{\kappa s_3^{(1)}}\, \xi^{\frac{\kappa+1}{2}} \\
q_3^{(1)}(\xi) &= \xi s_1^{(1)} \\
q_4^{(1)}(\xi) &= \xi s_2^{(1)} \\
q_5^{(1)}(\xi) &= \frac{3\kappa-1}{(\kappa-1)^2} s_3^{(1)} \xi^{\kappa} - \frac{2}{\kappa-1} s_4^{(1)} \sqrt{\kappa s_3^{(1)}}\, \xi^{\frac{\kappa+1}{2}} + \xi \frac{\left(s_4^{(1)}\right)^2 + \left(s_1^{(1)}\right)^2 + \left(s_2^{(1)}\right)^2}{2}.
\end{aligned}$$

Curve corresponding to $\mathbf{r_2}(\mathbf{q}) = \left(1, u, v, w, \frac{\mathbf{v}^2}{2}\right)^T$:

$$\begin{aligned}
q_1^{(2)}(\xi) &= \xi \\
q_2^{(2)}(\xi) &= \xi s_2^{(2)} \\
q_3^{(2)}(\xi) &= \xi s_3^{(2)} \\
q_4^{(2)}(\xi) &= \xi s_4^{(2)} \\
q_5^{(2)}(\xi) &= \frac{s_1^{(2)}}{\kappa-1} + \xi \frac{\left(s_2^{(2)}\right)^2 + \left(s_3^{(2)}\right)^2 + \left(s_4^{(2)}\right)^2}{2}.
\end{aligned}$$

Curve corresponding to $\mathbf{r_3}(\mathbf{q}) = \left(1, u, v-c, w, \frac{\mathbf{v}^2}{2} - vc\right)^T$:

$$\begin{aligned}
q_1^{(3)}(\xi) &= \xi \\
q_2^{(3)}(\xi) &= \xi s_2^{(3)} \\
q_3^{(3)}(\xi) &= \xi s_3^{(3)} + 2\sqrt{\kappa s_1^{(3)}}\, \xi^{\frac{1}{2}} \\
q_4^{(3)}(\xi) &= \xi s_4^{(3)} \\
q_5^{(3)}(\xi) &= \frac{2\kappa^2-2\kappa+1}{\kappa-1} s_1^{(3)} + 2 s_3^{(3)} \sqrt{\kappa s_1^{(3)}}\, \xi^{\frac{1}{2}} + \xi \frac{\left(s_2^{(3)}\right)^2 + \left(s_3^{(3)}\right)^2 + \left(s_4^{(3)}\right)^2}{2}.
\end{aligned}$$

Curve corresponding to $\mathbf{r_4}(\mathbf{q}) = \left(1, u, v, w - c, \frac{\mathbf{v}^2}{2} - wc\right)^T$:

$$q_1^{(4)}(\xi) = \xi$$

$$q_2^{(4)}(\xi) = \xi s_2^{(4)}$$

$$q_3^{(4)}(\xi) = \xi s_3^{(4)}$$

$$q_4^{(4)}(\xi) = \xi s_4^{(4)} + 2\sqrt{\kappa s_1^{(4)}}\xi^{\frac{1}{2}}$$

$$q_5^{(4)}(\xi) = \frac{2\kappa^2 - 2\kappa + 1}{\kappa - 1} s_1^{(4)} + 2s_4^{(4)}\sqrt{\kappa s_1^{(4)}}\xi^{\frac{1}{2}} + \xi\frac{\left(s_2^{(4)}\right)^2 + \left(s_3^{(4)}\right)^2 + \left(s_4^{(4)}\right)^2}{2}.$$

Curve corresponding to $\mathbf{r_5}(\mathbf{q}) = \left(1, u + c, v, w, \frac{\mathbf{v}^2}{2} + \frac{c^2}{\kappa - 1} + uc\right)^T$:

$$q_1^{(5)}(\xi) = \xi$$

$$q_2^{(5)}(\xi) = \xi s_4^{(5)} + \frac{2}{\kappa - 1}\sqrt{\kappa s_3^{(5)}}\xi^{\frac{\kappa+1}{2}}$$

$$q_3^{(5)}(\xi) = \xi s_1^{(5)}$$

$$q_4^{(5)}(\xi) = \xi s_2^{(5)}$$

$$q_5^{(5)}(\xi) = \frac{3\kappa - 1}{(\kappa - 1)^2} s_3^{(5)}\xi^{\kappa} + \frac{2}{\kappa - 1} s_4^{(5)}\sqrt{\kappa s_3^{(5)}}\xi^{\frac{\kappa+1}{2}} + \xi\frac{\left(s_4^{(5)}\right)^2 + \left(s_1^{(5)}\right)^2 + \left(s_2^{(5)}\right)^2}{2},$$

where $s_i^{(k)} = \psi_i^{(k)}(\mathbf{p})$ for $i = 1, 2, \ldots, 4$ and $k = 1, 2, \ldots, 5$. These curves are infinitely smooth in $\mathbb{R}^+$, for parameters from $\mathbb{R}^+$ they lie in the admissible state set and they are determined by (2.2.66).

Remark 2.2.7
For future explanation we need to know how the matrix $\mathbf{A}(\mathbf{q})$ eigenvalues behave along the above computed curves. In a similar way as before we obtain

$$\lambda_1(\mathbf{q}^{(1)}(\xi)) = u(\mathbf{q}^{(1)}(\xi)) - c(\mathbf{q}^{(1)}(\xi)) = s_4^{(1)} - \frac{\kappa + 1}{\kappa - 1}\sqrt{\kappa s_3^{(1)}}\xi^{\frac{\kappa-1}{2}}$$

$$\lambda_2(\mathbf{q}^{(2)}(\xi) = s_2^{(2)}$$

$$\lambda_3(\mathbf{q}^{(3)}(\xi) = s_2^{(3)}$$

$$\lambda_4(\mathbf{q}^{(4)}(\xi) = s_2^{(4)}$$

$$\lambda_1(\mathbf{q}^{(1)}(\xi)) = u(\mathbf{q}^{(1)}(\xi)) + c(\mathbf{q}^{(1)}(\xi)) = s_4^{(5)} + \frac{\kappa + 1}{\kappa - 1}\sqrt{\kappa s_3^{(5)}}\xi^{\frac{\kappa-1}{2}}.$$

We see that only $\lambda_1(\mathbf{q})$ and $\lambda_5(\mathbf{q})$ can change their sign along the corresponding curves.

Theorem 2.2.8
Let $\mathbf{p_1}$ and $\mathbf{p_2}$ be two different points in $\mathcal{Q}$. Let $\psi_i^{(k)}(\mathbf{p_1}) = \psi_i^{(k)}(\mathbf{p_2})$ where $i = 1, 2, \ldots, 4$ and $k \in \{1, 2, \ldots, 5\}$. Then they are connected by a curve $\mathbf{q}^{(k)}$.

Proof: Let us fix a $\xi_0 \in \mathbb{R}^+$ and let us suppose that $\mathbf{p_1}$ and $\mathbf{p_2}$ lie on different curves. The explicit form of the curves allows us to see that they cut each other with the parameter value ξ_0. But we know they are unique. Hence, $\mathbf{p_1}$ and $\mathbf{p_2}$ are connected by a curve $\mathbf{q}^{(k)}$ which contains the point $\mathbf{q}^{(k)}(\xi_0)$.

Remark 2.2.9
When we know these four invariants, we have a curve in the admissible state set $\mathcal{Q}$. Additional knowledge of the density gives us a unique point. You notice that here the $\mathbf{r_1}(\mathbf{q}), \mathbf{z_1}(\mathbf{q}), \mathbf{z_2}(\mathbf{q}), \mathbf{z_3}(\mathbf{q}), \mathbf{r_5}(\mathbf{q})$ eigenvector basis of the matrix $\mathbf{A}(\mathbf{q})$ from subsection **2.2.3** fails.

2.2.9 Optimal path in the admissible state set

Let $\mathbf{q_L}$, $\mathbf{q_R}$ be two different states in $\mathcal{Q}$. Our aim is to find a continuous path from $\mathbf{q_L}$ to $\mathbf{q_R}$ in $\mathcal{Q}$ the parts of which are parts of geometrical images of the curves $\mathbf{q}^{(1)}, \ldots, \mathbf{q}^{(5)}$.

We are looking for four states $\mathbf{q_A}, \mathbf{q_B}, \mathbf{q_C}$ and $\mathbf{q_D}$ in $\mathcal{Q}$ so that

$$\mathbf{q}^{(1)}(\varrho_L) = \mathbf{q_L}, \;\; \mathbf{q}^{(1)}(\varrho_A) = \mathbf{q}^{(2)}(\varrho_A) = \mathbf{q_A}, \;\; \mathbf{q}^{(2)}(\varrho_B) = \mathbf{q}^{(3)}(\varrho_B) = \mathbf{q_B}, \;\; \ldots, \;\; \mathbf{q}^{(5)}(\varrho_R) = \mathbf{q_R},$$

where ϱ_L is the density corresponding to the state $\mathbf{q_L}$ etc. The situation is shown in Fig.2.2.10 (here $\tilde{\mathbf{q}}^{(k)}$ means the geometrical image of $\mathbf{q}^{(k)}$ $k = 1, \ldots, 5$).

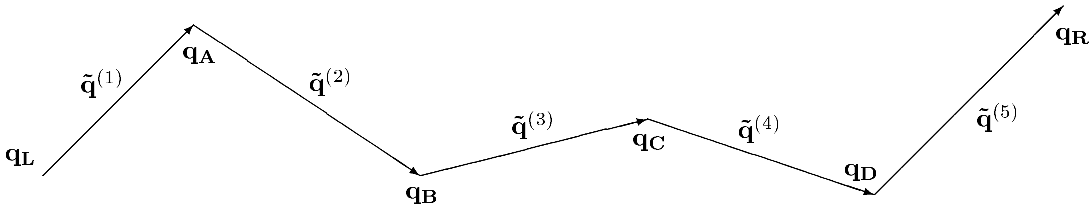

Fig.2.2.10

We have five curves and for each one of them we know four Riemann invariants. Hence, we can write down the following twenty equations:

$$\begin{array}{rclc}
\psi_i^{(1)}(\mathbf{q_L}) & = & \psi_i^{(1)}(\mathbf{q_A}) & i = 1, \ldots, 4 \\
\psi_i^{(2)}(\mathbf{q_A}) & = & \psi_i^{(2)}(\mathbf{q_B}) & i = 1, \ldots, 4 \\
\psi_i^{(3)}(\mathbf{q_B}) & = & \psi_i^{(3)}(\mathbf{q_C}) & i = 1, \ldots, 4 \\
\psi_i^{(4)}(\mathbf{q_C}) & = & \psi_i^{(4)}(\mathbf{q_D}) & i = 1, \ldots, 4 \\
\psi_i^{(5)}(\mathbf{q_D}) & = & \psi_i^{(5)}(\mathbf{q_R}) & i = 1, \ldots, 4
\end{array}$$

i.e.

$$
\begin{array}{llcl}
(a) & v_L & = & v_A \\
(b) & w_L & = & w_A \\
(c) & p_L/\varrho_L^\kappa & = & p_A/\varrho_A^\kappa \\
(d) & u_L + 2c_L/(\kappa-1) & = & u_A + 2c_A/(\kappa-1) \\
(e) & p_A & = & p_B \\
(f) & u_A & = & u_B \\
(g) & v_A & = & v_B \\
(h) & w_A & = & w_B \\
(i) & p_B & = & p_C \\
(j) & u_B & = & u_C \\
(k) & v_B - 2c_B & = & v_C - 2c_C \\
(l) & w_B & = & w_C \\
(m) & p_C & = & p_D \\
(n) & u_C & = & u_D \\
(o) & v_C & = & v_D \\
(p) & w_C - 2c_C & = & w_D - 2c_D \\
(q) & v_D & = & v_R \\
(r) & w_D & = & w_R \\
(s) & p_D/\varrho_D^\kappa & = & p_R/\varrho_R^\kappa \\
(t) & u_D - 2c_D/(\kappa-1) & = & u_R - 2c_R/(\kappa-1)
\end{array}
$$

By the remark 2.2.9, the solution to this system (the intersection states $\mathbf{q_A}, \ldots, \mathbf{q_D}$) is unique. Curves $\mathbf{q}^{(1)}, \ldots, \mathbf{q}^{(5)}$ need not to be ordered this way, but any permutation leads to much more complicated relations.

Let us denote

$$s = p/\varrho^\kappa, \quad \alpha = \left(\frac{s_R}{s_L}\right)^{\frac{1}{2\kappa}}, \quad z_L = \frac{\kappa-1}{2}u_L + c_L \quad \text{and} \quad z_R = \frac{\kappa-1}{2}u_R - c_R.$$

According to $(e)(i)(m)$

$$\frac{c_D^2}{c_A^2} = \frac{p_D}{p_A}\frac{\varrho_A}{\varrho_D} = \frac{\varrho_A}{\varrho_D}.$$

Equation (c) yields

$$\frac{c_L^2}{c_A^2} = \frac{p_L}{p_A}\frac{\varrho_A}{\varrho_L} = \frac{s_L}{s_A}\left(\frac{\varrho_L}{\varrho_A}\right)^{\kappa-1} = \left(\frac{\varrho_L}{\varrho_A}\right)^{\kappa-1}.$$

From $(c)(e)(i)(m)(s)$ it follows

$$s_L\varrho_A^\kappa = p_A = p_D = s_R\varrho_D^\kappa,$$

hence

$$\frac{\varrho_A}{\varrho_D} = \left(\frac{s_R}{s_L}\right)^{\frac{1}{\kappa}} = \alpha^2 \quad \text{and} \quad \frac{c_D}{c_A} = \left(\frac{s_R}{s_L}\right)^{\frac{1}{2\kappa}} = \alpha.$$

We can rewrite equations (d) and (t) as

$$z_L = u_A\frac{\kappa-1}{2} + c_A \quad \text{and} \quad z_R = u_D\frac{\kappa-1}{2} - c_D.$$

According to $(f)(j)(n)$

$$z_L - z_R = c_A + c_D = c_A + \alpha c_A = (1+\alpha)c_A,$$

hence

(2.2.67) $$c_A = \frac{z_L - z_R}{1+\alpha}, \quad c_D = \alpha c_A, \quad \varrho_A = \varrho_L\left(\frac{c_A}{c_L}\right)^{\frac{2}{\kappa-1}} \quad \text{and} \quad \varrho_D = \frac{\varrho_A}{\alpha^2}.$$

From (d) it follows

$$u_A = \frac{2}{\kappa-1}(z_L - c_A)$$

and according to $(f)(j)(n)(a)(q)(b)(r)$ we obtain

$$u_D = u_A, \quad v_A = v_L, \quad v_D = v_R, \quad w_A = w_L \quad \text{and} \quad w_D = w_R.$$

Further, it remains to specify the states $\mathbf{q_B}$ and $\mathbf{q_C}$:
According to $(f)(g)(h)$

$$u_B = u_A, \quad v_B = v_L \quad \text{and} \quad w_B = w_L.$$

Equations $(n)(o)(l)(h)$ yield

$$u_C = u_D, \quad v_C = v_R \quad \text{and} \quad w_C = w_L.$$

From (p) it follows

(2.2.68) $$w_L - 2c_C = w_R - 2c_D \quad \text{i.e.} \quad c_C = c_D + \frac{w_L - w_R}{2}.$$

According to (k)

$$v_L - 2c_B = v_R - 2c_C = v_R - w_L + w_R - 2c_D$$

and therefore

(2.2.69) $$c_B = \frac{v_L - v_R}{2} + \frac{w_L - w_R}{2} + c_D.$$

From (e) it follows

(2.2.70) $$\varrho_A c_A^2 = \varrho_B c_B^2 \quad \text{i.e.} \quad \varrho_B = \left(\frac{c_A}{c_B}\right)^2 \varrho_A.$$

Analogously, the equation (m) gives

(2.2.71) $$\varrho_D c_D^2 = \varrho_C c_C^2 \quad \text{and} \quad \varrho_C = \left(\frac{c_D}{c_C}\right)^2 \varrho_D.$$

In the end it remains to make sure that the computed states lie in $\mathcal{Q}$. Before we do this, let us make an important remark.

Remark 2.2.11
As we mentioned in the remark 2.2.7, eigenvalues $\lambda_1(\mathbf{q}^{(1)}(\xi))$ and $\lambda_5(\mathbf{q}^{(5)}(\xi))$ can change their signs. Here the value $|u|$ is equal to the speed of sound. Therefore we call them *sonic points*.

a) Along the curve $\mathbf{q}^{(1)}(\xi)$:

$$u_L^s = c_L^s \quad \text{and} \quad \psi_i^{(1)}(\mathbf{q_L}) = \psi_i^{(1)}(\mathbf{q_L^s}) \quad i = 1, \ldots, 4,$$

hence

$$\begin{array}{rcl} u_L + 2c_L/(\kappa - 1) & = & u_L^s + 2c_L^s/(\kappa - 1) \\ z_L & = & \frac{\kappa+1}{2} c_L^s \\ c_L^s & = & 2z_L/(\kappa + 1) \end{array}.$$

Further

$$v_L^s = v_L, \quad w_L^s = w_L \quad \text{and} \quad \frac{p_L}{\varrho_L^\kappa} = \frac{p_L^s}{(\varrho_L^s)^\kappa}$$

and consequently

$$\varrho_L^s = \varrho_L \left(\frac{c_L^s}{c_L} \right)^{\frac{2}{\kappa - 1}}.$$

b) Along the curve $\mathbf{q}^{(5)}(\xi)$:

$$u_R^s = -c_R^s \quad \text{and} \quad \psi_i^{(5)}(\mathbf{q_5}) = \psi_i^{(5)}(\mathbf{q_5^s}) \quad i = 1, \ldots, 4.$$

Analogously as in the previous case

$$\begin{array}{rcl} u_R - 2c_R/(\kappa - 1) & = & u_R^s - 2c_R^s/(\kappa - 1) \\ z_R & = & -\frac{\kappa+1}{2} c_R^s \\ c_R^s & = & -2z_R/(\kappa + 1) \end{array}.$$

Further

$$v_R^s = v_R, \quad w_R^s = w_R \quad \text{and} \quad \frac{p_R}{\varrho_R^\kappa} = \frac{p_R^s}{(\varrho_R^s)^\kappa}.$$

Finally

$$\varrho_R^s = \varrho_R \left(\frac{c_R^s}{c_R} \right)^{\frac{2}{\kappa - 1}}.$$

The state $\mathbf{q}$ is admissible if and only if $\varrho > 0$ and $p > 0$. The speed of sound is defined as a positive quantity. From the condition $c_A > 0$ we obtain

$$\frac{\kappa-1}{2}(u_L-u_R)+c_L+c_R>0. \tag{2.2.72}$$

In case this condition holds true, by (2.2.67) we have $\varrho_A>0$ and $\varrho_D>0$. From the condition $c_C>0$ and (2.2.68) it follows

$$\frac{\alpha}{\alpha+1}\left(\frac{\kappa-1}{2}(u_L-u_R)+c_L+c_R\right)+\frac{w_L-w_R}{2}>0. \tag{2.2.73}$$

The relation (2.2.71) yields $\varrho_C>0$. According to $c_B>0$ and (2.2.69) we also have

$$\frac{\alpha}{\alpha+1}\left(\frac{\kappa-1}{2}(u_L-u_R)+c_L+c_R\right)+\frac{v_L-v_R}{2}+\frac{w_L-w_R}{2}>0. \tag{2.2.74}$$

In case this condition is satisfied, by (2.2.70) also $\varrho_B>0$.

By the previous explanation, $\mathbf{q_L}$ and $\mathbf{q_A}$ being admissible implies $\mathbf{q_L^s}$ being also an admissible state. Analogously, the state $\mathbf{q_L^s}$ is admissible. In case the flow in the domain Ω contains no shocks, we immediately see that we can construct such a fine mesh that conditions (2.2.72), (2.2.73) and (2.2.74) are satisfied. For a flow containing shock waves this particular problem remains still open.

2.3 Riemann problem

In this paragraph we will deal with the one-dimensional Riemann problem. Its approximate solution is an essential part of almost all numerical schemes for the solution of the Euler equations. It will also play an important role in our case.

Definition 2.3.1
Let n be a natural number, $\mathbf{f}\in C^1(\mathbb{R}^n)$. We call *Riemann problem* the problem given by a general hyperbolic system

$$\frac{\partial}{\partial t}\mathbf{q}(x,t)+\frac{\partial}{\partial x}\mathbf{f}(\mathbf{q}(\mathbf{x},\mathbf{t}))=0 \tag{2.3.75}$$

for almost all $(x,t)\in\mathbb{R}\times\mathbb{R}^+$ with the initial condition

$$\mathbf{q}(x,0)=\left\{\begin{array}{ll}\mathbf{q}_L: & x<0\\ \\ \mathbf{q}_R: & x>0\end{array}\right\}, \tag{2.3.76}$$

where $\mathbf{q}_L$, $\mathbf{q}_R$ are arbitrary constants and $\mathbf{q}(x,t)\in\mathbb{R}^n$ for $(x,t)\in\mathbb{R}\times\mathbb{R}^+$.

Remark 2.3.2
System (2.3.75) is hyperbolic if to the matrix

$$\mathbf{A}(\mathbf{q})=\frac{\mathbf{Df}}{\mathbf{Dq}}(\mathbf{q})$$

another real diagonal matrix $\mathbf{D}(\mathbf{q}) = \mathrm{diag}(\lambda_1(\mathbf{q}), \lambda_2(\mathbf{q}), \ldots, \lambda_n(\mathbf{q}))$ and a regular matrix $\mathbf{R}(\mathbf{q})$ exist such that

$$\mathbf{A}(\mathbf{q})\mathbf{R}(\mathbf{q}) = \mathbf{R}(\mathbf{q})\mathbf{D}(\mathbf{q}) \qquad \text{for all } \mathbf{q} \in \mathbb{R}^n. \tag{2.3.77}$$

Columns of $\mathbf{R}(\mathbf{q})$ are the matrix $\mathbf{A}(\mathbf{q})$ eigenvectors and the diagonal elements of the matrix $\mathbf{D}(\mathbf{q})$ are the corresponding eigenvalues. We consider the eigenvalues ordered in the same way as in subsection **2.2.2**, i.e. $\lambda_1(\mathbf{q}) \leq \lambda_2(\mathbf{q}) \leq \ldots \leq \lambda_n(\mathbf{q})$.

Theorem 2.3.3
In case there is a unique solution to the Riemann problem (2.3.75) (2.3.76), it can be written in the form $\mathbf{q}(x,t) = \hat{q}(x/t)$.

Proof: For any $\alpha \in \mathbb{R}^+$ we set $\mathbf{q}_\alpha(x,t) = \mathbf{q}(\alpha x, \alpha t)$, where $\mathbf{q} = \mathbf{q}(x,t)$ is a solution to the Riemann problem (2.3.75) (2.3.76). The function $\mathbf{q}_\alpha(x,t)$ is also a solution, therefore $\mathbf{q}(x,t) = \mathbf{q}_\alpha(x,t) = \mathbf{q}(\alpha x, \alpha t)$ for all $\alpha \in \mathbb{R}^+$ and $(x,t) \in \mathbb{R} \times \mathbb{R}^+$. Let $t \in \mathbb{R}^+$, then for $\alpha = 1/t$ is $\mathbf{q}(x,t) = \mathbf{q}(x/t, 1)$ for all $x \in \mathbb{R}$. Hence, we can set $\hat{\mathbf{q}}(\xi) = \mathbf{q}(\xi, 1)$.

Lemma 2.3.4:
For $n = 1$ let us consider the Riemann problem (2.3.75) (2.3.76) with the flux $\mathbf{f}(\mathbf{q}) = a\mathbf{q}$, $a \in \mathbb{R}$. Then there exists its unique solution in the form

$$\mathbf{q}(x,t) = \mathbf{q}_L(1 - H(x - at)) + \mathbf{q}_R H(x - at). \tag{2.3.78}$$

The function $H : \mathbb{R} \to \mathbb{R}$ is defined by the relation

$$H(x) = \left\{ \begin{array}{ll} 0: & x < 0 \\ \\ 1: & x \geq 0 \end{array} \right\}$$

and it is called *Heavysider shock function*.

Proof: The equation has the form

$$\frac{\partial}{\partial t}\mathbf{q}(x,t) + a\frac{\partial}{\partial x}\mathbf{q}(x,t) = 0$$

and its solution is constant along the characteristics $x(t) = at + c$, where $t > 0$ and $c \in \mathbb{R}$. For $(x,t) \in \mathbb{R} \times \mathbb{R}^+$ it is

$$\mathbf{q}(x,t) = \mathbf{q}(x - at, 0) = \left\{ \begin{array}{ll} \mathbf{q}_L: & x - at < 0 \\ \\ \mathbf{q}_R: & x - at \geq 0 \end{array} \right\}.$$

Lemma 2.3.5:
Let us consider the Riemann problem (2.3.75) (2.3.76) with the flux $\mathbf{f}(\mathbf{q}) = \mathbf{A}\mathbf{q}$, where $\mathbf{A}$ is

a constant diagonalizable real matrix of the form $n \times n$, Let $\mathbf{r}_1, \mathbf{r}_2, \ldots, \mathbf{r}_n$ be its eigenvectors and $\lambda_1 \leq \lambda_2 \leq \ldots \leq \lambda_n$ the corresponding eigenvalues. Vectors $\mathbf{q}_L, \mathbf{q}_R$ can be expressed as

$$\mathbf{q}_L = \sum_{i=1}^{n} \alpha_i \mathbf{r}_i, \qquad \mathbf{q}_R = \sum_{i=1}^{n} \beta_i \mathbf{r}_i \tag{2.3.79}$$

and there is a unique solution to the Riemann problem in the form

$$\mathbf{q}(x,t) = \sum_{i=1}^{n} \left(\alpha_i(1 - H(x - \lambda_i t)) + \beta_i H(x - \lambda_i t)\right) \mathbf{r}_i. \tag{2.3.80}$$

Proof: The system (2.3.75) is hyperbolic and its linear independent eigenvectors $\mathbf{r}_1, \mathbf{r}_2, \ldots, \mathbf{r}_n$ generate $\mathbb{R}^n$. Vectors $\mathbf{q}_L, \mathbf{q}_R$ can be written as a linear combination

$$\mathbf{q}(x,t) = \sum_{i=1}^{n} \xi_i(x,t) \mathbf{r}_i, \tag{2.3.81}$$

where $\xi_i : \mathbb{R} \times \mathbb{R}^+ \to \mathbb{R}$, $i = 1, 2, \ldots, n$. According to (2.3.75) we obtain

$$\sum_{i=1}^{n} \left[\frac{\partial \xi_i}{\partial t}(x,t) + \lambda_i \frac{\partial \xi_i}{\partial x}(x,t) \right] \mathbf{r}_i = 0. \tag{2.3.82}$$

Linear independence of $\mathbf{r}_1, \mathbf{r}_2, \ldots, \mathbf{r}_n$ implies

$$\frac{\partial \xi_i}{\partial t}(x,t) + \lambda_i \frac{\partial \xi_i}{\partial x}(x,t) = 0$$

$$\xi_i(x,0) = \left\{ \begin{array}{ll} \alpha_i : & x < 0 \\ \beta_i : & x \geq 0 \end{array} \right\}$$

for $i = 1, 2, \ldots, n$. Lemma 2.3.4 implies that

$$\xi_i(x,t) = \alpha_i(1 - H(x - \lambda_i t)) + \beta_i H(x - \lambda_i t) \qquad i = 1, 2, \ldots, n \tag{2.3.83}$$

is a unique solution to this problem. Putting (2.3.83) into (2.3.81) we obtain (2.3.80).

In the following paragraph we will need to know the value of $\mathbf{f}(\mathbf{q}_R(0))$, where $\mathbf{q}_R(x/t)$ is the solution to the Riemann problem (2.3.75) (2.3.76). Since we are not able to solve a general hyperbolic system, we must try to find a good approximation $\mathbf{f}_R(\mathbf{q}_L, \mathbf{q}_R)$ of the value $\mathbf{f}(\mathbf{q}_R(0))$. The function $\mathbf{f}_R : \mathbb{R}^n \times \mathbb{R}^n \to \mathbb{R}^n$ is *an approximate Riemann solver.*

Let us consider the scalar Riemann problem. In case $f(q) = aq$ where $a \in \mathbb{R}$ is a constant, the lemma 2.3.4 for $t > 0$ leads to

$$q(0,t) = q_L(1 - H(-at)) + q_R H(-at) = q_L H(a) + q_R H(-a).$$

Let us denote $a^+ = max(a, 0)$, $a^- = min(a, 0)$ the positive and the negative part of a, respectively. The exact Riemann solver has the form

$$f_R(q_L, q_R) = aq(0, t) = a^+ q_L + a^- q_R.$$

In the nonlinear case it is difficult to express the solution to the Riemann problem. According to (2.3.75) we know that the solution is constant along the characteristics $x(t)$ satisfying

$$\frac{\mathrm{d}x(t)}{\mathrm{d}t} = \frac{\mathrm{d}f}{\mathrm{d}q}(q(x(t), t)).$$

Hence, if

$$\frac{\mathrm{d}f}{\mathrm{d}q}(q) \geq 0 \qquad \text{for all} \quad q \in \mathbb{R},$$

the exact Riemann solver has the form

$$f_R(q_L, q_R) = f(q_L)$$

and in case

$$\frac{\mathrm{d}f}{\mathrm{d}q}(q) \leq 0 \qquad \text{for all} \quad q \in \mathbb{R},$$

it is

$$f_R(q_L, q_R) = f(q_R).$$

This result motivates the splitting of $f(q)$ to its positive part $f^+(q)$ and its negative part $f^-(q)$ in such a way that for all $q \in \mathbb{R}$ it holds

$$f(q) = f^+(q) + f^-(q)$$
$$\frac{\mathrm{d}f^+}{q}(q) \geq 0 \quad \text{and} \quad \frac{\mathrm{d}f^-}{q}(q) \leq 0.$$

We consider the approximate Riemann solver in the form

$$f_R(q_L, q_R) = f^+(q_L) + f^-(q_R). \tag{2.3.84}$$

Now we return to the vector Riemann problem (2.3.75) (2.3.76) again. Let $\mathbf{R}$ be the matrix the columns of which are the eigenvectors $\mathbf{r}_1, \mathbf{r}_2, \ldots, \mathbf{r}_n$ of the matrix $\mathbf{A}$ and $D = \mathrm{diag}(\lambda_1, \lambda_2, \ldots, \lambda_n)$ the diagonal matrix as mentioned above. Let k be a natural number such that $\lambda_1 \leq \lambda_2 \leq \ldots \leq \lambda_k \leq 0 < \lambda_{k+1} \leq \ldots \leq \lambda_n$. By the lemma 2.3.5

$$\mathbf{q}(0, t) = \sum_{i=1}^{k} \beta_i \mathbf{r}_i + \sum_{i=k+1}^{n} \alpha_i \mathbf{r}_i$$

and

$$\mathbf{f}(\mathbf{q}(0, t)) = \sum_{i=1}^{k} \beta_i \lambda_i \mathbf{r}_i + \sum_{i=k+1}^{n} \alpha_i \lambda_i \mathbf{r}_i. \tag{2.3.85}$$

Further, we define diagonal matrices

$$\mathbf{D}^+ = \mathrm{diag}(\lambda_1^+, \lambda_2^+, \dots, \lambda_n^+) \qquad \mathbf{D}^- = \mathrm{diag}(\lambda_1^-, \lambda_2^-, \dots, \lambda_n^-) \qquad |\mathbf{D}| = \mathbf{D}^+ - \mathbf{D}^-$$

and matrices $\mathbf{A}^+ = \mathbf{R}\mathbf{D}^+\mathbf{R}^{-1} \qquad \mathbf{A}^- = \mathbf{R}\mathbf{D}^-\mathbf{R}^{-1} \qquad |\mathbf{A}| = \mathbf{A}^+ - \mathbf{A}^-.$

We see that the matrix $\mathbf{A}^+$ is similar to the matrix $\mathbf{D}^+$. Therefore they have the same eigenvalues. Eigenvectors of $\mathbf{D}^+$ are identical with the canonical basis vectors, which means the eigenvector set of $\mathbf{A}^+$ is identical with the eigenvector set of the matrix $\mathbf{A}$. In case of the matrix $\mathbf{A}^-$ the situation is analogous. Using (2.3.77) and (2.3.79) we obtain

$$\begin{aligned}
\mathbf{A}^+\mathbf{q}_L &= \sum_{i=1}^{n} \alpha_i \lambda_i^+ \mathbf{r}_i = \sum_{i=k+1}^{n} \alpha_i \lambda_i \mathbf{r}_i \\
\mathbf{A}^-\mathbf{q}_R &= \sum_{i=1}^{n} \beta_i \lambda_i^- \mathbf{r}_i = \sum_{i=1}^{k} \beta_i \lambda_i \mathbf{r}_i.
\end{aligned}$$

According to (2.3.85) the Riemann solver has the form

$$\mathbf{f}_R(\mathbf{q}_L, \mathbf{q}_R) = \mathbf{A}^+(\mathbf{q}_L) + \mathbf{A}^-(\mathbf{q}_R) = \frac{1}{2}(\mathbf{A}(\mathbf{q}_L) + \mathbf{A}(\mathbf{q}_R) - |\mathbf{A}|(\mathbf{q}_R - \mathbf{q}_L)). \tag{2.3.86}$$

Let us now consider the Riemann problem (2.3.75) (2.3.76) for a general nonlinear system. Having resolved the scalar and the linear case, we can do the following heuristic generalization: We set

$$\mathbf{f}_R(\mathbf{q}_L, \mathbf{q}_R) = \mathbf{f}^+(\mathbf{q}_L) + \mathbf{f}^-(\mathbf{q}_R), \tag{2.3.87}$$

where functions $\mathbf{f}^+, \mathbf{f}^- : \mathbb{R}^n \to \mathbb{R}^n$ satisfy

$$\mathbf{f}(\mathbf{q}) = \mathbf{f}^+(\mathbf{q}) + \mathbf{f}^-(\mathbf{q}), \qquad \text{for all } \mathbf{q} \in \mathbb{R}^n \text{ and} \tag{2.3.88}$$

$$\frac{\mathbf{Df}^+}{\mathbf{Dq}}(\mathbf{q}) \qquad \text{has no negative eigenvalues} \tag{2.3.89}$$

$$\frac{\mathbf{Df}^-}{\mathbf{Dq}}(\mathbf{q}) \qquad \text{has no positive eigenvalues.} \tag{2.3.90}$$

Of course, this flux splitting is not unique and can be done in many different ways. In our paper, we will develop the Osher-Solomon method.

Analogously as in the linear case, we define the matrices

$$\begin{aligned}
\mathbf{D}^+(\mathbf{q}) &= \mathrm{diag}(\lambda_1^+(\mathbf{q}), \lambda_2^+(\mathbf{q}), \dots, \lambda_n^+(\mathbf{q})) \\
\mathbf{D}^-(\mathbf{q}) &= \mathrm{diag}(\lambda_1^-(\mathbf{q}), \lambda_2^-(\mathbf{q}), \dots, \lambda_n^-(\mathbf{q})) \\
|\mathbf{D}|(\mathbf{q}) &= \mathbf{D}^+(\mathbf{q}) - \mathbf{D}^-(\mathbf{q})
\end{aligned}$$

and

$$\begin{aligned}
\mathbf{A}^+(\mathbf{q}) &= \mathbf{R}(\mathbf{q})\mathbf{D}^+(\mathbf{q})\mathbf{R}^{-1}(\mathbf{q}) \\
\mathbf{A}^-(\mathbf{q}) &= \mathbf{R}(\mathbf{q})\mathbf{D}^-(\mathbf{q})\mathbf{R}^{-1}(\mathbf{q}) \\
|\mathbf{A}|(\mathbf{q}) &= \mathbf{A}^+(\mathbf{q}) - \mathbf{A}^-(\mathbf{q}).
\end{aligned}$$

Let us assume existence of two functions $\mathbf{f}^+, \mathbf{f}^-$ satisfying (2.3.88) so that

$$\frac{\mathrm{D}\mathbf{f}^+}{\mathrm{D}\mathbf{q}}(\mathbf{q}) = \mathbf{A}^+(\mathbf{q}) \quad \text{and} \quad \frac{\mathrm{D}\mathbf{f}^-}{\mathrm{D}\mathbf{q}}(\mathbf{q}) = \mathbf{A}^-(\mathbf{q}) \tag{2.3.91}$$

for all $\mathbf{q} \in \mathbb{R}^n$. These functions satisfy conditions (2.3.89), (2.3.90) and they can be expressed in the form

$$\mathbf{f}^+(\mathbf{q}) = \mathbf{f}^+(\mathbf{q}_L) + \int_{\mathbf{q}_L}^{\mathbf{q}} \mathbf{A}^+(\mathbf{q})\mathrm{d}\mathbf{q} \tag{2.3.92}$$

$$\mathbf{f}^-(\mathbf{q}) = \mathbf{f}^-(\mathbf{q}_L) + \int_{\mathbf{q}_L}^{\mathbf{q}} \mathbf{A}^-(\mathbf{q})\mathrm{d}\mathbf{q}. \tag{2.3.93}$$

Putting (2.3.92) into (2.3.87) we obtain the approximate Riemann solver

$$\mathbf{f}_R(\mathbf{q}_L, \mathbf{q}_R) = \mathbf{f}(\mathbf{q}_R) - \int_{\mathbf{q}_L}^{\mathbf{q}_R} \mathbf{A}^+(\mathbf{q})\mathrm{d}\mathbf{q} \tag{2.3.94}$$

or equivalently

$$\mathbf{f}_R(\mathbf{q}_L, \mathbf{q}_R) = \mathbf{f}(\mathbf{q}_L) + \int_{\mathbf{q}_L}^{\mathbf{q}_R} \mathbf{A}^-(\mathbf{q})\mathrm{d}\mathbf{q} = \frac{1}{2}\left(\mathbf{f}(\mathbf{q}_L) + \mathbf{f}(\mathbf{q}_R) - \int_{\mathbf{q}_L}^{\mathbf{q}_R} |\mathbf{A}|(\mathbf{q})\mathrm{d}\mathbf{q}\right).$$

Unfortunately, functions $\mathbf{f}^+$ and $\mathbf{f}^-$ do not exist in general and the above written integrals depend on the trace in $\mathbb{R}^n$.

2.4 Approximate solution to the Riemann problem

In this subsection we are going to construct the numerical flux $\Phi(\tilde{\mathbf{q}_\mathbf{i}}(t), \tilde{\mathbf{q}_\mathbf{j}}(t), \nu_{ij}, \mu_2(\partial\Omega_{ij}))$ which approximates the integral (2.1.21)

$$\int_{\partial\Omega_{ij}} \mathbf{f}(\mathbf{q}(\mathbf{x},t))\nu_{ij\,1} + \mathbf{g}(\mathbf{q}(\mathbf{x},t))\nu_{ij\,2} + \mathbf{h}(\mathbf{q}(\mathbf{x},t))\nu_{ij\,3}\mathrm{d}\mathbf{S} \tag{2.4.95}$$

using values $\mathbf{q}_\mathbf{i}(t), \mathbf{q}_\mathbf{j}(t)$ obtained from the function $\mathbf{q}(x,t)$ on elements Ω_i, Ω_j. The normal vector ν_{ij} from (2.4.95) can be expressed in polar coordinates:

$$\nu_{ij} = (\cos\alpha_{ij}\cos\beta_{ij}, \sin\alpha_{ij}\cos\beta_{ij}, \sin\beta_{ij})^T, \tag{2.4.96}$$

where α_{ij} and β_{ij} are angles, which the normal vector forms with the xz and yz axis planes, respectively. According to (2.2.52) we can rewrite the integral (2.4.95) as

$$\int_{\partial\Omega_{ij}} \mathbf{T}(\alpha_{ij},\beta_{ij})^{-1}\mathbf{f}(\mathbf{T}(\alpha_{ij},\beta_{ij})\mathbf{q}(\mathbf{x},t))\mathrm{d}\mathbf{S}. \tag{2.4.97}$$

For simplicity, we denote $\mathbf{T}(\alpha_{ij},\beta_{ij})$ by the symbol $\mathbf{T}_{ij}$. We will approximate the integral (2.4.97) by the value

$$\mu_2(\partial\Omega_{ij})\mathbf{T}_{ij}{}^{-1}\mathbf{f}(\mathbf{T}_{ij}\mathbf{q}_{ij}(t)), \tag{2.4.98}$$

where $\mathbf{q}_{ij}(t)$ is a suitably chosen approximation of $\mathbf{q}(x,t)$ on the side $\partial\Omega_{ij}$ of the finite volumes Ω_i and Ω_j depending on $\mathbf{q_i}(t)$ and $\mathbf{q_j}(t)$. Our main aim now is to find this approximation. Let us fix a time point $t=t'$ and denote $\mathbf{q_i}=\mathbf{q_i}(t')$, $\mathbf{q_j}=\mathbf{q_j}(t')$ and $\mathbf{q}_{ij}=\mathbf{q}_{ij}(t')$.

Since the system of the Euler equation is very complicated, we would not succeed by using such simple approximations as linear combinations of $\mathbf{q_i}$ and $\mathbf{q_j}$ etc. To construct a good scheme for solving it, we must use some deeper knowledge.

Let us construct a new local coordinate system. Its origin lies somewhere inside $\partial\Omega_{ij}$ (not important where, it can be its center for example) and the outside normal vector ν_{ij} has in its new coordinates the form

$$\tilde{\nu}_{ij} = (1,0,0)^T.$$

Here is the transformation rule:

$$\tilde{\mathbf{x}} - \tilde{\mathbf{o}} = \mathbf{T}_{ij}(\mathbf{x} - \mathbf{o}). \tag{2.4.99}$$

In this relation $\mathbf{x}$ means global coordinates, $\tilde{\mathbf{x}}$ local coordinates, $\mathbf{o}$ is the origin of the local coordinate system in global coordinates and $\tilde{\mathbf{o}}$ the origin of the local coordinate system in the local coordinates (i.e. $(0,0,0)^T$).

It holds

$$\tilde{\mathbf{q}}(\tilde{\mathbf{x}},t) = \mathbf{T}_{ij}\mathbf{q}(\mathbf{x},t). \tag{2.4.100}$$

The matrix $\mathbf{T}_{ij}$ is specified without taking care of rotation around the normal vector ν_{ij}, which does not matter to us since we are solving the one-dimensional Riemann problem in the normal direction.

The equation (13) has in the local coordinates the form

$$\frac{\partial}{\partial t}\tilde{\mathbf{q}}(\tilde{\mathbf{x}},t) + \frac{\partial}{\partial x}\mathbf{f}(\tilde{\mathbf{q}}(\tilde{\mathbf{x}},t)) + \frac{\partial}{\partial y}\mathbf{g}(\tilde{\mathbf{q}}(\tilde{\mathbf{x}},t)) + \frac{\partial}{\partial z}\mathbf{h}(\tilde{\mathbf{q}}(\tilde{\mathbf{x}},t)) = 0 \tag{2.4.101}$$

again due to (2.4.100) and the regularity of the matrix $\mathbf{T}_{ij}$. Relation (2.4.98) yields

$$\mu_2(\partial\Omega_{ij})\mathbf{T}_{ij}{}^{-1}\mathbf{f}(\tilde{\mathbf{q}}_{ij}), \tag{2.4.102}$$

where the value $\tilde{\mathbf{q}}_{ij} = \mathbf{T}_{ij}\mathbf{q}_{ij}$ can be understood as an approximation of $\tilde{\mathbf{q}}(\tilde{\mathbf{o}}, t')$ depending on $\tilde{\mathbf{q}}(\tilde{\mathbf{x}}, t') = \tilde{\mathbf{q}}_{\mathbf{i}}$ for $\tilde{x} < 0$ and $\tilde{\mathbf{q}}(\tilde{\mathbf{x}}, t') = \tilde{\mathbf{q}}_{\mathbf{j}}$ for $\tilde{x} > 0$. We neglect the dependence on $\tilde{y}$ and $\tilde{z}$ since our approximation remains constant near the origin.

The appropriate Riemann problem to the equation (2.4.101) is

$$\frac{\partial}{\partial t}\hat{\mathbf{q}}(\tilde{x}, t) + \frac{\partial}{\partial \tilde{x}}\mathbf{f}(\hat{\mathbf{q}}(\tilde{x}, t)) = 0 \tag{2.4.103}$$

for $(\tilde{x}, t) \in \mathbb{R} \times (t', \infty)$ with the initial condition

$$\hat{\mathbf{q}}(\tilde{x}, t') = \left\{ \begin{array}{ll} \tilde{\mathbf{q}}_{\mathbf{i}} : & \tilde{x} < 0 \\ & \\ \tilde{\mathbf{q}}_{\mathbf{j}} : & \tilde{x} > 0 \end{array} \right\}, \tag{2.4.104}$$

where $\hat{\mathbf{q}} : \mathbb{R} \times (t', \infty) \to \mathbb{R}^5$. By the theorem 2.3.3 the solution to (2.4.103) (2.4.104) can be expressed in the form $\hat{\mathbf{q}}(\tilde{x}, t) = \hat{\mathbf{q}}_R(\tilde{x}/t)$. The value $\hat{\mathbf{q}}(0, t) = \hat{\mathbf{q}}_R(0)$ is therefore constant for all $t > t'$ and it seems suitable to approximate $\tilde{\mathbf{q}}_{ij}$ by $\hat{\mathbf{q}}_R(0)$. Substituting this in (2.4.102), we obtain an approximation of the integral (2.4.95) in the form

$$\mu_2(\partial\Omega_{ij})\mathbf{T}_{ij}{}^{-1}\mathbf{f}(\hat{\mathbf{q}}_R(0)). \tag{2.4.105}$$

Correspondingly to what we said in section **2.3**, we will approximate the value $\mathbf{f}(\hat{\mathbf{q}}_R(0))$ by the approximate Riemann solver $\mathbf{f}_R(\mathbf{T}_{ij}\mathbf{q}_{\mathbf{i}}, \mathbf{T}_{ij}\mathbf{q}_{\mathbf{j}})$ which was defined by the relation (2.3.94). Now we have the numerical flux

$$\Phi_{ij}(\mathbf{q}_{\mathbf{i}}, \mathbf{q}_{\mathbf{j}}) = \mu_2(\partial\Omega_{ij})\mathbf{T}_{ij}{}^{-1}\mathbf{f}_R(\mathbf{T}_{ij}\mathbf{q}_{\mathbf{i}}, \mathbf{T}_{ij}\mathbf{q}_{\mathbf{j}}) \tag{2.4.106}$$

where

$$\mathbf{f}_R(\mathbf{q}_{\mathbf{L}}, \mathbf{q}_{\mathbf{R}}) = \mathbf{f}(\mathbf{q}_{\mathbf{R}}) - \int_{\mathbf{q}_{\mathbf{L}}}^{\mathbf{q}_{\mathbf{R}}} \mathbf{A}^+(\mathbf{q})\mathrm{d}\mathbf{q} \tag{2.4.107}$$

or equivalently

$$\mathbf{f}_R(\mathbf{q}_{\mathbf{L}}, \mathbf{q}_{\mathbf{R}}) = \mathbf{f}(\mathbf{q}_{\mathbf{L}}) + \int_{\mathbf{q}_{\mathbf{L}}}^{\mathbf{q}_{\mathbf{R}}} \mathbf{A}^-(\mathbf{q})\mathrm{d}\mathbf{q} = \frac{1}{2}\left(\mathbf{f}(\mathbf{q}_{\mathbf{L}}) + \mathbf{f}(\mathbf{q}_{\mathbf{R}}) - \int_{\mathbf{q}_{\mathbf{L}}}^{\mathbf{q}_{\mathbf{R}}} |\mathbf{A}|(\mathbf{q})\mathrm{d}\mathbf{q}\right). \tag{2.4.108}$$

We can approximate them heuristic by a suitable numerical quadrature or compute them along a suitably chosen curve in $\mathbb{R}^n$.

The most popular schemes obtained as a result of numerical quadrature are the Vijayasundaram scheme:

$$\int_{\mathbf{q_L}}^{\mathbf{q_R}} |\mathbf{A}|(\mathbf{q})\mathrm{d}\mathbf{q} \approx |\mathbf{A}|\left(\frac{\mathbf{q_L}+\mathbf{q_R}}{2}\right)(\mathbf{q_R}-\mathbf{q_L})$$

$$\frac{1}{2}(\mathbf{f}(\mathbf{q_L})+\mathbf{f}(\mathbf{q_R})) \approx \mathbf{f}\left(\frac{\mathbf{q_L}+\mathbf{q_R}}{2}\right) = \mathbf{A}\left(\frac{\mathbf{q_L}+\mathbf{q_R}}{2}\right)\frac{\mathbf{q_L}+\mathbf{q_R}}{2},$$

the Van Leer scheme:

$$\int_{\mathbf{q_L}}^{\mathbf{q_R}} |\mathbf{A}|(\mathbf{q})\mathrm{d}\mathbf{q} \approx |\mathbf{A}|\left(\frac{\mathbf{q_L}+\mathbf{q_R}}{2}\right)(\mathbf{q_R}-\mathbf{q_L})$$

and the Steger-Warming scheme:

$$\int_{\mathbf{q_L}}^{\mathbf{q_R}} \mathbf{A}^-(\mathbf{q})\mathrm{d}\mathbf{q} \approx \mathbf{A}^-(\mathbf{q_R})(\mathbf{q_R}) - \mathbf{A}^-(\mathbf{q_L})(\mathbf{q_L}).$$

There is a great disadvantage of this approach, namely the matrices $\mathbf{A}, \mathbf{A}^-$ or $\mathbf{A}^+$ must be computed for every side $\partial\Omega_{ij}$ in each iteration, which costs a lot of time. We are now going to construct a scheme which does not need it.

2.5 Osher-Solomon numerical flux

Let $\mathbf{q_L}$, $\mathbf{q_R}$ be two arbitrary states satisfying conditions (2.2.72), (2.2.73) and (2.2.74). We have shown that it is possible to connect them with a unique piecewise smooth curve described in section **2.2.8**. We use this result now for the integration of matrices $\mathbf{A}(\mathbf{q})$, $\mathbf{A}^+(\mathbf{q})$, $\mathbf{A}^-(\mathbf{q})$ and $|\mathbf{A}|(\mathbf{q})$. Since (2.4.107) and (2.4.108) are equivalent, we can choose the first of them.

$$(2.5.109) \qquad \int_{\mathbf{q_L}}^{\mathbf{q_A}} \mathbf{A}^+(\mathbf{q})\mathrm{d}\mathbf{q} = \int_{\varrho_L}^{\varrho_A} \mathbf{A}^+(\mathbf{q}^{(1)}(\xi))\frac{\mathrm{d}\mathbf{q}^{(1)}}{\mathrm{d}\xi}(\xi)\mathrm{d}\xi =$$

$$= \int_{\varrho_L}^{\varrho_A} \mathbf{A}^+(\mathbf{q}^{(1)}(\xi))\mathbf{r_1}(\mathbf{q}^{(1)}(\xi))\mathrm{d}\xi = \int_{\varrho_L}^{\varrho_A} \lambda_1{}^+(\mathbf{q}^{(1)}(\xi))\mathbf{r_1}(\mathbf{q}^{(1)}(\xi))\mathrm{d}\xi =$$

$$= \int_{\varrho_L}^{\varrho_A} H(\lambda_1(\mathbf{q}^{(1)}(\xi)))\lambda_1(\mathbf{q}^{(1)}(\xi))\mathbf{r_1}(\mathbf{q}^{(1)}(\xi))\mathrm{d}\xi = \int_{\varrho_L}^{\varrho_A} H(\lambda_1(\mathbf{q}^{(1)}(\xi)))\mathbf{A}(\mathbf{q}^{(1)}(\xi))\mathbf{r_1}(\mathbf{q}^{(1)}(\xi))\mathrm{d}\xi =$$

$$= \int_{\mathbf{q_L}}^{\mathbf{q_A}} H(\lambda_1(\mathbf{q}))\mathbf{A}(\mathbf{q})\mathrm{d}\mathbf{q} = \int_{\mathbf{q_L}}^{\mathbf{q_A}} H(\lambda_1(\mathbf{q}))\frac{\mathbf{Df}}{\mathbf{Dq}}(\mathbf{q})\mathrm{d}\mathbf{q} \qquad .$$

The remaining integrals can be evaluated in a similar way. By the remark 2.2.7 the eigenvalues $\lambda_1(\mathbf{q})$, $\lambda_5(\mathbf{q})$ can change their signs along the curves $\mathbf{q}^{(1)}(\xi)$, $\mathbf{q}^{(5)}(\xi)$, respectively. The eigenvalues $\lambda_2(\mathbf{q})$, $\lambda_3(\mathbf{q})$ and $\lambda_4(\mathbf{q})$ are constant along their curves. Thus,

$\lambda_1(\mathbf{q_L}) \geq 0$ and $\lambda_1(\mathbf{q_A}) \geq 0$

$$\int_{\mathbf{q_L}}^{\mathbf{q_A}} \mathbf{A}^+(\mathbf{q})\mathrm{d}\mathbf{q} = \int_{\mathbf{q_L}}^{\mathbf{q_A}} \frac{\mathrm{D}\mathbf{f}}{\mathrm{D}\mathbf{q}}(\mathbf{q})\mathrm{d}\mathbf{q} = \mathbf{f}(\mathbf{q_A}) - \mathbf{f}(\mathbf{q_L})$$

$\lambda_1(\mathbf{q_L}) \geq 0$ and $\lambda_1(\mathbf{q_A}) < 0$

$$\int_{\mathbf{q_L}}^{\mathbf{q_A}} \mathbf{A}^+(\mathbf{q})\mathrm{d}\mathbf{q} = \int_{\mathbf{q_L}}^{\mathbf{q_L^s}} \frac{\mathrm{D}\mathbf{f}}{\mathrm{D}\mathbf{q}}(\mathbf{q})\mathrm{d}\mathbf{q} = \mathbf{f}(\mathbf{q_L^s}) - \mathbf{f}(\mathbf{q_L})$$

$\lambda_1(\mathbf{q_L}) < 0$ and $\lambda_1(\mathbf{q_A}) \geq 0$

$$\int_{\mathbf{q_L}}^{\mathbf{q_A}} \mathbf{A}^+(\mathbf{q})\mathrm{d}\mathbf{q} = \int_{\mathbf{q_L^s}}^{\mathbf{q_A}} \frac{\mathrm{D}\mathbf{f}}{\mathrm{D}\mathbf{q}}(\mathbf{q})\mathrm{d}\mathbf{q} = \mathbf{f}(\mathbf{q_A}) - \mathbf{f}(\mathbf{q_L^s})$$

$\lambda_1(\mathbf{q_L}) < 0$ and $\lambda_1(\mathbf{q_A}) < 0$

$$\int_{\mathbf{q_L}}^{\mathbf{q_A}} \mathbf{A}^+(\mathbf{q})\mathrm{d}\mathbf{q} = 0.$$

Calculation along the curve $\mathbf{q}^{(5)}(\xi)$ proceeds in a similar way.

$\lambda_5(\mathbf{q_D}) \geq 0$ and $\lambda_5(\mathbf{q_R}) \geq 0$

$$\int_{\mathbf{q_D}}^{\mathbf{q_R}} \mathbf{A}^+(\mathbf{q})\mathrm{d}\mathbf{q} = \int_{\mathbf{q_D}}^{\mathbf{q_R}} \frac{\mathrm{D}\mathbf{f}}{\mathrm{D}\mathbf{q}}(\mathbf{q})\mathrm{d}\mathbf{q} = \mathbf{f}(\mathbf{q_R}) - \mathbf{f}(\mathbf{q_D})$$

$\lambda_5(\mathbf{q_D}) \geq 0$ and $\lambda_5(\mathbf{q_R}) < 0$

$$\int_{\mathbf{q_D}}^{\mathbf{q_R}} \mathbf{A}^+(\mathbf{q})\mathrm{d}\mathbf{q} = \int_{\mathbf{q_D}}^{\mathbf{q_R^s}} \frac{\mathrm{D}\mathbf{f}}{\mathrm{D}\mathbf{q}}(\mathbf{q})\mathrm{d}\mathbf{q} = \mathbf{f}(\mathbf{q_R^s}) - \mathbf{f}(\mathbf{q_D})$$

$\lambda_5(\mathbf{q_D}) < 0$ and $\lambda_5(\mathbf{q_R}) \geq 0$

$$\int_{\mathbf{q_D}}^{\mathbf{q_R}} \mathbf{A}^+(\mathbf{q})\mathrm{d}\mathbf{q} = \int_{\mathbf{q_R^s}}^{\mathbf{q_R}} \frac{\mathrm{D}\mathbf{f}}{\mathrm{D}\mathbf{q}}(\mathbf{q})\mathrm{d}\mathbf{q} = \mathbf{f}(\mathbf{q_R}) - \mathbf{f}(\mathbf{q_R^s})$$

$\lambda_5(\mathbf{q_D}) < 0$ and $\lambda_5(\mathbf{q_D}) < 0$

$$\int_{\mathbf{q_D}}^{\mathbf{q_R}} \mathbf{A}^+(\mathbf{q})\mathrm{d}\mathbf{q} = 0.$$

The Riemann invariant u is constant along the curves $\mathbf{q}^{(2)}(\xi)$, $\mathbf{q}^{(3)}(\xi)$ and $\mathbf{q}^{(4)}(\xi)$.

Hence, $\lambda_2(\mathbf{q_A}) \geq 0$ yields

$$\int_{\mathbf{q_A}}^{\mathbf{q_D}} \mathbf{A}^+(\mathbf{q})\mathrm{d}\mathbf{q} = \mathbf{f}(\mathbf{q_D}) - \mathbf{f}(\mathbf{q_A})$$

and in case $\lambda_2(\mathbf{q_A}) < 0$, it is

$$\int_{\mathbf{q_A}}^{\mathbf{q_D}} \mathbf{A}^+(\mathbf{q})\mathrm{d}\mathbf{q} = 0.$$

The last step is to add our particular results together:

$$\int_{\mathbf{q_L}}^{\mathbf{q_R}} \mathbf{A}^+(\mathbf{q})\mathrm{d}\mathbf{q} = \tag{2.5.110}$$

$$= \int_{\mathbf{q_L}}^{\mathbf{q_A}} \mathbf{A}^+(\mathbf{q})\mathrm{d}\mathbf{q} + \int_{\mathbf{q_A}}^{\mathbf{q_B}} \mathbf{A}^+(\mathbf{q})\mathrm{d}\mathbf{q} + \int_{\mathbf{q_B}}^{\mathbf{q_C}} \mathbf{A}^+(\mathbf{q})\mathrm{d}\mathbf{q} + \int_{\mathbf{q_C}}^{\mathbf{q_D}} \mathbf{A}^+(\mathbf{q})\mathrm{d}\mathbf{q} + \int_{\mathbf{q_D}}^{\mathbf{q_R}} \mathbf{A}^+(\mathbf{q})\mathrm{d}\mathbf{q} \qquad .$$

Substituting this term into (2.4.107) we get the Osher-Solomon approximate Riemann solver $\mathbf{f}_R(\mathbf{q_L}, \mathbf{q_R})$ for all states $\mathbf{q_L}, \mathbf{q_R} \in \mathcal{Q}$ satisfying conditions (2.2.72), (2.2.73) and (2.2.74). The scheme is shown in Diagram 2.5.1.

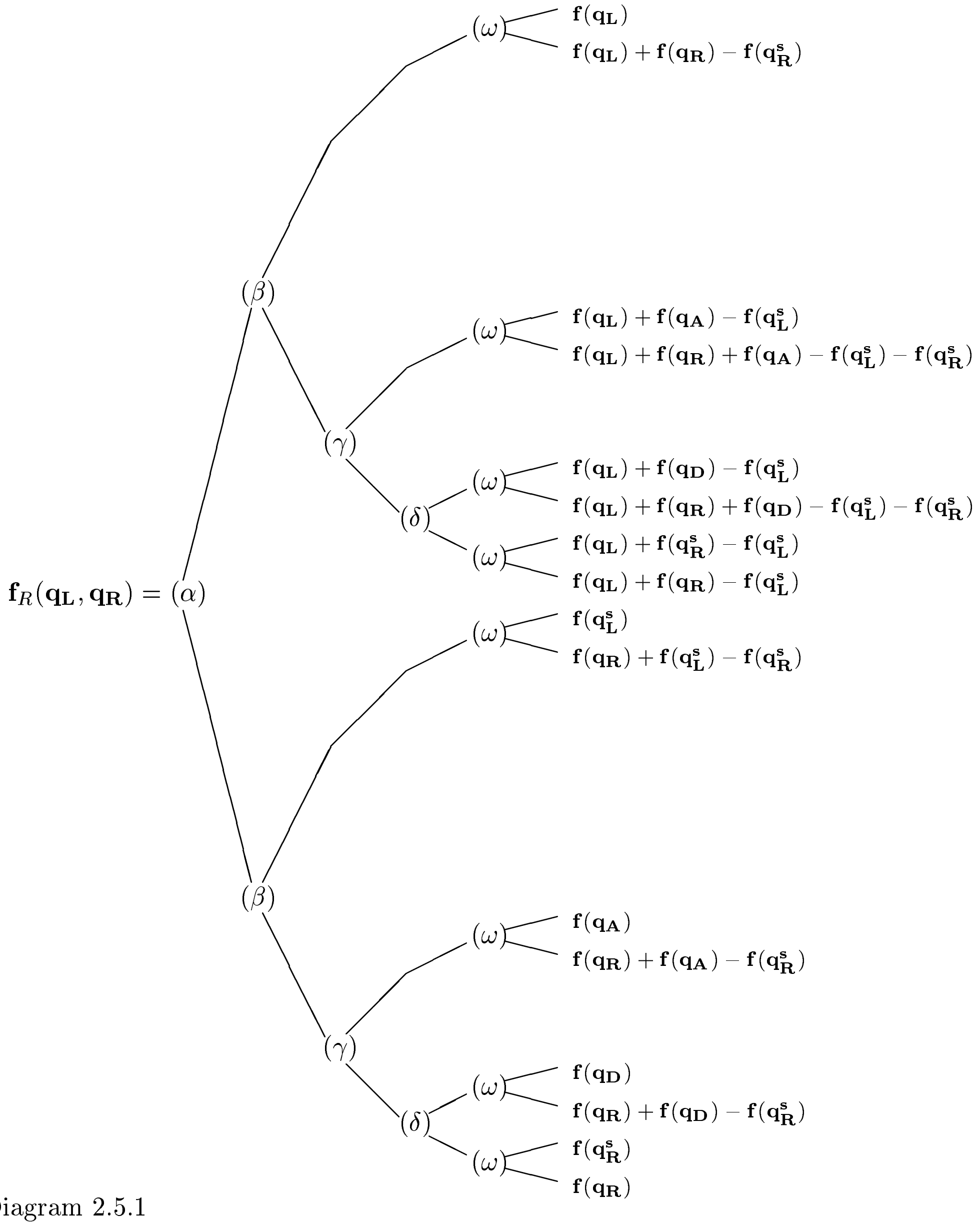

Diagram 2.5.1
Osher-Solomon approximate Riemann solver $\mathbf{f}_R(\mathbf{q_L}, \mathbf{q_R})$

The following five conditions must be tested every time:

$(\alpha) \ldots \lambda_1(\mathbf{q_L}) = u_L - c_L \geq 0$
$(\beta) \ldots \lambda_1(\mathbf{q_A}) = u_A - c_A \geq 0$
$(\gamma) \ldots \lambda_2(\mathbf{q_A}) = u_A \geq 0$
$(\delta) \ldots \lambda_5(\mathbf{q_D}) = u_D + c_D = u_A + c_D \geq 0$
$(\omega) \ldots \lambda_5(\mathbf{q_R}) = u_R + c_R \geq 0$

In the previous diagram, the direction upward means that the condition is satisfied. The reader may notice that some conditions determine conditions following after them. At this moment it remains to make sure the Osher-Solomon numerical flux is conservative and consistent.

Theorem 2.5.2
The Osher-Solomon approximate Riemann solver $\mathbf{f}_R(\mathbf{q_L}, \mathbf{q_R})$ has the property $\mathbf{f}_R(\mathbf{q}, \mathbf{q}) = \mathbf{f}(\mathbf{q})$ for every $\mathbf{q} \in \mathcal{Q}$, which means that the numerical flux (2.4.106) is consistent (see the relation (2.1.22)) with the differential equation (13).

Proof: Let $\mathbf{q_L} = \mathbf{q_R} = \mathbf{q}$. The reader can go through the solution to the system of equations in section **2.2.9** now and make sure that $\mathbf{q_L} = \mathbf{q_R}$ yields $\mathbf{q_A} = \mathbf{q_B} = \mathbf{q_C} = \mathbf{q_D} = \mathbf{q_L}$. Remark 2.2.11 implies that also $\mathbf{q_L^s} = \mathbf{q_R^s} = \mathbf{q_L}$. Conditions (2.2.72), (2.2.73) and (2.2.74) for $\mathbf{q_L} = \mathbf{q_R}$ are satisfied, which means it remains now only to put these particular results into the Diagram 2.5.1. If we do it, we obtain

$$\Phi(\mathbf{q}, \mathbf{q}, \nu, a) = a\mathbf{T}^{-1}(\alpha, \beta)\mathbf{f}(\mathbf{T}(\alpha, \beta)\mathbf{q}) =$$
$$= a(\mathbf{f}(\mathbf{q}) \cos\alpha \cos\beta, \mathbf{g}(\mathbf{q}) \sin\alpha \cos\beta, \mathbf{h}(\mathbf{q}) \sin\beta) =$$
$$= a(\mathbf{f}(\mathbf{q})\nu_1 + \mathbf{g}(\mathbf{q})\nu_2 + \mathbf{h}(\mathbf{q})\nu_3)$$

which verifies the relation (2.1.22).

Theorem 2.5.3:
The Osher-Solomon numerical flux (2.4.106) meets $\Phi(\mathbf{q_1}, \mathbf{q_2}, \nu, a) = -\Phi(\mathbf{q_2}, \mathbf{q_1}, -\nu, a)$ for two arbitrary states $\mathbf{q_1}, \mathbf{q_2} \in \mathcal{Q}$ satisfying (2.2.72), (2.2.73) and (2.2.74), for every $\nu \in \mathbb{R}^3$ $|\nu| = 1$ and for every $a \in \mathbb{R}^+$. In other words, it is conservative if and only if it is defined (see (2.1.23)).

Proof: We have to verify that

$$\mathbf{T}(\alpha, \beta)^{-1}\mathbf{f}_R(\mathbf{T}(\alpha, \beta)\mathbf{q_1}, \mathbf{T}(\alpha, \beta)\mathbf{q_2}) = \tag{2.5.111}$$
$$= \mathbf{T}(\alpha + \pi, -\beta)^{-1}\mathbf{f}_R(\mathbf{T}(\alpha + \pi, -\beta)\mathbf{q_2}, \mathbf{T}(\alpha + \pi, -\beta)\mathbf{q_1})$$

for all $\mathbf{q_1}, \mathbf{q_2} \in \mathcal{Q}$ and $\alpha, \beta \in \langle 0, 2\pi)$. Matrix $\mathbf{T}(\alpha, \beta)$ was defined by the relation (2.2.51). Setting $\mathbf{q_L} = \mathbf{T}(\alpha, \beta)\mathbf{q_1}$, $\mathbf{q_R} = \mathbf{T}(\alpha, \beta)\mathbf{q_2}$ we can rewrite (2.5.111) as

$$\mathbf{T}(\alpha + \pi, -\beta)\mathbf{T}(\alpha, \beta)^{-1}\mathbf{f}_R(\mathbf{q_L}, \mathbf{q_R}) = \tag{2.5.112}$$
$$= -\mathbf{f}_R(\mathbf{T}(\alpha + \pi, -\beta)\mathbf{T}(\alpha, \beta)^{-1}\mathbf{q_L}, \mathbf{T}(\alpha + \pi, -\beta)\mathbf{T}(\alpha, \beta)^{-1}\mathbf{q_R})$$

and because of

$$\mathbf{T}(\alpha + \pi, -\beta)\mathbf{T}(\alpha, \beta)^{-1} = \mathbf{T}(\pi, 0),$$

the relation (2.5.112) can be written as follows:

$$\mathbf{f}_R(\mathbf{q_L},\mathbf{q_R}) = -\mathbf{T}(\pi,0)^{-1}\mathbf{f}_R(\mathbf{T}(\pi,0)\mathbf{q_R},\mathbf{T}(\pi,0)\mathbf{q_L}) \tag{2.5.113}$$

It is suitable to denote

$$\begin{array}{rcl} \tilde{\mathbf{q}}_{\mathbf{L}} &=& \mathbf{T}(\pi,0)\mathbf{q_R} \\ \tilde{\mathbf{q}}_{\mathbf{R}} &=& \mathbf{T}(\pi,0)\mathbf{q_L} \end{array} \tag{2.5.114}$$

now. The reader can easily make sure that $\mathbf{T}(\pi,0) = \mathrm{diag}(1,-1,-1,1,1)$, which yields

$$\begin{array}{c} \tilde{\varrho}_L = \varrho_R, \tilde{u}_L = -u_R, \tilde{v}_L = -v_R, \tilde{w}_L = w_R, \tilde{p}_L = p_R, \tilde{c}_L = c_R, \\ \tilde{\varrho}_R = \varrho_L, \tilde{u}_R = -u_L, \tilde{v}_R = -v_L, \tilde{w}_R = w_L, \tilde{p}_R = p_L, \tilde{c}_R = c_L \end{array}. \tag{2.5.115}$$

Analogously as for the states $\mathbf{q_L}$, $\mathbf{q_R}$ in subsection **2.2.9** we obtain

$$\tilde{\alpha} = \left(\frac{\tilde{s}_R}{\tilde{s}_L}\right)^{\frac{1}{2\kappa}} = \left(\frac{\frac{\tilde{p}_R}{\tilde{\varrho}_R^\kappa}}{\frac{\tilde{p}_L}{\tilde{\varrho}_L^\kappa}}\right)^{\frac{1}{2\kappa}} = \left(\frac{s_L}{s_R}\right)^{\frac{1}{2\kappa}} = \frac{1}{\alpha}$$

$$\tilde{z}_L = -\frac{\kappa-1}{2}u_R + c_R = -z_R$$

$$\tilde{z}_R = -\frac{\kappa-1}{2}u_L - c_L = -z_L$$

$$\tilde{c}_A = \frac{\tilde{z}_L - \tilde{z}_R}{1+\tilde{\alpha}} = \frac{-z_R + z_L}{1+\frac{1}{\alpha}} = \alpha\frac{z_L - z_R}{1+\alpha} = \alpha c_A = c_D \tag{2.5.116}$$

$$\tilde{c}_D = \tilde{\alpha}\tilde{c}_A = c_A \tag{2.5.117}$$

$$c_R^2 = \kappa\frac{p_R}{\varrho_R} = \kappa s_R \varrho_R^{\kappa-1} = \alpha^{2\kappa}\kappa s_L \varrho_L^{\kappa-1}\left(\frac{\varrho_R}{\varrho_L}\right)^{\kappa-1} = \alpha^{2\kappa}c_L^2\left(\frac{\varrho_R}{\varrho_L}\right)^{\kappa-1}$$

$$\varrho_D = \frac{1}{\alpha^2}\varrho_A = \frac{1}{\alpha^2}\left(\frac{c_D}{\alpha c_L}\right)^{\frac{2}{\kappa-1}}\varrho_L = \left(\frac{c_D}{c_R}\right)^{\frac{2}{\kappa-1}}\varrho_R$$

$$\tilde{\varrho}_A = \tilde{\varrho}_L\left(\frac{\tilde{c}_A}{\tilde{c}_L}\right)^{\frac{2}{\kappa-1}} = \left(\frac{c_D}{c_R}\right)^{\frac{2}{\kappa-1}}\varrho_R = \varrho_D$$

$$\tilde{\varrho_D} = \frac{\tilde{\varrho}_A}{\tilde{\alpha}^2} = \alpha^2\varrho_D = \varrho_A$$

$$\tilde{u}_A = \frac{2}{\kappa-1}(\tilde{z}_L - \tilde{c}_A) = \frac{2}{\kappa-1}(-z_R - \alpha c_A) = -u_A = -u_D \tag{2.5.118}$$

$$\tilde{u}_D = \tilde{u}_A \tag{2.5.119}$$

and

$$\begin{array}{c} \tilde{v}_A = \tilde{v}_L = -v_R = -v_D \\ \tilde{v}_D = \tilde{v}_R = -v_L = -v_A \\ \tilde{w}_A = \tilde{w}_L = w_R = w_D \\ \tilde{w}_D = \tilde{w}_R = w_L = w_A \end{array}$$

and finally we have

(2.5.120)
$$\begin{array}{rcl}\tilde{\mathbf{q}}_{\mathbf{A}} & = & \mathbf{T}(\pi,0)\mathbf{q}_{\mathbf{D}} \\ \tilde{\mathbf{q}}_{\mathbf{D}} & = & \mathbf{T}(\pi,0)\mathbf{q}_{\mathbf{A}}\end{array}.$$

In case that the sonic points $\mathbf{q}^{\mathbf{s}}_{\mathbf{L}}$ or $\mathbf{q}^{\mathbf{s}}_{\mathbf{R}}$ exist, the remark 2.2.11 says that also $\tilde{\mathbf{q}}^{\mathbf{s}}_{\mathbf{R}}$ or $\tilde{\mathbf{q}}^{\mathbf{s}}_{\mathbf{L}}$ exist, respectively, and

$$\tilde{v}^s_R = \tilde{v}_R = -v_L = -v^s_L$$

$$\tilde{w}^s_R = \tilde{w}_R = w_L = w^s_L$$

$$\tilde{c}^s_R = -\frac{2\tilde{z}_R}{\kappa+1} = \frac{2z_L}{\kappa+1} = c^s_L$$

$$\tilde{u}^s_R = -\tilde{c}^s_R = -c^s_L = -u^s_L$$

$$\tilde{\varrho}^s_R = \tilde{\varrho}_R\left(\frac{\tilde{c}^s_R}{\tilde{c}_R}\right)^{\frac{2}{\kappa-1}} = \left(\frac{c^s_L}{c_L}\right)^{\frac{2}{\kappa-1}} = \varrho^s_L.$$

With the sonic point $\tilde{\mathbf{q}}^{\mathbf{s}}_{\mathbf{L}}$ we proceed analogously and find that

(2.5.121)
$$\begin{array}{rcl}\tilde{\mathbf{q}}^{\mathbf{s}}_{\mathbf{L}} & = & \mathbf{T}(\pi,0)\mathbf{q}^{\mathbf{s}}_{\mathbf{R}} \\ \tilde{\mathbf{q}}^{\mathbf{s}}_{\mathbf{R}} & = & \mathbf{T}(\pi,0)\mathbf{q}^{\mathbf{s}}_{\mathbf{L}}\end{array}.$$

Let us now return to the scheme of the approximate Riemann solver again. Using relations (2.5.114), (2.5.120) and (2.5.121) for $\mathbf{f}_R(\tilde{\mathbf{q}}_{\mathbf{L}},\tilde{\mathbf{q}}_{\mathbf{R}})$ we construct a scheme similar to the Diagram 2.5.1. Conditions (α), (β), $\dots,(\omega)$ have now the form

$(\hat{\alpha})\dots\tilde{\lambda_1}(\tilde{\mathbf{q}}_{\mathbf{L}}) = \tilde{u}_L - \tilde{c}_L \geq 0$
$(\hat{\beta})\dots\tilde{\lambda_1}(\tilde{\mathbf{q}}_{\mathbf{A}}) = \tilde{u}_A - \tilde{c}_A \geq 0$
$(\hat{\gamma})\dots\tilde{\lambda_2}(\tilde{\mathbf{q}}_{\mathbf{A}}) = \tilde{u}_A \geq 0$
$(\hat{\delta})\dots\tilde{\lambda_5}(\tilde{\mathbf{q}}_{\mathbf{D}}) = \tilde{u}_D - \tilde{c}_D = \tilde{u}_A - \tilde{c}_D \geq 0$
$(\hat{\omega})\dots\tilde{\lambda_5}(\tilde{\mathbf{q}}_{\mathbf{R}}) = \tilde{u}_R + \tilde{c}_R \geq 0$

Let us give a short explanation why it is not important whether conditions (α), (β), (γ), (δ), (ω) and $(\hat{\alpha})$, $(\hat{\beta})$, $\dots,(\hat{\omega})$ are strict or not.

In case $u_L = c_L$, the state $\mathbf{q}_{\mathbf{L}}$ equals to the sonic point $\mathbf{q}^{\mathbf{s}}_{\mathbf{L}}$. Analogously, in case $u_A = c_A$, it is $\mathbf{q}_{\mathbf{A}} = \mathbf{q}^{\mathbf{s}}_{\mathbf{L}}$. There is a small difference in case $u_A = 0$ – we do not have $\mathbf{q}_{\mathbf{A}} = \mathbf{q}_{\mathbf{D}}$, but we know that u_A is a Riemann invariant and stays constant along the curves $\mathbf{q}^{(2)}$, $\mathbf{q}^{(3)}$ and $\mathbf{q}^{(4)}$, which yields $u_D = 0$. Now, according to the flux definition (14) we have $\mathbf{f}(\mathbf{q}_{\mathbf{A}}) = \mathbf{f}(\mathbf{q}_{\mathbf{D}})$. In the end, in case $u_R = -c_R$ it is $\mathbf{q}_{\mathbf{R}} = \mathbf{q}^{\mathbf{s}}_{\mathbf{R}}$ and in case $u_D = -c_D$, it holds $\mathbf{q}_{\mathbf{D}} = \mathbf{q}^{\mathbf{s}}_{\mathbf{R}}$.

Conditions $(\hat{\alpha})$, $(\hat{\beta})$, $\dots,(\hat{\omega})$ can be rewritten as $(\tilde{\alpha})$, $(\tilde{\beta})$, $\dots,(\tilde{\omega})$, which are equivalent to (α), (β), $\dots,(\omega)$, respectively. The scheme with the solver $\mathbf{f}_R(\tilde{\mathbf{q}}_{\mathbf{L}},\tilde{\mathbf{q}}_{\mathbf{R}})$ is shown in Diagram 2.5.4. Using (2.2.52) with $\alpha = \pi$, $\beta = 0$, we obtain immediately that the equality (2.5.113) is valid.

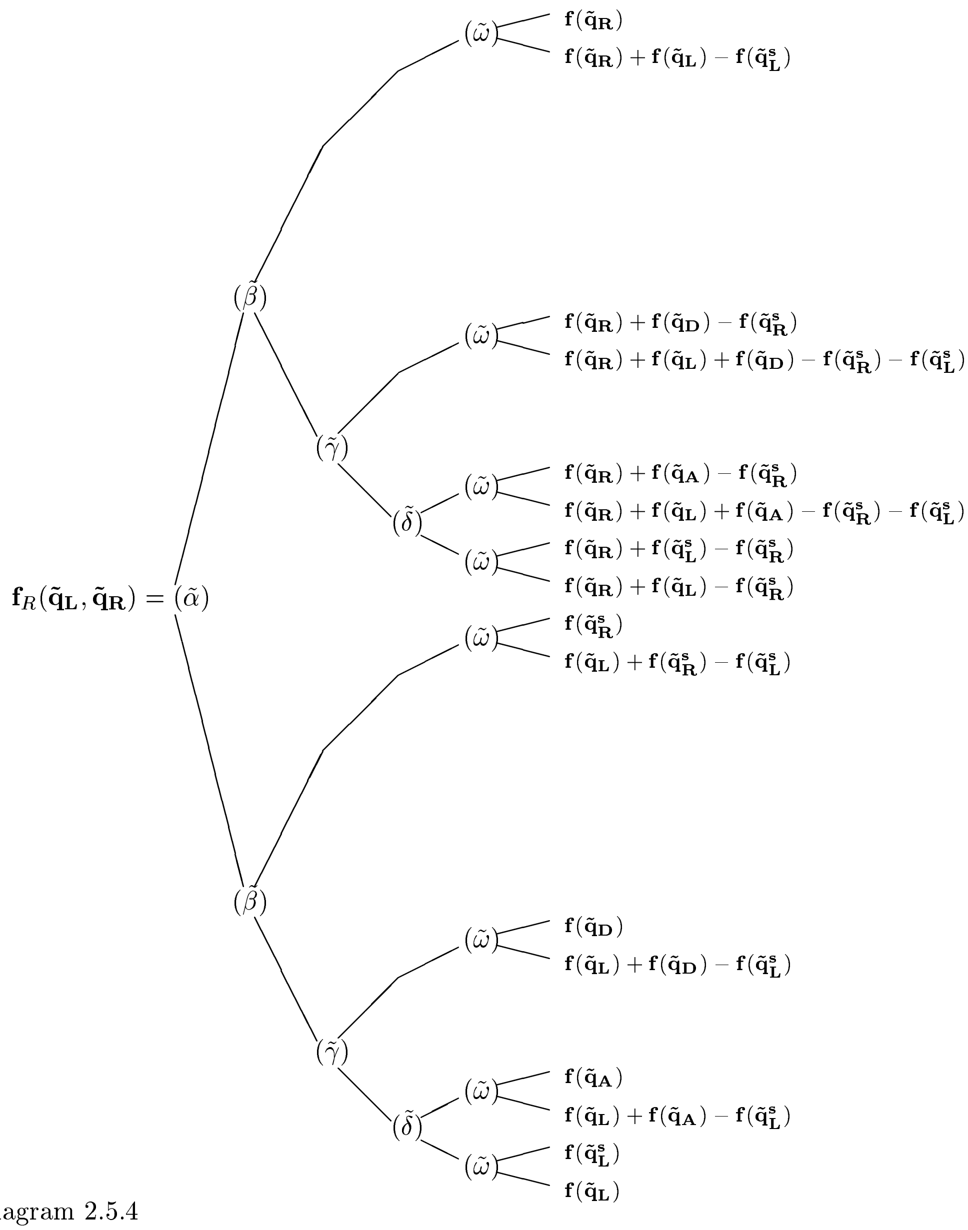

Diagram 2.5.4
Osher-Solomon approximate Riemann solver $\mathbf{f}_R(\tilde{\mathbf{q}}_\mathbf{L}, \tilde{\mathbf{q}}_\mathbf{R})$

$(\tilde{\alpha}) \ldots \tilde{\lambda_5}(\tilde{\mathbf{q}}_\mathbf{R}) = \tilde{u}_R + \tilde{c}_R \leq 0$
$(\tilde{\beta}) \ldots \tilde{\lambda_5}(\tilde{\mathbf{q}}_\mathbf{D}) = \tilde{u}_D + \tilde{c}_D = \tilde{u}_A + \tilde{c}_D \leq 0$
$(\tilde{\gamma}) \ldots \tilde{\lambda_2}(\tilde{\mathbf{q}}_\mathbf{A}) = \tilde{u}_A \leq 0$
$(\tilde{\delta}) \ldots \tilde{\lambda_1}(\tilde{\mathbf{q}}_\mathbf{A}) = \tilde{u}_A - \tilde{c}_A \leq 0$
$(\tilde{\omega}) \ldots \tilde{\lambda_1}(\tilde{\mathbf{q}}_\mathbf{L}) = \tilde{u}_L - \tilde{c}_L \leq 0$

At this moment we have finished our search for the numerical flux through sides lying inside of Ω. In the following section we will be concerned with the boundary conditions.

2.6 Boundary conditions

In this section we will deal with the choice of boundary conditions on the inlet and outlet sides of Ω to the system of equations (7). Let $\mathbf{q}(\mathbf{x}, t)$ be a solution to the equation (13) in the domain $\Omega \times (0, \mathcal{T})$. We restrict ourselves to a fixed time $t_0 \in (0, \mathcal{T})$. Linearized equation (13) has the form

$$(2.6.122) \quad \frac{\partial \mathbf{q}(\mathbf{x},t)}{\partial t} + \mathbf{A}(\overline{\mathbf{q}}(\mathbf{x},t_0))\frac{\partial \mathbf{q}(\mathbf{x},t)}{\partial x} + \mathbf{B}(\overline{\mathbf{q}}(\mathbf{x},t_0))\frac{\partial \mathbf{q}(\mathbf{x},t)}{\partial y} + \mathbf{C}(\overline{\mathbf{q}}(\mathbf{x},t_0))\frac{\partial \mathbf{q}(\mathbf{x},t)}{\partial z} = 0$$

for $(\mathbf{x}, t) \in \Omega \times (0, \mathcal{T})$. As you notice, we use our old notations

$$\mathbf{A}(\mathbf{q}) = \frac{\mathbf{Df}}{\mathbf{Dq}}(\mathbf{q}), \quad \mathbf{B}(\mathbf{q}) = \frac{\mathbf{Dg}}{\mathbf{Dq}}(\mathbf{q}) \text{ and } \mathbf{C}(\mathbf{q}) = \frac{\mathbf{Dh}}{\mathbf{Dq}}(\mathbf{q}).$$

The function $\overline{\mathbf{q}}(\mathbf{x}, t_0)$ is given by the relation (2.1.18). Let us use the symbol $B(\mathbf{q})$ for our boundary operator. The boundary condition can be written in the form

$$(2.6.123) \qquad B(\mathbf{q}(\mathbf{x}, t)) = 0$$

for $(\mathbf{x}, t) \in \partial\Omega \times (0, \mathcal{T})$ again. We consider a real element Ω_i, $i \in \{1, 2, \ldots, N\}$, $j \in \{N+1, N+2, \ldots, M\}$ and its side $\partial\Omega_{ij} \subset \partial\Omega$. Let us construct analogously as in section **2.4** a local coordinate system. Its x-axis is oriented in the direction of the outside normal vector ν_{ij}. Equation (2.6.122) yields

$$(2.6.124) \quad \frac{\partial \tilde{\mathbf{q}}(\tilde{\mathbf{x}},t)}{\partial t} + \mathbf{A}(\tilde{\overline{\mathbf{q}}}(\tilde{\mathbf{x}},t_0))\frac{\partial \tilde{\mathbf{q}}(\tilde{\mathbf{x}},t)}{\partial x} + \mathbf{B}(\tilde{\overline{\mathbf{q}}}(\tilde{\mathbf{x}},t_0))\frac{\partial \tilde{\mathbf{q}}(\tilde{\mathbf{x}},t)}{\partial y} + \mathbf{C}(\tilde{\overline{\mathbf{q}}}(\tilde{\mathbf{x}},t_0))\frac{\partial \tilde{\mathbf{q}}(\tilde{\mathbf{x}},t)}{\partial z} = 0$$

for $(\mathbf{x}, t) \in \Omega \times (0, \mathcal{T})$. We denote local coordinate system variables by the tilde again.

Let us proceed from (2.6.124) and (2.6.123) to the boundary Riemann problem

$$(2.6.125) \qquad \frac{\partial \hat{\mathbf{q}}(x,t)}{\partial t} + \mathbf{A}(\tilde{\mathbf{q}}_{\mathbf{i}})\frac{\partial \hat{\mathbf{q}}(x,t)}{\partial x} = 0 \qquad (x,t) \in \mathbb{R}^- \times \mathbb{R}^+$$

$$(2.6.126) \qquad \hat{\mathbf{q}}(x, 0) = \tilde{\mathbf{q}}_{\mathbf{i}} \qquad x < 0$$

$$(2.6.127) \qquad \hat{B}(\hat{\mathbf{q}}(0, t)) = 0 \qquad t > 0.$$

Here $\tilde{\mathbf{q}}_{\mathbf{i}}$ means $\tilde{\overline{\mathbf{q}}}(\tilde{\mathbf{x}}, t_0)$ restricted at Ω_i and the operator $\hat{B} : \mathcal{Q} \to \mathbb{R}^p$, $p \in \{0, 1, \ldots, 5\}$ represents a set of p prescribed boundary conditions, which is our aim to specify so that problem (2.6.125) ... (2.6.127) has a unique solution.

By the theorem 2.3.3 the unique solution to the boundary Riemann problem can be represented as $\hat{\mathbf{q}}(x,t) = \hat{\mathbf{q}}_R(x/t)$, $(x,t) \in \mathbb{R}^- \times \mathbb{R}^+$. This function is constant in time for $x = 0$. Therefore it seems to be suitable to choose the value $\hat{\mathbf{q}}_R(0)$ as an approximation of $\tilde{\mathbf{q}}(\tilde{\mathbf{x}}, t_0)$ on the side $\partial\Omega_{ij}$. Let us denote $\hat{\mathbf{q}}_\mathbf{b} = \hat{\mathbf{q}}_R(0)$.

Vectors $\tilde{\mathbf{q}}_\mathbf{i}$, $\hat{\mathbf{q}}_\mathbf{b}$ and the solution $\hat{\mathbf{q}}(x,t)$ itself can be expressed in the matrix $\mathbf{A}(\tilde{\mathbf{q}}_\mathbf{i})$ eigenvector basis:

$$\text{(2.6.128)} \quad \tilde{\mathbf{q}}_\mathbf{i} = \sum_{k=1}^{5} \alpha_k \mathbf{r_k}(\tilde{\mathbf{q}}_\mathbf{i}) \qquad \hat{\mathbf{q}}_\mathbf{b} = \sum_{k=1}^{5} \beta_k \mathbf{r_k}(\tilde{\mathbf{q}}_\mathbf{i}) \qquad \hat{\mathbf{q}}(x,t) = \sum_{k=1}^{5} \vartheta_k(x,t) \mathbf{r_k}(\tilde{\mathbf{q}}_\mathbf{i}),$$

where α_k, β_k are constants and $\vartheta_k : \mathbb{R}_0^- \times \mathbb{R}_0^+ \to \mathbb{R}$ for $k = 1, 2, \ldots, 5$. Putting (2.6.128) into (2.6.125) and (2.6.126) for $k = 1, 2, \ldots, 5$, we obtain problems

$$\text{(2.6.129)} \qquad \frac{\partial \vartheta_k}{\partial t}(x,t) + \lambda_k(\tilde{\mathbf{q}}_\mathbf{i}) \frac{\partial \vartheta_k}{\partial x}(x,t) = 0 \qquad (x,t) \in \mathbb{R}^- \times \mathbb{R}^+$$

$$\text{(2.6.130)} \qquad \vartheta_k(x,0) = \alpha_k \qquad x < 0$$

$$\text{(2.6.131)} \qquad \vartheta_k(0,t) = \beta_k \qquad t > 0.$$

Here $\lambda_k(\tilde{\mathbf{q}}_\mathbf{i})$ are again the eigenvalues of the matrix $\mathbf{A}(\tilde{\mathbf{q}}_\mathbf{i})$. We know that the solution $\vartheta_k(x,t)$ to the equation (2.6.129) is constant along the characteristics $x(t) = \lambda_k(\tilde{\mathbf{q}}_\mathbf{i})t + x_0$ (x_0 is an arbitrary constant). The situation is shown in Fig.2.6.1.

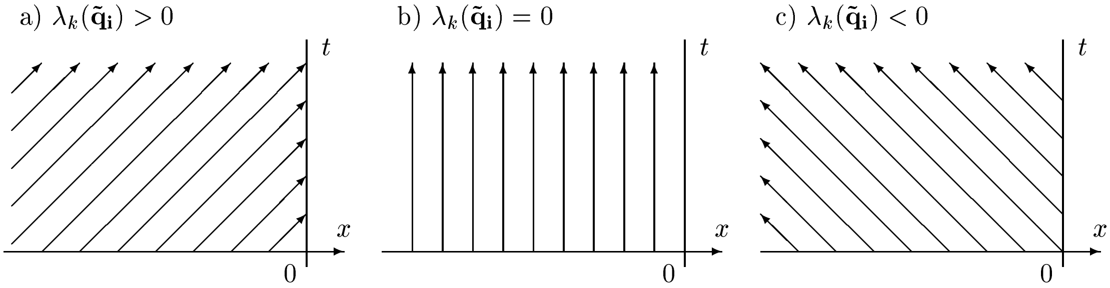

Fig.2.6.1
Characteristics of the equation (2.6.129) depending on $\lambda_k(\tilde{\mathbf{q}}_\mathbf{i})$

For the solution $\vartheta_k(x,t)$ at $(x,t) \in \mathbb{R}^- \times \mathbb{R}^+$ it holds

$$\text{(2.6.132)} \qquad \vartheta_k(x,t) = \left\{ \begin{array}{ll} \vartheta_k(x - \lambda_k(\tilde{\mathbf{q}}_\mathbf{i})t, 0) & x - \lambda_k(\tilde{\mathbf{q}}_\mathbf{i})t < 0 \\ \vartheta_k(0, t - \frac{x}{\lambda_k(\tilde{\mathbf{q}}_\mathbf{i})}) & x - \lambda_k(\tilde{\mathbf{q}}_\mathbf{i})t > 0 \end{array} \right\}$$

and for $\lambda_k(\tilde{\mathbf{q}}_\mathbf{i})t \geq 0$ we consequently obtain

$$\vartheta_k(x,t) = \vartheta_k(x - \lambda_k(\tilde{\mathbf{q}}_\mathbf{i})t, 0). \tag{2.6.133}$$

In case $\lambda_k(\tilde{\mathbf{q}}_\mathbf{i}) \geq 0$ there is no necessity to prescribe any boundary condition. In case the eigenvalue is negative, the solution is specified only for such $(x,t) \in \mathbb{R}^- \times \mathbb{R}^+$ that $x - \lambda_k(\tilde{\mathbf{q}}_\mathbf{i})t < 0$. We see it very well in Fig.2.6.1. Here a) shows how information is propagated from the domain. In case the eigenvalue is zero, information neither is propagated into nor from it. The last figure explains, why we need to prescribe a boundary condition in case of the negative eigenvalue.

For $(x,t) \in \mathbb{R}^- \times \mathbb{R}^+$ and $k \in \{1, 2, \ldots, 5\}$ we obtain

$$\text{if } \lambda_k(\tilde{\mathbf{q}}_\mathbf{i}) \geq 0 \text{ then } \vartheta_k(x,t) = \alpha_k \tag{2.6.134}$$

$$\text{if } \lambda_k(\tilde{\mathbf{q}}_\mathbf{i}) < 0 \text{ then } \vartheta_k(x,t) = \left\{ \begin{array}{ll} \alpha_k & \text{for } x - \lambda_k(\tilde{\mathbf{q}}_\mathbf{i})t < 0 \\ \beta_k & \text{for } x - \lambda_k(\tilde{\mathbf{q}}_\mathbf{i})t > 0 \end{array} \right\}. \tag{2.6.135}$$

If the number of the negative eigenvalues is p, relations (2.6.134), (2.6.130) and (2.6.131) yield $\beta_k = \alpha_k$ for $k = p+1, p+2, \ldots, 5$. The relation (2.6.128) gives

$$\hat{\mathbf{q}}_\mathbf{b} = \sum_{k=1}^{p} \beta_k \mathbf{r_k}(\tilde{\mathbf{q}}_\mathbf{i}) + \sum_{k=p+1}^{5} \alpha_k \mathbf{r_k}(\tilde{\mathbf{q}}_\mathbf{i}), \tag{2.6.136}$$

where $\beta_1, \beta_2, \ldots, \beta_p$ are real constants. We see that the number of components of the the solution vector which need to be specified by a boundary condition equals to the number of negative eigenvalues of the matrix $\mathbf{A}(\tilde{\mathbf{q}}_\mathbf{i})$.

Of course, for practical applications it would be much more suitable to give directly some components of the solution vector instead of β_k, but the choice of these components is not trivial. Let us now have a short look at it.

In case $p = 0$ or $p = 5$, the situation is clear. In case $p = 0$ there is no need to prescribe any boundary conditions - we set $\hat{\mathbf{q}}_\mathbf{b} = \tilde{\mathbf{q}}_\mathbf{i}$. In case $p = 5$ we choose $\hat{\mathbf{q}}_\mathbf{b}$ from $\mathcal{Q}$ arbitrary. The rest is a bit more complicated. Under notation

$$\alpha = (\alpha_1, \alpha_2, \alpha_3, \alpha_4, \alpha_5)^T$$

the relation (2.6.128) yields

$$\alpha = \mathbf{R}^{-1}(\tilde{\mathbf{q}}_\mathbf{i})\tilde{\mathbf{q}}_\mathbf{i}.$$

Here the matrix $\mathbf{R}(\mathbf{q})$ comes from (2.2.48). The reader can easily verify that

$$\alpha = \frac{\varrho_i}{2\kappa}(1, 2(\kappa - 1), 0, 0, 1)^T.$$

At first, we will analyse the case $p = 1$ using the following notation:

$$\tilde{\mathbf{q}}_\mathbf{i} = (\varrho_i, \varrho_i\tilde{u}_i, \varrho_i\tilde{v}_i, \varrho_i\tilde{w}_i, E_i)^T$$
$$\hat{\mathbf{q}}_\mathbf{b} = (\varrho_b, \varrho_b\tilde{u}_b, \varrho_b\tilde{v}_b, \varrho_b\tilde{w}_b, E_b)^T$$

$$\delta = \frac{2\kappa\beta_1 - \varrho_i}{2\varrho_i\kappa}.$$

Relation (2.6.136) yields

$$\hat{\mathbf{q}}_{\mathbf{b}} = \varrho_i \begin{pmatrix} \delta+1 \\ (\delta+1)\tilde{u}_i - \delta c_i \\ (\delta+1)\tilde{v}_i \\ (\delta+1)\tilde{w}_i \\ (\delta+1)\frac{\tilde{\mathbf{v}}_i^2}{2} - \delta\tilde{u}_i c_i + \frac{c_i^2}{\kappa-1}\frac{\kappa\delta+1}{\kappa} \end{pmatrix},$$

where c_i is the speed of sound and $\tilde{\mathbf{v}}_i^2$ square of the velocity vector corresponding to the state $\tilde{\mathbf{q}}_{\mathbf{i}}$. Using (11) we obtain

$$p_b = (1 + \kappa\delta - \frac{\delta^2\kappa(\kappa-1)}{2(\delta+1)}).$$

The state $\hat{\mathbf{q}}_{\mathbf{b}}$ is admissible if its density $\delta + 1$ (as well as the corresponding pressure) is positive. When $\kappa \in (1,3)$, this is equivalent to

$$\delta > \frac{-(\kappa+1) + \sqrt{(3\kappa-1)(\kappa-1)}}{\kappa(3-\kappa)}. \tag{2.6.137}$$

If we prescribed the density ϱ_b, we would also have δ, β and consequently the boundary state $\hat{\mathbf{q}}_{\mathbf{b}}$, but we would have to satisfy the condition (2.6.137). We would like to prescribe some variables without taking care of others. If we prescribed $\tilde{u}_b \neq \tilde{u}_i - c_i$, we would obtain

$$\delta = \frac{\tilde{u}_i - \tilde{u}_b}{c_i - \tilde{u}_i + \tilde{u}_b}.$$

We see that denominator of this fraction could become zero. Relation (2.6) says that $\tilde{v}_b = \tilde{v}_i$ and $\tilde{w}_b = \tilde{w}_i$, which means we can't prescribe them. What we can prescribe is the pressure p_b. The reader can easily verify that in case $p_i > 0, p_b > 0$ and $\kappa \in (1,3)$ there is a unique $\delta > -1$ given by

$$\frac{\frac{p_b}{p_i} - (\kappa+1) + \sqrt{\left(\frac{p_b}{p_i}\right)^2 - 2\frac{p_b}{p_i}(\kappa-1)^2 + (\kappa-1)(3-\kappa)}}{\kappa(3-\kappa)}.$$

This quantity specifies the boundary state $\hat{\mathbf{q}}_{\mathbf{b}}$.

At this moment, what remains to be analyzed is the case $p = 4$. Let us introduce a new local notation

$$\delta_k = \frac{2\kappa\beta_k}{\varrho_i} \qquad k = 1,2,3,4$$

$$\vartheta = \delta_1 + \delta_2 + \delta_3 + \delta_4 + 1.$$

Substitution into (2.6.136) gives

$$\hat{\mathbf{q}}_{\mathbf{b}} = \frac{\varrho_i}{2\kappa} \begin{pmatrix} \vartheta \\ \vartheta\tilde{u}_i + (1-\delta_1)c_i \\ \vartheta\tilde{v}_i - \delta_3 c_i \\ \vartheta\tilde{w}_i - \delta_4 c_i \\ \frac{\vartheta\tilde{\mathbf{v}}_i^2}{2} - c_i(\delta_1\tilde{u}_i + \delta_3\tilde{v}_i + \delta_4\tilde{w}_i) + \frac{c_i^2}{\kappa-1} + \tilde{u}_i c_i * \delta_1\frac{c_i^2}{\kappa-1} \end{pmatrix} \tag{2.6.138}$$

and for the pressure

$$p_b = p_i \left(1 + \delta_1 - (\kappa - 1)\frac{(1-\delta_1)^2 + \delta_3^2 + \delta_4^2}{2\vartheta} \right).$$

Relation (2.6.138) further yields

$$\begin{array}{rcl} \varrho_b & = & \frac{\varrho_i}{2\kappa}\vartheta \\ \tilde{u}_b & = & \tilde{u}_i + \frac{1-\delta_1}{\vartheta}c_i \\ \tilde{v}_b & = & \tilde{v}_i - \frac{\delta_3 c_i}{\vartheta}c_i \\ \tilde{w}_b & = & \tilde{w}_i - \frac{\delta_4 c_i}{\vartheta}c_i \end{array}$$

and in case that

$$2 - \frac{2\kappa}{c_i}(\tilde{u}_b - \tilde{u}_i)(\varrho_b - \varrho_i) > (\kappa-1)\kappa\frac{\varrho_b - \varrho_i}{c_i^2}((\tilde{u}_b - \tilde{u}_i)^2 + (\tilde{v}_b - \tilde{v}_i)^2 + (\tilde{w}_b - \tilde{w}_i)^2),$$

the pressure p will also be positive.

Prescribing three velocity components and the pressure we would get a restricting condition again. If we wanted to give both density and pressure, the constants $\delta_1, \delta_2, \delta_3$ and δ_4 would not exist in general, because one of them would always be a solution to a quadratic equation with possibly complex roots. We see that the specification of $\beta_1, \beta_2, \beta_3$ and β_4 requires to prescribe the density and three velocity components.

Now we could start investigations which further quantities (like speed of sound, entropy etc.) we could prescribe. Since we do not think there is necessity to do it now, we proceed to the next section.

2.7 Numerical flux through boundary sides

In the previous section we briefly investigated what variables can be prescribed at the boundary of Ω. Consequently, we are going to construct relations describing numerical flux through a side $\partial\Omega_{ij} \subset \partial\Omega$. Since ideas we will use in this section are similar to those from section **2.4**, there is no need to explain them in detail as above.

2.7.1 Inlet and outlet

We will to approximate integral (2.1.21) by the term (2.4.98) using again the complete notation from section **2.4**. The value $\mathbf{T}_{ij}\mathbf{q}_{ij}$ will be approximated by $\hat{\mathbf{q}}_{\mathbf{b}} = \hat{\mathbf{q}}_R(0)$ again, where $\hat{\mathbf{q}}(\mathbf{x},t) = \hat{\mathbf{q}}_R(x/t)$ is an exact solution to the boundary Riemann problem

$$\frac{\partial}{\partial t}\hat{\mathbf{q}}(x,t) + \frac{\partial}{\partial x}\mathbf{f}(\hat{\mathbf{q}}(x,t)) = 0 \qquad (x,t) \in \mathbb{R}^- \times \mathbb{R}^+ \tag{2.7.139}$$

$$\hat{\mathbf{q}}(x,0) = \tilde{\mathbf{q}}_{\mathbf{i}} = \mathbf{T}_{ij}(\mathbf{q}_{\mathbf{i}}) \qquad x < 0 \tag{2.7.140}$$

$$\hat{B}(\hat{\mathbf{q}}(0,t)) = 0 \qquad t > 0. \tag{2.7.141}$$

Here the operator $\hat{B} : \mathcal{Q} \to \mathbb{R}^p$ $p \in \{1, 2, \dots, 5\}$ represents the p boundary conditions. In case of the linearized problem number of prescribed boundary conditions equals to the number of negative eigenvalues of the matrix $\mathbf{A}(\tilde{\mathbf{q}}_{\mathbf{i}})$. Our boundary state can be written in the form

$$\hat{\mathbf{q}}_{\mathbf{b}} = \sum_{k=1}^{p} \beta_k \mathbf{r}_{\mathbf{k}}(\tilde{\mathbf{q}}_{\mathbf{i}}) + \sum_{k=p+1}^{5} \alpha_k \mathbf{r}_{\mathbf{k}}(\tilde{\mathbf{q}}_{\mathbf{i}}) = \tilde{\mathbf{q}}_{\mathbf{i}} + \sum_{k=1}^{p} (\beta_k - \alpha_k)\mathbf{r}_{\mathbf{k}}(\tilde{\mathbf{q}}_{\mathbf{i}}). \tag{2.7.142}$$

Constants $\beta_1, \beta_2, \dots, \beta_5$ are to be specified by the boundary condition. By (2.7.142) $\tilde{\mathbf{q}}_{\mathbf{i}}$ and $\hat{\mathbf{q}}_{\mathbf{b}}$ can be connected by a piecewise linear continuous curve in $\mathbb{R}^5$ consisting of abscissas $\mathbf{q}^{(1)}, \mathbf{q}^{(2)}, \dots, \mathbf{q}^{(p)}$ so that to every of them the appropriate eigenvector of $\mathbf{A}(\tilde{\mathbf{q}}_{\mathbf{i}})$ is tangential, as follows:

$$\begin{gathered}
\mathbf{q}^{(j)} : (0, \xi_j) \to \mathbb{R}^5 \qquad j = 1, 2, \dots, p \\
\mathbf{q}^{(1)}(0) = \tilde{\mathbf{q}}_{\mathbf{i}} \\
\mathbf{q}^{(j)}(\xi_j) = \mathbf{q}^{(j+1)}(0) \qquad j = 1, 2, \dots, p-1 \\
\mathbf{q}^{(p)}(\xi_p) = \hat{\mathbf{q}}_{\mathbf{b}}.
\end{gathered}$$

These curves can be written for example in the form

$$\mathbf{q}^{(j)}(\xi) = \tilde{\mathbf{q}}_{\mathbf{i}} + \sum_{k=1}^{j-1} (\beta_k - \alpha_k)\mathbf{r}_{\mathbf{k}}(\tilde{\mathbf{q}}_{\mathbf{i}}) + \xi \mathbf{r}_{\mathbf{j}}(\tilde{\mathbf{q}}_{\mathbf{i}}) \qquad \xi \in (0, \beta_j - \alpha_j) \qquad j = 1, 2, \dots, p.$$

We will generalize this idea to the nonlinear system. Let us suppose that analogously as in the previous case the states $\tilde{\mathbf{q}}_{\mathbf{i}}$ and $\hat{\mathbf{q}}_{\mathbf{b}}$ can be connected by a piecewise smooth curve consisting of parts of the curves $\mathbf{q}^{(1)}, \mathbf{q}^{(2)}, \dots, \mathbf{q}^{(p)}$, which we defined in subsection **2.2.8**.

These curves must satisfy

$$\mathbf{q}^{(1)}(0) = \tilde{\mathbf{q}}_{\mathbf{i}} \tag{2.7.143}$$
$$\mathbf{q}^{(j)}(\xi_j) = \mathbf{q}^{(j+1)}(0) \qquad j = 1, 2, \ldots, p-1 \tag{2.7.144}$$
$$\mathbf{q}^{(p)}(\xi_p) = \hat{\mathbf{q}}_{\mathbf{b}}. \tag{2.7.145}$$

There are $p-1$ unknown states between $\tilde{\mathbf{q}}_{\mathbf{i}}$ and $\hat{\mathbf{q}}_{\mathbf{b}}$ and every one of them contains five unknown components. With further five unknown components of the boundary state $\hat{\mathbf{q}}_{\mathbf{b}} \in \mathbb{R}^5$ we have $5p$ unknowns. Knowing that every one of the mentioned curves is accompanied by four Riemann invariants and having p equations more from the boundary condition, we can write a new system of equations. The solution is the unknown boundary state $\hat{\mathbf{q}}_{\mathbf{b}}$.

Let us now analyze various situations which can appear at an inlet or outlet element of the domain.

In case $p = 0$, it is $\tilde{u}_i - c_i \geq 0$ which means the sonic or subsonic outlet. The equation (2.7.142) yields $\hat{\mathbf{q}}_{\mathbf{b}} = \tilde{\mathbf{q}}_{\mathbf{i}}$ and

$$\mathbf{f}_R(\tilde{\mathbf{q}}_{\mathbf{i}}, \hat{\mathbf{q}}_{\mathbf{b}}) = \mathbf{f}(\hat{\mathbf{q}}_{\mathbf{b}}) - \int_{\tilde{\mathbf{q}}_{\mathbf{i}}}^{\hat{\mathbf{q}}_{\mathbf{b}}} \mathbf{A}^{+}(\mathbf{q}) \mathrm{d}\mathbf{q} = \mathbf{f}(\hat{\mathbf{q}}_{\mathbf{b}}).$$

In case $p = 1$, it is $\tilde{u}_i - c_i < 0$ and $\tilde{u}_i \geq 0$ which means the subsonic outlet. Remembering Riemann invariants corresponding to the curve $\mathbf{q}^{(1)}$, we easily obtain

$$\begin{aligned}
\varrho_b &= \left(\frac{p_b}{p_i}\right)^{\frac{1}{\kappa}} \varrho_i \\
c_b &= \sqrt{\kappa \frac{p_b}{\varrho_b}} \\
\tilde{u}_b &= \tilde{u}_i + \frac{2}{\kappa - 1}(c_i - c_b) \\
\tilde{v}_b &= \tilde{v}_i, \quad \tilde{w}_b = \tilde{w}_i.
\end{aligned}$$

Remark 2.2.11 says that the first eigenvalue of the matrix $\mathbf{A}(\mathbf{q})$ can change its sign along the curve $\mathbf{q}^{(1)}$. Since we prescribe only the boundary pressure p_b, we should verify whether this sign change is possible. Relation

$$\lambda_1(\hat{\mathbf{q}}_{\mathbf{b}}) = \tilde{u}_b - c_b \geq 0$$

yields

$$\tilde{u}_i + \frac{2}{\kappa - 1} c_i \geq \frac{\kappa + 1}{\kappa - 1} \sqrt{\kappa \frac{p_b}{\left(\frac{p_b}{p_i}\right)^{\frac{1}{\kappa}} \varrho_i}}$$

and consequently

$$p_b \leq \left(\frac{\tilde{u}_i + \frac{2}{\kappa - 1} c_i}{\frac{\kappa+1}{\kappa-1} \sqrt{\kappa \frac{p_i^{1/\kappa}}{\varrho_i}}} \right)^{\frac{2}{1 - 1/\kappa}}.$$

Analogously as in remark 2.2.11 we compute

$$\tilde{u}_i^s = c_i^s, \qquad \tilde{u}_i^s + \frac{2}{\kappa-1}c_i^s = \tilde{u}_i + \frac{2}{\kappa-1}c_i$$

$$\tilde{u}_i^s = \frac{\kappa-1}{\kappa+1}(\tilde{u}_i + \frac{2}{\kappa-1}c_i)$$

$$p_i^s = \frac{\varrho_i^s(\tilde{u}_i^s)^2}{\kappa} = \frac{p_i}{\varrho_i}(\varrho_i^s)^\kappa, \qquad \varrho_i^s = \left(\frac{(\tilde{u}_i^s)^2\varrho_i}{\kappa p_i}\right)^{\frac{1}{\kappa-1}}$$

and finally $\tilde{v}_i^s = \tilde{v}_i$, $\tilde{w}_i^s = \tilde{w}_i$.

Relation $$\int_{\tilde{\mathbf{q}}_\mathbf{i}}^{\hat{\mathbf{q}}_\mathbf{b}} \mathbf{A}^+(\mathbf{q})\mathrm{d}\mathbf{q} = \left\{ \begin{array}{cc} 0 & \lambda_1(\hat{\mathbf{q}}_\mathbf{b}) < 0 \\ \mathbf{f}(\hat{\mathbf{q}}_\mathbf{b}) - \mathbf{f}(\tilde{\mathbf{q}}_\mathbf{i}^\mathbf{s}) & \lambda_1(\hat{\mathbf{q}}_\mathbf{b}) \geq 0 \end{array} \right\}$$

gives us the approximate Riemann solver

$$\mathbf{f}_R(\tilde{\mathbf{q}}_\mathbf{i}, \hat{\mathbf{q}}_\mathbf{b}) = \left\{ \begin{array}{cc} \mathbf{f}(\hat{\mathbf{q}}_\mathbf{b}) & \lambda_1(\hat{\mathbf{q}}_\mathbf{b}) < 0 \\ \mathbf{f}(\tilde{\mathbf{q}}_\mathbf{i}^\mathbf{s}) & \lambda_1(\hat{\mathbf{q}}_\mathbf{b}) \geq 0 \end{array} \right\}.$$

In case $p = 4$ we have $\tilde{u}_i < 0$ and $\tilde{u}_i + c_i \geq 0$ which means the subsonic or sonic inlet. Between the states $\tilde{\mathbf{q}}_\mathbf{i}$ and $\hat{\mathbf{q}}_\mathbf{b}$ there are three intersection points and the curve, which we will integrate along, consists of parts of the curves $\mathbf{q}^{(1)}, \mathbf{q}^{(2)}, \mathbf{q}^{(3)}$ and $\mathbf{q}^{(4)}$. There is only one of these three states $\tilde{\mathbf{q}}_\mathbf{H} = \mathbf{q}^{(1)}(\xi_1) = \mathbf{q}^{(2)}(0)$ important for us, because between it and the boundary state $\hat{\mathbf{q}}_\mathbf{b}$ the eigenvalue u of the matrix $\mathbf{A}$ cannot change its sign. According to the results from section **2.6**, the most suitable alternative is to prescribe $\varrho_b, \tilde{u}_b, \tilde{v}_b$ and $\tilde{w}_b$ and compute the boundary pressure p_b. Remembering Riemann invariants corresponding to the curves $\mathbf{q}^{(1)}, \mathbf{q}^{(2)}, \mathbf{q}^{(3)}$ and $\mathbf{q}^{(4)}$, we immediately obtain

$$c_H = c_i + \frac{\kappa-1}{2}(\tilde{u}_i - \tilde{u}_b), \quad \varrho_H = \left(\frac{c_H^2\varrho_i}{\kappa p_i}\right)^{\frac{1}{\kappa-1}} \varrho_i, \quad p_H = \frac{\varrho_H c_H^2}{\kappa}$$
$$\tilde{u}_H = \tilde{u}_b, \quad \tilde{v}_H = \tilde{v}_i, \quad \tilde{w}_H = \tilde{w}_i \quad \text{and} \quad p_H = p_b.$$

On the curve $\mathbf{q}^{(1)}$, between $\tilde{\mathbf{q}}_\mathbf{i}$ and $\hat{\mathbf{q}}_\mathbf{b}$ the sonic point $\tilde{\mathbf{q}}_\mathbf{i}^\mathbf{s}$ can exist. Using $\tilde{\mathbf{q}}_\mathbf{i}$ and $\tilde{\mathbf{q}}_\mathbf{H}$ we can compute it in the same way as in the previous case. Having these results, we can start the integration:

$$\int_{\tilde{\mathbf{q}}_\mathbf{i}}^{\tilde{\mathbf{q}}_\mathbf{H}} \mathbf{A}^+(\mathbf{q})\mathrm{d}\mathbf{q} = \left\{ \begin{array}{cc} 0 & \lambda_1(\tilde{\mathbf{q}}_\mathbf{H}) < 0 \\ \mathbf{f}(\tilde{\mathbf{q}}_\mathbf{H}) - \mathbf{f}(\tilde{\mathbf{q}}_\mathbf{i}^\mathbf{s}) & \lambda_1(\tilde{\mathbf{q}}_\mathbf{H}) \geq 0 \end{array} \right\}$$
$$\int_{\tilde{\mathbf{q}}_\mathbf{H}}^{\hat{\mathbf{q}}_\mathbf{b}} \mathbf{A}^+(\mathbf{q})\mathrm{d}\mathbf{q} = \left\{ \begin{array}{cc} 0 & \lambda_2(\hat{\mathbf{q}}_\mathbf{b}) < 0 \\ \mathbf{f}(\hat{\mathbf{q}}_\mathbf{b}) - \mathbf{f}(\tilde{\mathbf{q}}_\mathbf{H}) & \lambda_2(\hat{\mathbf{q}}_\mathbf{b}) \geq 0 \end{array} \right\}.$$

The approximate Riemann solver $\mathbf{f}_R(\tilde{\mathbf{q}}_{\mathbf{i}}, \hat{\mathbf{q}}_{\mathbf{b}})$ has the form

$$\mathbf{f}_R(\tilde{\mathbf{q}}_{\mathbf{i}}, \hat{\mathbf{q}}_{\mathbf{b}}) = \left\{ \begin{array}{cc} \mathbf{f}(\hat{\mathbf{q}}_{\mathbf{b}}) & \lambda_1(\tilde{\mathbf{q}}_{\mathbf{H}}) < 0, \lambda_2(\hat{\mathbf{q}}_{\mathbf{b}}) < 0 \\ \mathbf{f}(\hat{\mathbf{q}}_{\mathbf{b}}) + \mathbf{f}(\tilde{\mathbf{q}}_{\mathbf{i}}^{\mathbf{s}}) - \mathbf{f}(\tilde{\mathbf{q}}_{\mathbf{H}}) & \lambda_1(\tilde{\mathbf{q}}_{\mathbf{H}}) \geq 0, \lambda_2(\hat{\mathbf{q}}_{\mathbf{b}}) < 0 \\ \mathbf{f}(\tilde{\mathbf{q}}_{\mathbf{H}}) & \lambda_1(\tilde{\mathbf{q}}_{\mathbf{H}}) < 0, \lambda_2(\hat{\mathbf{q}}_{\mathbf{b}}) \geq 0 \\ \mathbf{f}(\tilde{\mathbf{q}}_{\mathbf{i}}^{\mathbf{s}}) & \lambda_1(\tilde{\mathbf{q}}_{\mathbf{H}}) \geq 0, \lambda_2(\hat{\mathbf{q}}_{\mathbf{b}}) \geq 0 \end{array} \right\}.$$

In the following subsection we will occupy ourselves with the numerical flux through solid walls.

2.7.2 Solid wall

To obtain a good description of the numerical flux through solid walls, we will not need to solve any Riemann problem this time, although it would be possible. The integral

$$\int_{\partial\Omega_{ij}} \mathbf{f}(\mathbf{q}(\mathbf{x},t))\nu_{ij\,1} + \mathbf{g}(\mathbf{q}(\mathbf{x},t))\nu_{ij\,2} + \mathbf{h}(\mathbf{q}(\mathbf{x},t))\nu_{ij\,3}\mathrm{d}S$$

defined by (2.1.21) has in the corresponding local coordinates the form

$$\int_{\partial\Omega_{ij}} \mathbf{f}(\tilde{\mathbf{q}}(\tilde{\mathbf{x}},t))\mathrm{d}S. \tag{2.7.146}$$

Since we neglect the viscosity, we require only $\tilde{u}(\tilde{\mathbf{x}},t) = 0$ at the solid wall, which does not contradict the solution to our problem. Using the flux definition, we can rewrite (2.7.146) as

$$\int_{\partial\Omega_{ij}} (0,p,0,0,0)^T(\tilde{\mathbf{x}},t)\mathrm{d}S.$$

Setting $p = p_i$, we obtain the approximate Riemann solver in the form

$$\mathbf{f}_R(\tilde{\mathbf{q}}_{\mathbf{i}}, \hat{\mathbf{q}}_{\mathbf{b}}) = \mu_2(\partial\Omega_{ij})(0,p_i,0,0,0)^T.$$

Our theoretical basis is now so strong that we can proceed to our first numerical experiments.

3 Numerical experiments

In this chapter we will present results of some computations performed with the aid of the four numerical fluxes developed above. Before we do this, let us make a useful remark: when we return to the matrix $\mathbf{A}(\mathbf{q})$ defined by (2.2.25) setting $w = 0$ and leaving out its fourth column and fourth row, we get exactly its two-dimensional form. Formally, following the whole technique (eigenvalues, eigenvectors, Riemann invariants etc.) once again with $w = 0$ leaving out fourth vector coordinates and forgetting zero-relations we construct the two-dimensional version of all the mentioned methods. We hope that having understood this indication, the reader is able to carry out remaining details by himself. Thus, our three-dimensional schemes can be easily used also for two-dimensional (and analogously for one-dimensional) problems which will be of great use for us, because we will see there is a big difference in time requirements. Now let us shortly mention the dimensionless Euler equations.

3.1 Dimensionless Euler equations

Let Ω be a three-dimensional bounded domain occupied by the fluid. We choose three constants $l_{ref}, u_{ref}, \varrho_{ref}$ – characteristic length of the domain, characteristic velocity and characteristic density of the flow. Further, we define the characteristic time $t_{ref} = l_{ref}/u_{ref}$. In the system (7) we divide the first equation by

$$\frac{\varrho_{ref} u_{ref}}{l_{ref}},$$

further three equations by

$$\frac{\varrho_{ref} u_{ref}^2}{l_{ref}},$$

the last equation by

$$\frac{\varrho_{ref} u_{ref}^3}{l_{ref}}$$

and use the notation

$$\begin{aligned} \tilde{t} &= t/t_{ref} \\ \tilde{\varrho} &= \varrho/\varrho_{ref} \\ \tilde{u} &= u/u_{ref} \\ \tilde{v} &= v/u_{ref} \\ \tilde{w} &= w/u_{ref} \\ \tilde{p} &= p/(\varrho_{ref} u_{ref}^2) \\ \tilde{E} &= E/(\varrho_{ref} u_{ref}^2) \end{aligned} \quad .$$

We see that the dimensionless system has again the form (7), which is a very agreeable fact because we do not have to change our methods or our software for its numerical solution. It is due to the zero right side in our case. In case of the non-homogeneous Euler equations and the Navier-Stokes equations the two systems are different. More details about similarity of flows can be found in [13].

3.2 Testing methods

In this section we will present conclusions we have obtained on the basis of two-dimensional numerical experiments. For this purpose we use the test GAMM channel (see also [14], [10], [21], [33] etc.).

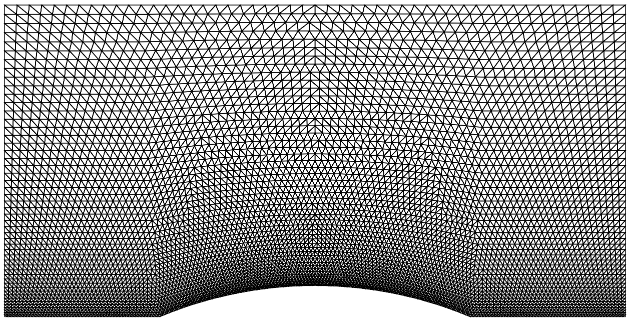

Fig.3.2.1 - Grid on the GAMM channel

This channel is 2m long, 1m high and there is a 10cm high circular cap centered in the middle of its bottom. The fluid (in our case air) flows through it in the x-direction. Since our scheme is not adaptive yet, the triangular mesh we use has to be quite fine. This triangulation (see Fig.3.2.1) contains 5924 grid points and 11476 elements. The inlet and outlet boundary conditions are identical with the initial one:

$$\begin{aligned} \varrho_0 &= 1.5\,\mathrm{kg/m^3} \\ u_0 &= 205.709277\,\mathrm{m/s} \\ v_0 &= 0\,\mathrm{m/s} \\ p_0 &= 101000\,\mathrm{Pa} \end{aligned}$$

i.e. $M = 0.67$, the dimensionless form of which is

$$\begin{aligned} \tilde{\varrho_0} &= 1 \\ \tilde{u_0} &= 1 \\ \tilde{v_0} &= 0 \\ \tilde{p_0} &= 1.5911911657 \end{aligned}.$$

Since the proposed FVM method is explicit, it is necessary to introduce a stability condition. To keep the developing solution l^1 stable, we take over the CFL condition from [38]:

$$\frac{\triangle t_k}{|\Omega_i|} \max_{j \in \mathcal{N}(i)} |\partial\Omega_{ij}| \varrho(\mathbf{A}(\mathbf{T_{ij}q_i^k})) \leq CFL.$$

For the l^∞ stability we use another CFL condition from [13]:

$$\frac{\triangle t_k}{|\Omega_i|} |\partial\Omega_i| \max_{j \in \mathcal{N}(i)} \varrho(\mathbf{A}(\mathbf{T_{ij}q_i^k})) \leq CFL.$$

The CFL value is so-called *Courant-Friedrichs-Lewy constant* lying in the open interval (0, 1). The reader can easily verify that for dimensionless computations these conditions remain unchanged. The approximate steady-state solution is considered stabilized when the residuum is small enough. In our numerical experiments we use a slightly weaker criterion, namely the l^∞ norm of the relative density error

$$\max_{i=1,\ldots,N} \frac{|\varrho_i^{k+1} - \varrho_i^k|}{\varrho_i^k}$$

or

$$\frac{1}{N}\sum_{i=1}^{N} \frac{|\varrho_i^{k+1} - \varrho_i^k|}{\varrho_i^k}$$

i.e. its l^1 norm. To describe the convergence history, we plot a graph of the decimal logarithm of these values. Since many time iterations are needed, we give their number in thousands. In our conception the time-step is left constant during one time step. In case at an element negative density or pressure are computed, they are set to a suitable small positive constant. This approach is slightly different from the approach used in [26].

In the following figures we show results of this comparison. The reader can look at them, compare them by himself and after having done it, there is our conclusion in the end. All the four computations proceeded under exactly identical conditions, there was the only difference in the numerical flux used.

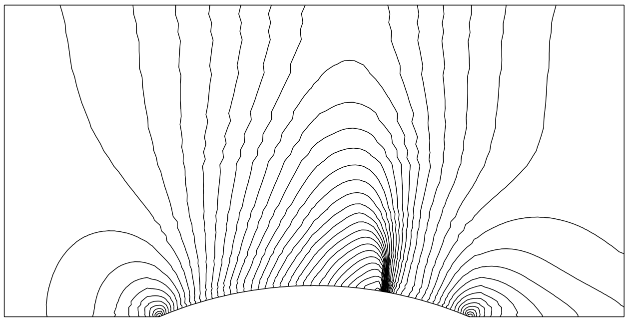

Fig.3.2.2 - Mach number isolines, Steger-Warming method

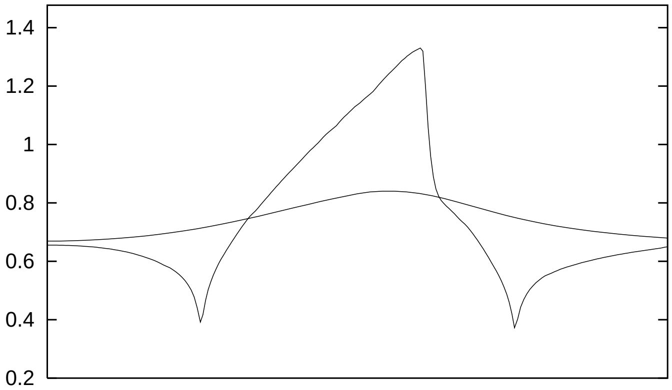

Fig.3.2.3 - Mach number at the solid walls, Steger-Warming method

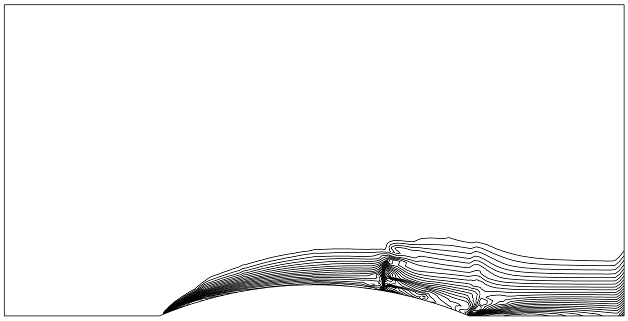

Fig.3.2.4 - Entropy distribution, Steger-Warming method

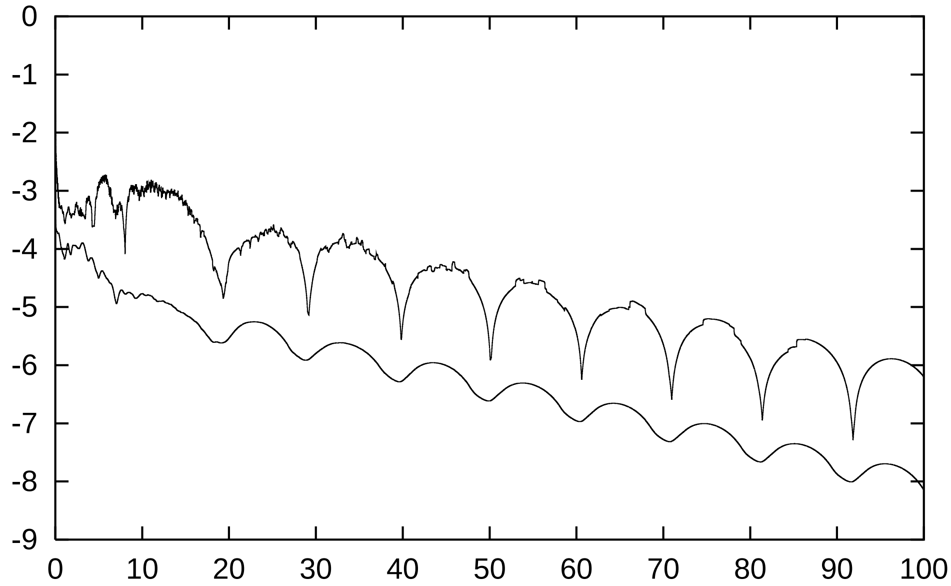

Fig.3.2.5 - Convergence histogram, Steger-Warming method

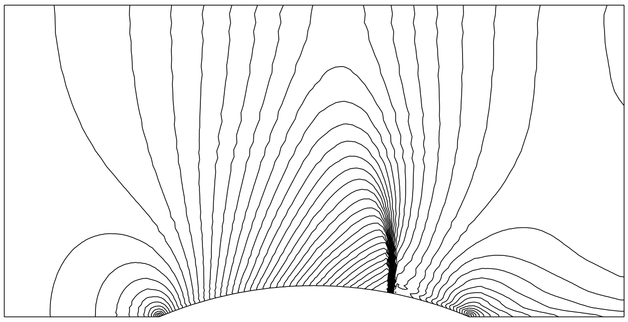

Fig.3.2.6 - Mach number isolines, VanLeer method

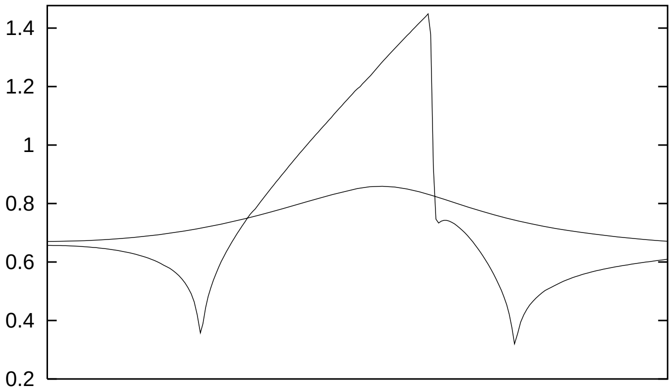

Fig.3.2.7 - Mach number at the solid walls, Van-Leer method

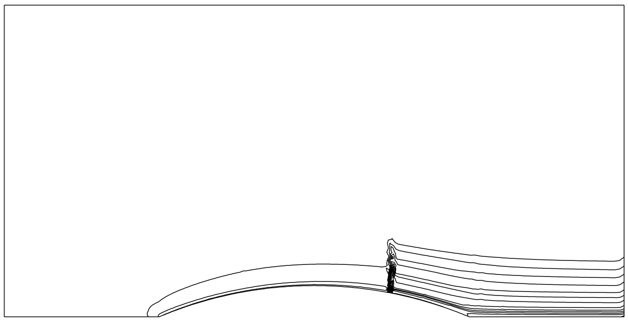

Fig.3.2.8 - Entropy distribution, VanLeer method

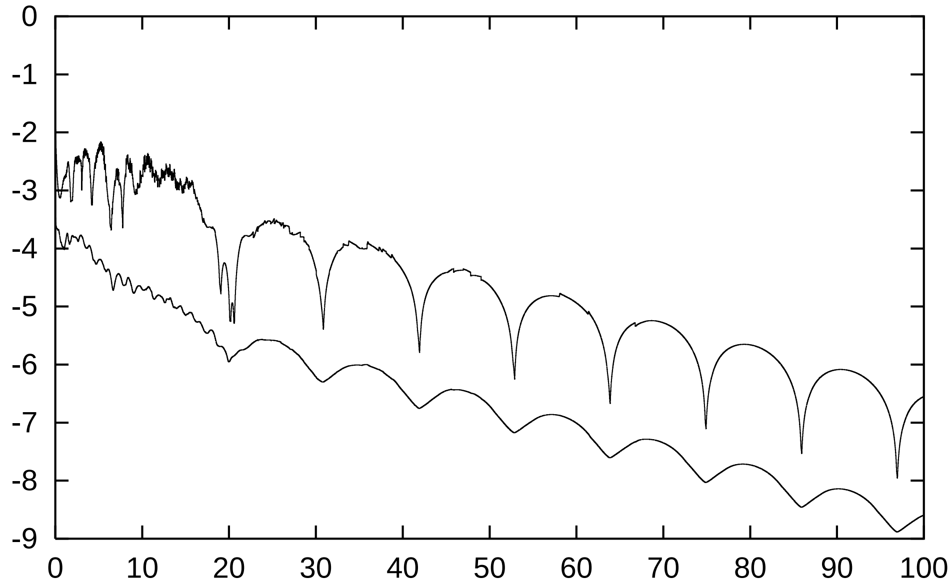

Fig.3.2.9 - Convergence histogram, VanLeer method

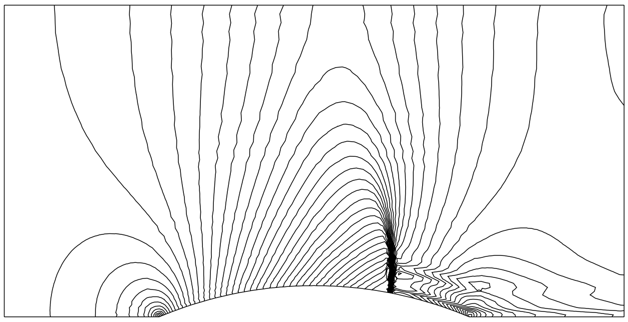

Fig.3.2.10 - Mach number isolines, Vijayasundaram method

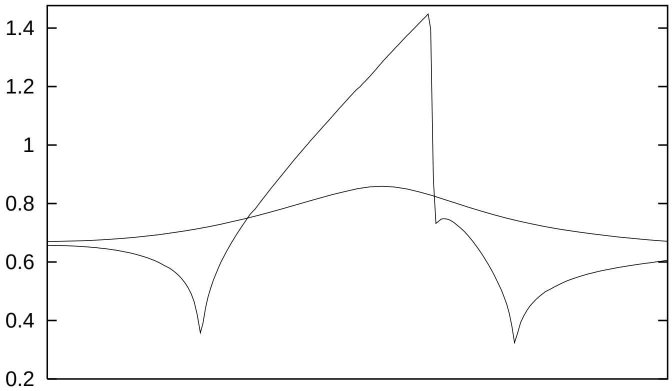

Fig.3.2.11 - Mach number at the solid walls, Vijayasundaram method

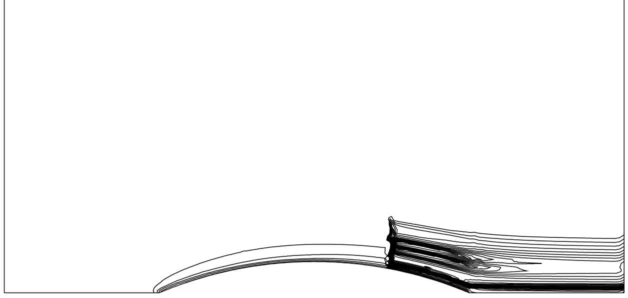

Fig.3.2.12 - Entropy distribution, Vijayasundaram method

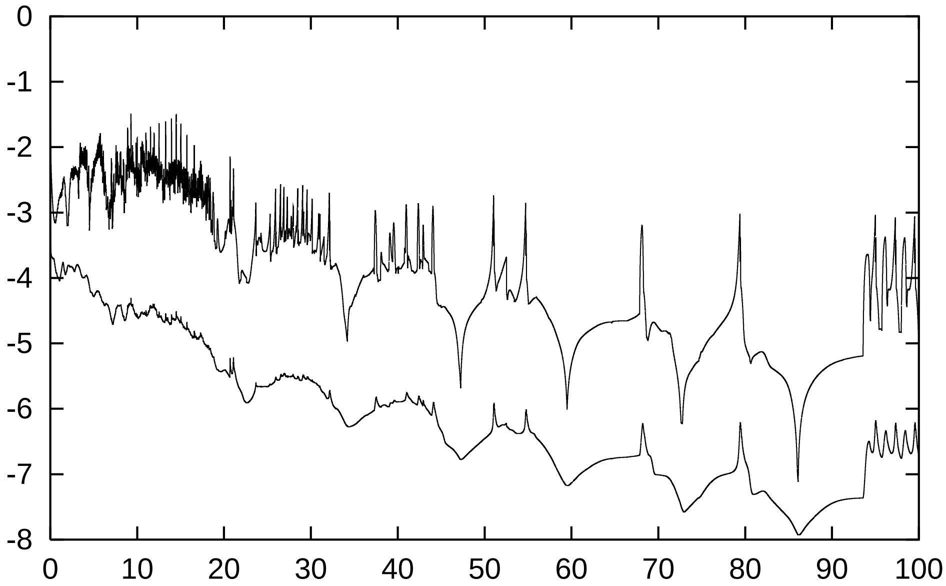

Fig.3.2.13 - Convergence histogram, Vijayasundaram method

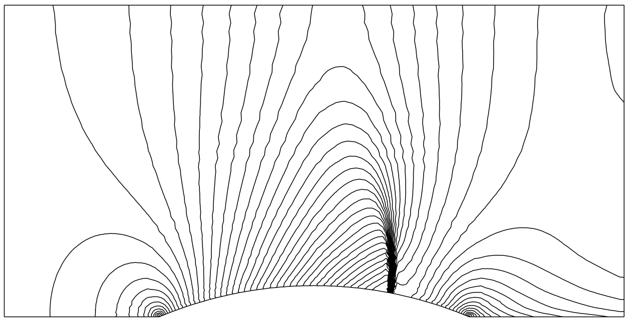

Fig.3.2.14 - Mach number isolines, Osher-Solomon method

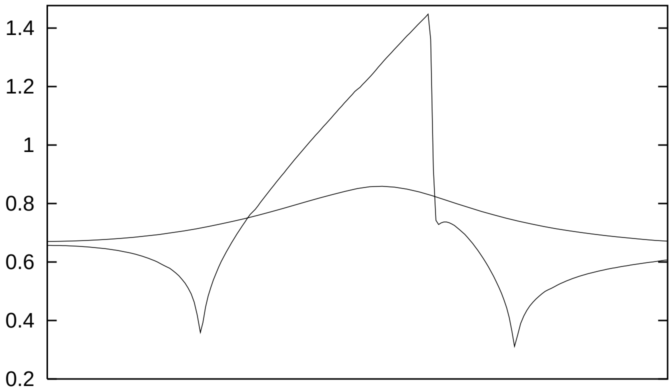

Fig.3.2.15 - Mach number at the solid walls, Osher-Solomon method

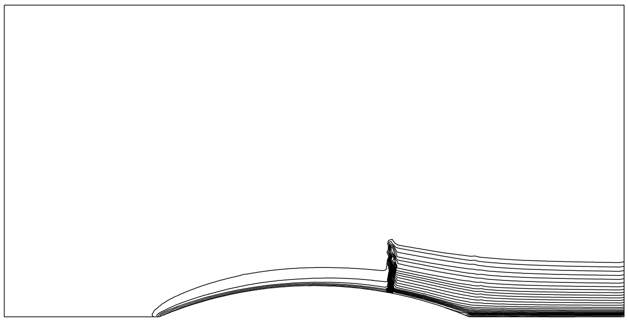

Fig.3.2.16 - Entropy distribution, Osher-Solomon method

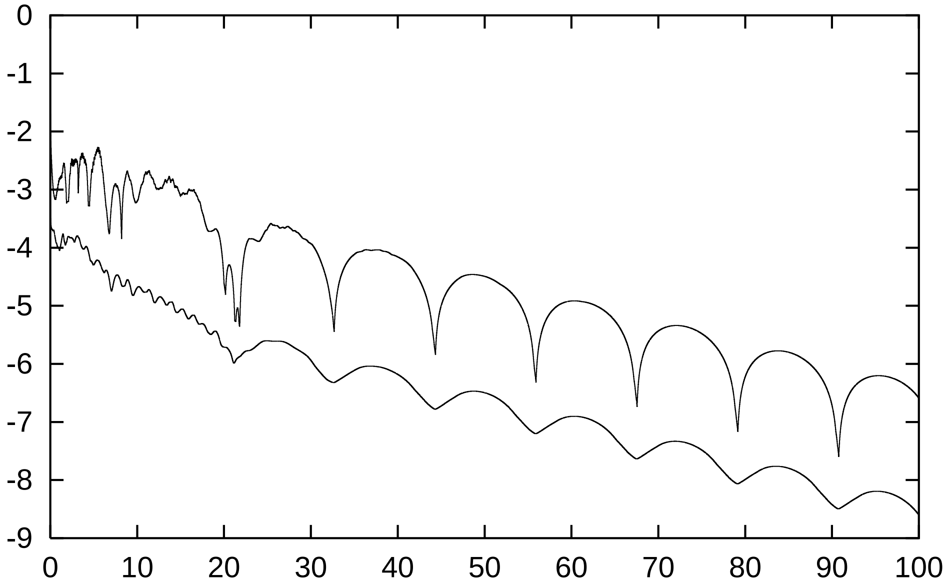

Fig.3.2.17 - Convergence histogram, Osher-Solomon method

3.2.1 Conclusion

In our opinion, a numerical scheme for solving the Euler equations is satisfactory when it is able to focus the shock wave (especially in our case it means to capture the so-called *Zierep singularity* i.e. Mach number at the cap is immediately after the shock increasing), to describe well the shock size (in our case Mach number at the cap falls from 1.44 to 0.72 approximately), to distribute entropy through the domain correctly and to keep prescribed boundary conditions. There are additional points of view – time requirement of the methods and their stability.

As far as boundary conditions are concerned, we found no great difference, which is probably due to our universal boundary treatment. We show later that there is also a strong dependence between the boundary numerical flux and the convergence history.

In case of the Steger-Warming scheme there is no Zierep singularity, the shock size is underestimated and the entropy is increasing along the circular cap disproportionately.

The other schemes captured the Zierep singularity much better (it is obvious that they were limited by the grid) and distributed the entropy more correctly as well. In case of the Vijayasundaram scheme there were great stability problems (see Fig.3.2.13) which caused defects in Mach number and entropy isolines (see Fig. 3.2.10 and Fig.3.2.12). This example documents clearly that we cannot rely on the convergence histogram absolutely – since the l^∞ norm falls under -7 and the l^1 norm under -8, we would probably say the solution is satisfactory.

There is one more important thing to be mentioned – the Osher-Solomon scheme needed approximately three-times less computer time than the other ones.

3.3 Testing fixed boundary conditions

Numerical treatment of boundary conditions has a fundamental influence on the progress of the computation and on its results. Especially the numerical flux through inlet and outlet sides is important because it decides which boundary informations and how much influence the solution inside. Since the relations we have deduced in **2.6** extrapolate physical quantities the characteristics of which are going out of the domain, we call them *extrapolated*. In some papers (see [31], [37] e.g.) boundary conditions are *fixed*. It means the inlet and outlet numerical flux is computed in the same way as the flux inside (nothing is extrapolated explicitly, boundary conditions are used in the full form) and it depends on the inside numerical flux only how it handles boundary informations.

To show differences of these two approaches, we performed one more two-dimensional numerical experiment the results of which are shown in Fig.3.3.1 - Fig.3.3.21. This computation proceeded by using the Osher-Solomon method. An advantage of the fixed approach (see Fig.3.3.10 - Fig.3.3.12) is acceleration of the iterative process. On the other hand (see Fig.3.3.1 - Fig.3.3.9) there are great discords in shape of isolines, position of the shock wave (in our case about 8cm), size of the shock and size of physical quantities at the solid walls. Let us now fix the boundary conditions and try to find, where the differences come from.

First, numerical fluxes developed by Steger-Warming, VanLeer and Vijayasundaram, to computation of which many matrix operations are needed, do not allow us to understand, how informations about the boundary condition are propagated into the domain. In this sense, the situation is more clear in case of the Osher-Solomon scheme and we will now take advantage of it. Let Ω_2 be a fictive outlet element, $\mathbf{q_2}$ its state vector and Ω_1 its neighbour outlet element with the state $\mathbf{q_1}$, both state vectors expressed in corresponding local coordinates. Let us consider the situation (see Diagram 2.5.1) $\lambda_1(\mathbf{q_1}) \geq 0$, $\lambda_1(\mathbf{q_A}) < 0$, $\lambda_2(\mathbf{q_1}) \geq 0$, $\lambda_5(\mathbf{q_D}) \geq 0$ and $\lambda_5(\mathbf{q_2}) \geq 0$, which can appear in case of subsonic outlet condition prescribed. Handling classically, we would extrapolate all the physical quantities from Ω_1 to Ω_2 (which is correct) but the fixed scheme gives the flux $\mathbf{f}(\mathbf{q_1}) + \mathbf{f}(\mathbf{q_A}) - \mathbf{f}(\mathbf{q_1^S})$ i.e. allows that information from Ω_2 influences the state $\mathbf{q_1}$ in the next time step. This was the simplest example but we see that there are really a very few situations only in which the boundary informations are handled correctly.

Further, it is very easy to show that for a steady flow the continuity equation gives

$$\int_{\partial\Omega} \varrho\mathbf{v}.\mathbf{n}\mathrm{dS} = 0. \tag{3.3.147}$$

Being aware of our solid wall boundary condition, this can be changed to the form

$$\int_{\partial\Omega_{\text{inlet}}} \varrho\mathbf{v}.\mathbf{n}\mathrm{dS} + \int_{\partial\Omega_{\text{outlet}}} \varrho\mathbf{v}.\mathbf{n}\mathrm{dS} = 0. \tag{3.3.148}$$

In case we extrapolate, we do not have to prescribe ϱ and $\mathbf{v}$ at outlet, which is very agreeable because due to the conservativity of FVM the relation (3.3.148) will be satisfied. In case we fix the boundary conditions, characteristics are not respected. Well, we can arrange the outlet density and velocity together in order that they meet (3.3.148), but we do not know anything about their proportion. In other words, in the beginning of the computation we would have to prescribe its results. Otherwise, our result would be a solution to a quite different problem (see Fig.3.3.13 - Fig.3.3.21; here the x-axis follows direction upward in the domain).

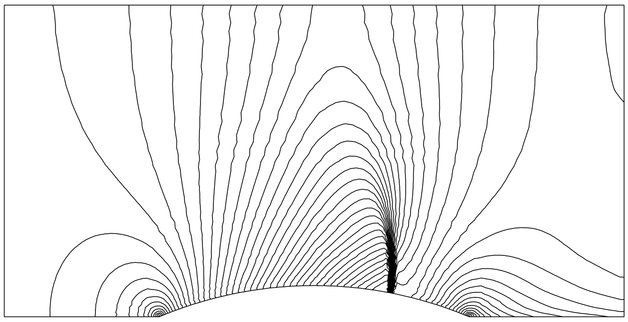

Fig.3.3.1 - Mach number isolines: both inlet and outlet extrapolated

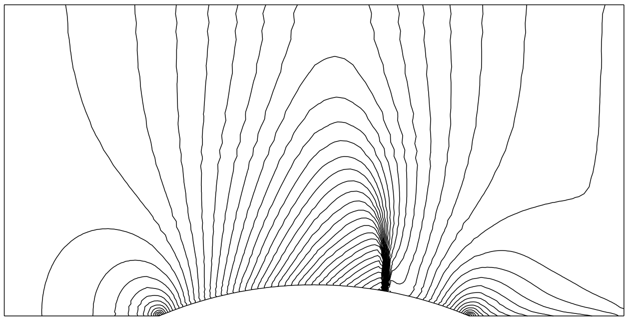

Fig.3.3.2 - Mach number isolines: inlet fixed, outlet extrapolated

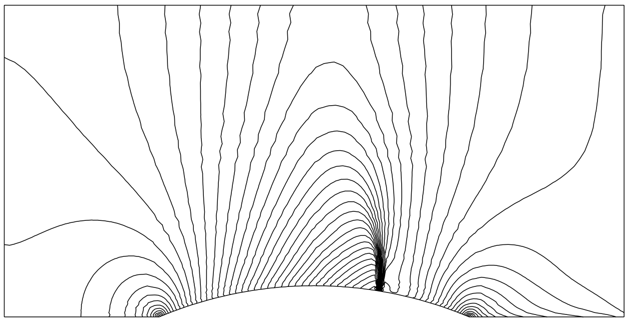

Fig.3.3.3 - Mach number isolines: both inlet and outlet fixed

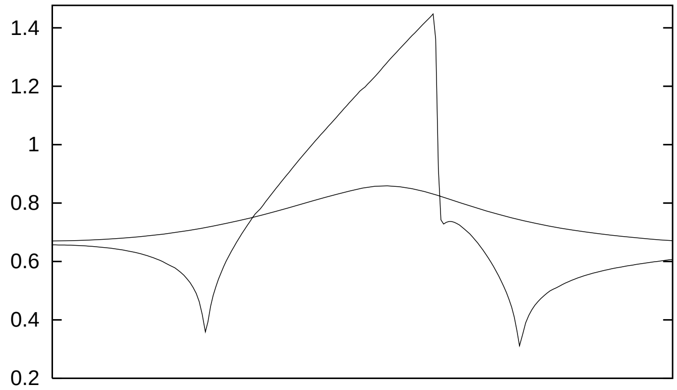

Fig.3.3.4 - Mach number at the walls: both inlet and outlet extrapolated

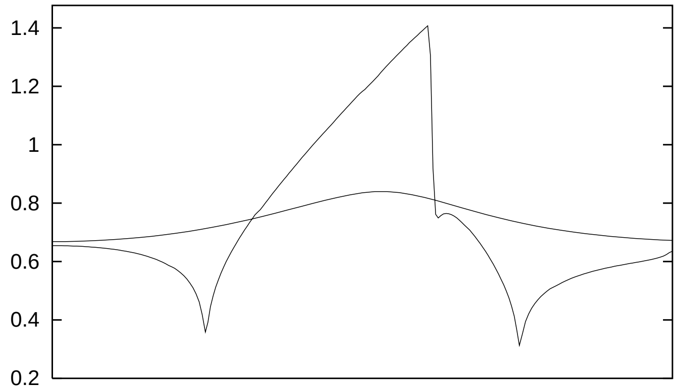

Fig.3.3.5 - Mach number at the walls: inlet fixed, outlet extrapolated

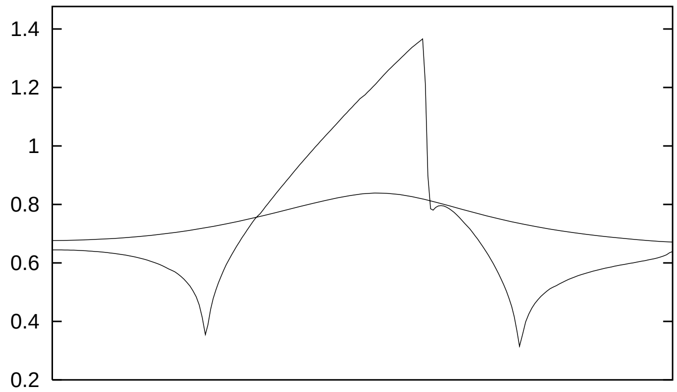

Fig.3.3.6 - Mach number at the walls: both inlet and outlet fixed

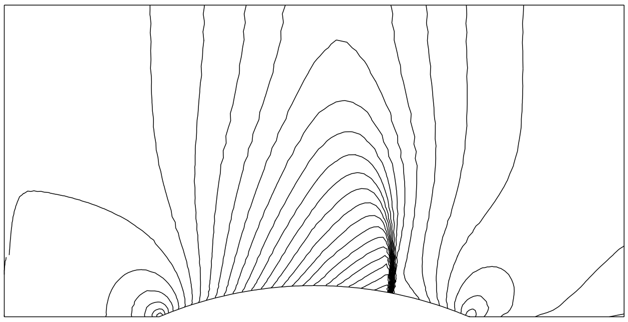

Fig.3.3.7 - Density isolines: both inlet and outlet extrapolated

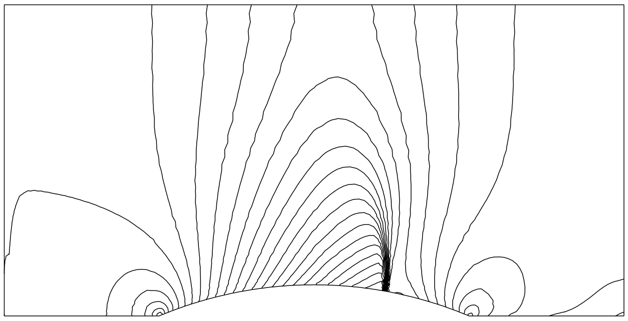

Fig.3.3.8 - Density isolines: inlet fixed, outlet extrapolated

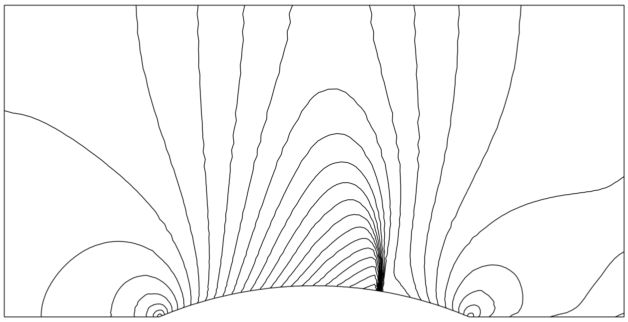

Fig.3.3.9 - Density isolines: both inlet and outlet fixed

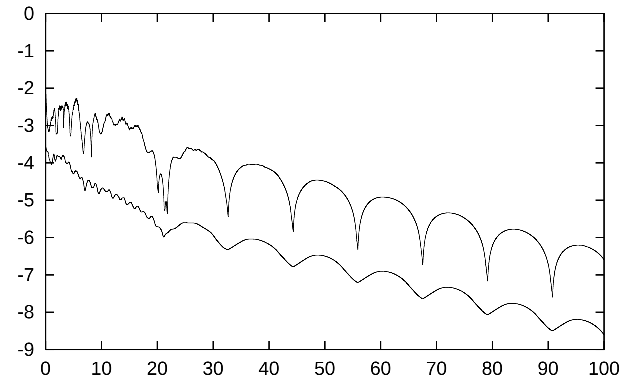

Fig.3.3.10 - Convergence histogram: both inlet and outlet extrapolated

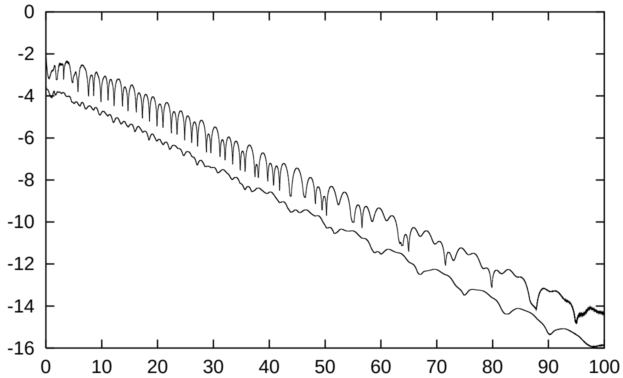

Fig.3.3.11 - Convergence histogram: inlet fixed, outlet extrapolated

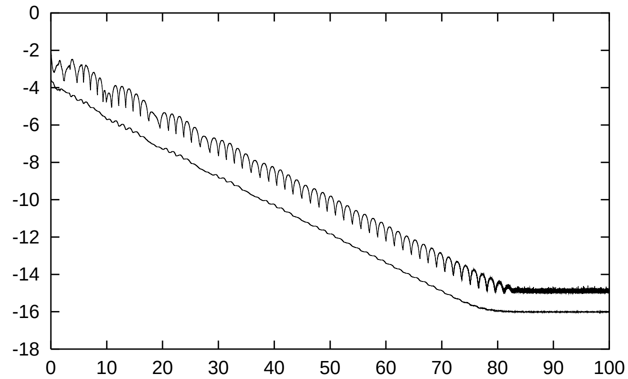

Fig.3.3.12 - Convergence histogram: both inlet and outlet fixed

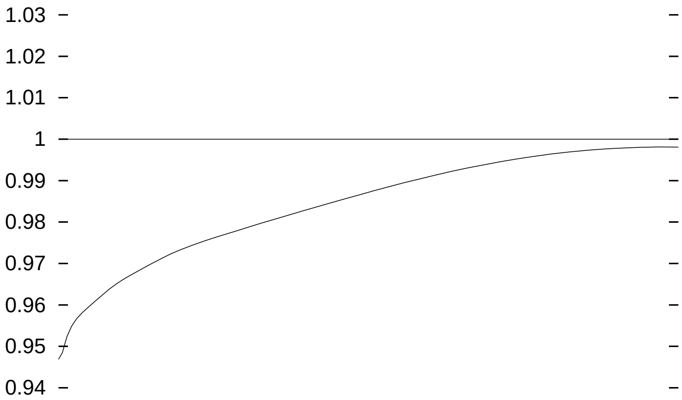

Fig.3.3.13 - Density at inlet and outlet: both inlet and outlet extrapolated

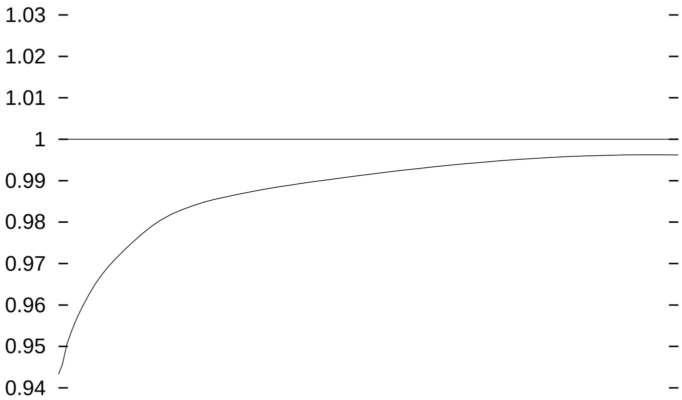

Fig.3.3.14 - Density at inlet and outlet: inlet fixed, outlet extrapolated

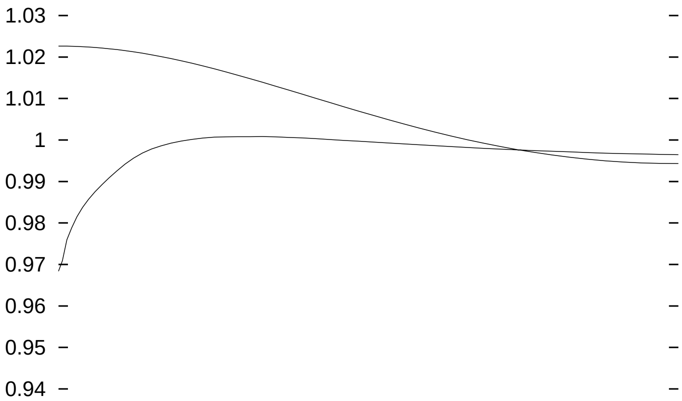

Fig.3.3.15 - Density at inlet and outlet: both inlet and outlet fixed

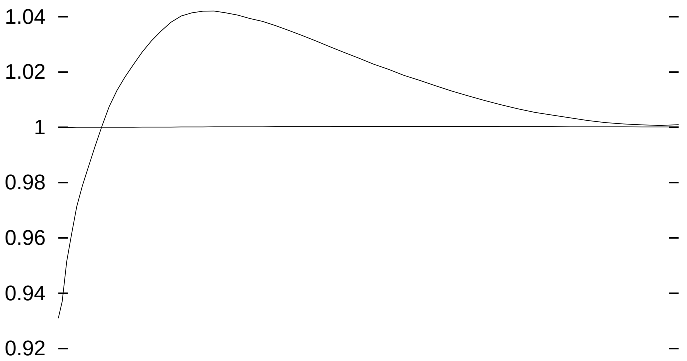

Fig.3.3.16 - Normal velocity at inlet and outlet: both inlet and outlet extrapolated

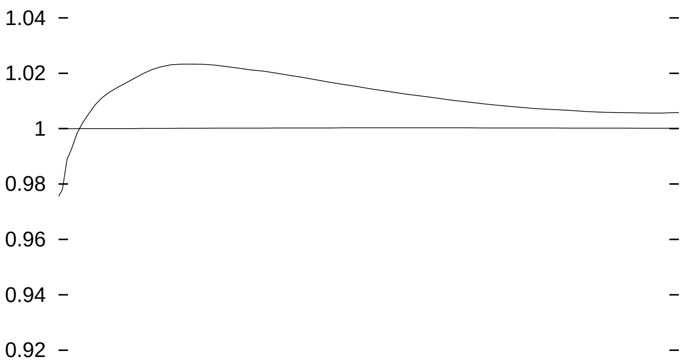

Fig.3.3.17 - Normal velocity at inlet and outlet: inlet fixed, outlet extrapolated

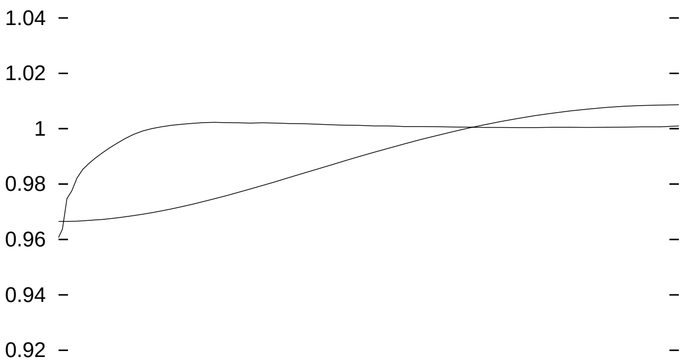

Fig.3.3.18 - Normal velocity at inlet and outlet: both inlet and outlet fixed

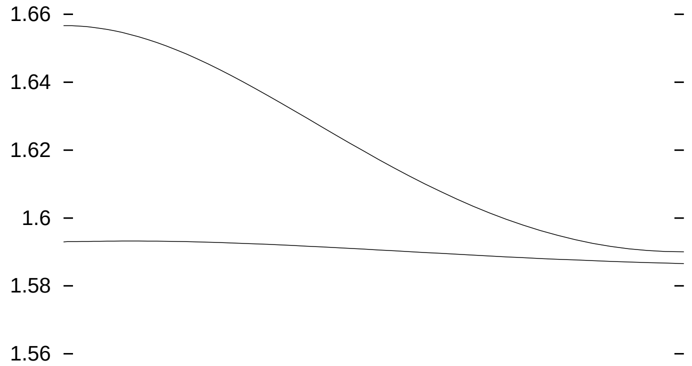

Fig.3.3.19 - Pressure at inlet and outlet: both inlet and outlet extrapolated

Fig.3.3.20 - Pressure at inlet and outlet: inlet fixed, outlet extrapolated

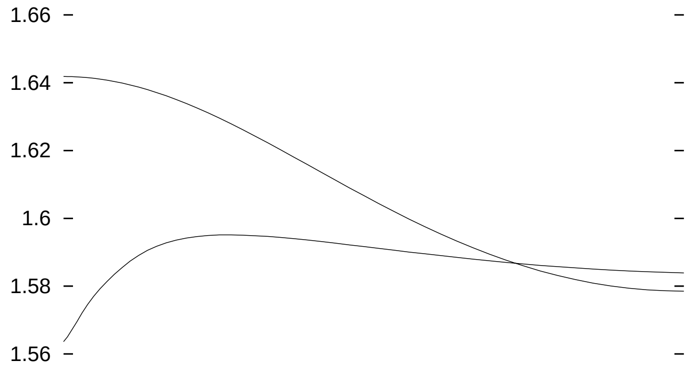

Fig.3.3.21 - Pressure at inlet and outlet: both inlet and outlet fixed

3.4 Basic three-dimensional problems

After having presented results of some two-dimensional numerical experiments concerning properties of the schemes and of some further inlet-outlet treatments, we proceed to our first three-dimensional computations, using the Osher scheme with extrapolated boundary numerical flux. First, our aim is to verify experimentally compatibility of the two- and three-dimensional scheme, therefore we will perform a few computations on prism-grids which are suitable for this purpose. After this, we start using tetrahedron-grids which are obviously the most suitable ones for complicated three-dimensional domains.

3.4.1 GAMM channel

Let us consider the three-dimensional analogy of the GAMM channel the depth of which is 10cm. The prism-grid (see Fig.3.4.1) corresponding to the triangular one we used in previous computations, contains 35544 grid points and 57380 elements.

Fig.3.4.1 - Grid on the three-dimensional GAMM channel

At the inlet and outlet sides we prescribe the same dimensionless condition as before:

$$\tilde{\varrho}_0 = 1, \;\; \tilde{u}_0 = 1, \;\; \tilde{v}_0 = 0, \;\; \tilde{w}_0 = 0, \;\; \tilde{p}_0 = 1.5911911657 \ .$$

There were two computations performed: first, the initial condition was identical with the inlet-outlet one, further, for this purpose extended two-dimensional results were used.

Both the results (see Fig.3.4.2 - Fig.3.4.7) are in our opinion very satisfactory. There are practically no differences between them and the two-dimensional one. Maximal range of the dimensionless velocity z-component is about 1e-6. In the second case, the computation stopped a few iterations after its beginning because of the relative density error criterion satisfied.

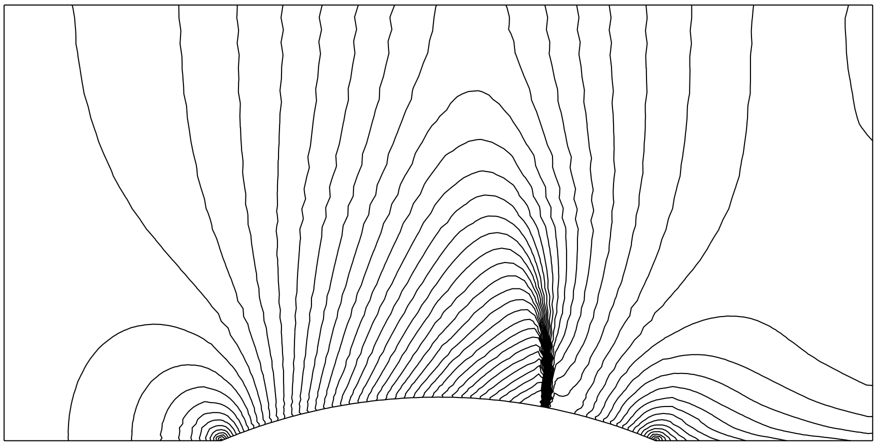

Fig.3.4.2 - Mach number isolines

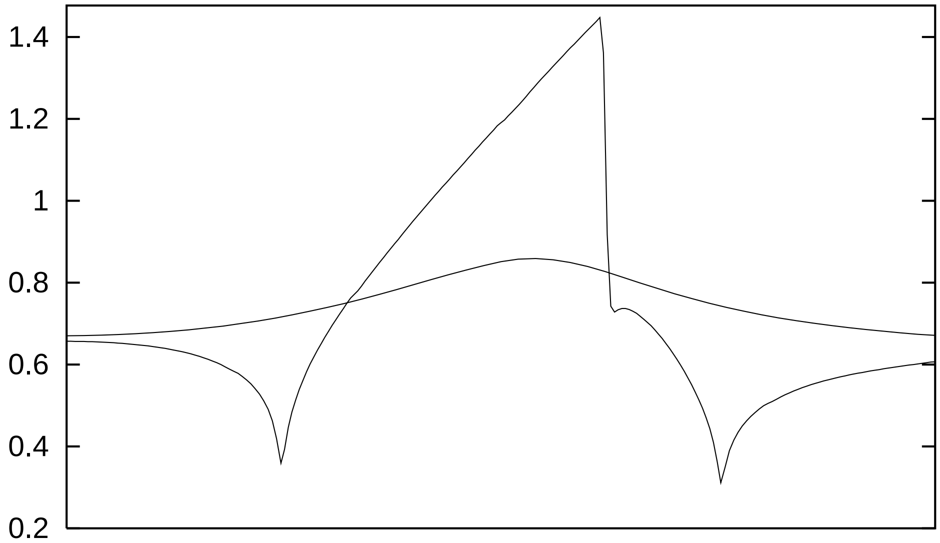

Fig.3.4.3 - Mach number at the solid walls

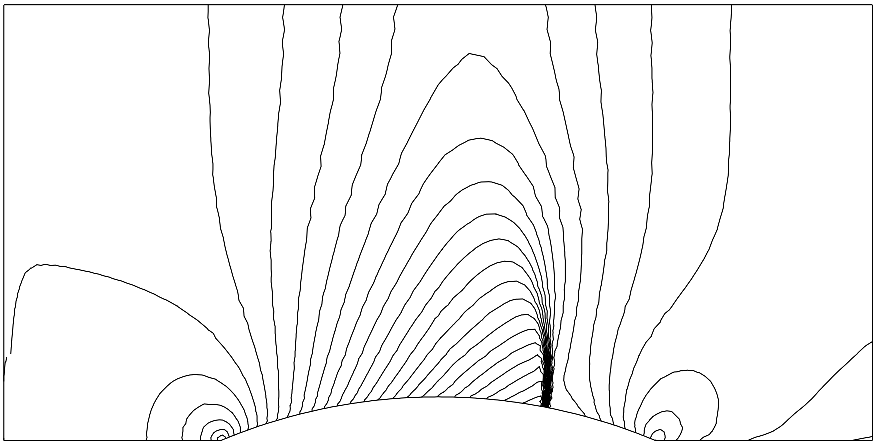

Fig.3.4.4 - Density isolines

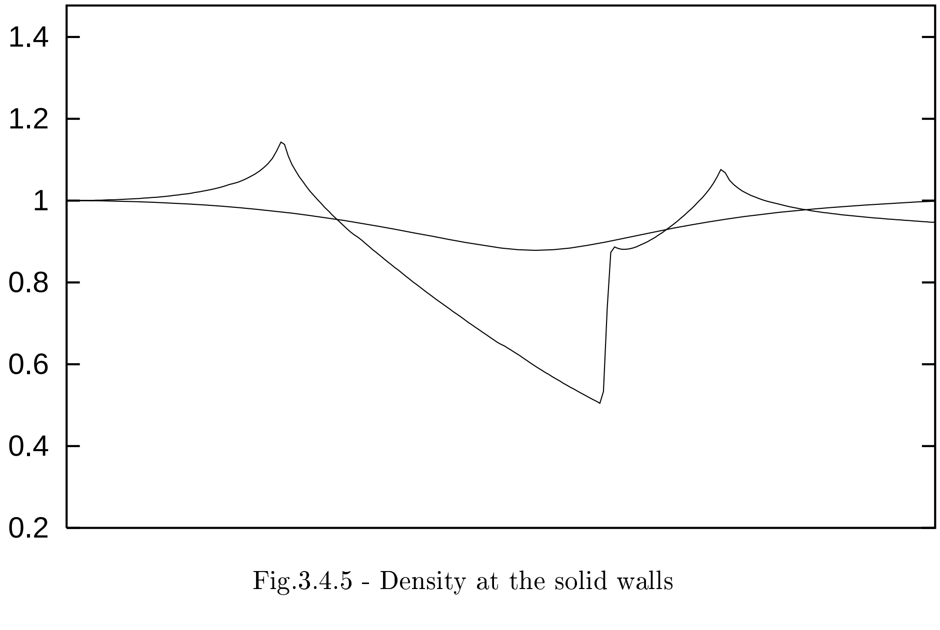

Fig.3.4.5 - Density at the solid walls

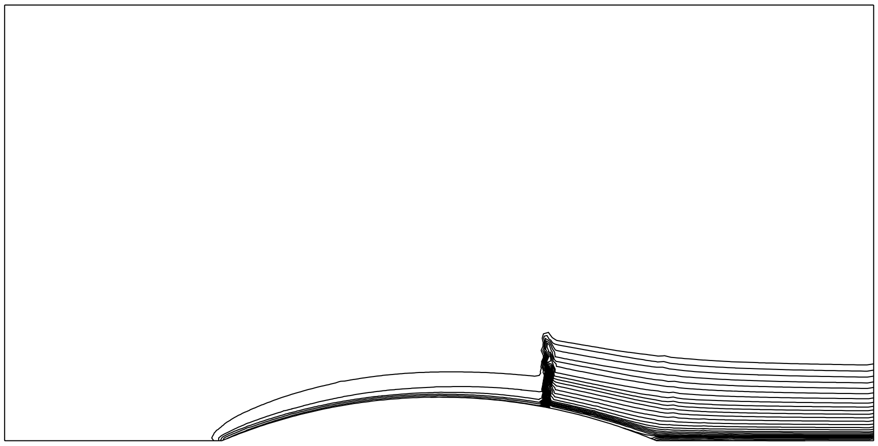

Fig.3.4.6 - Entropy distribution

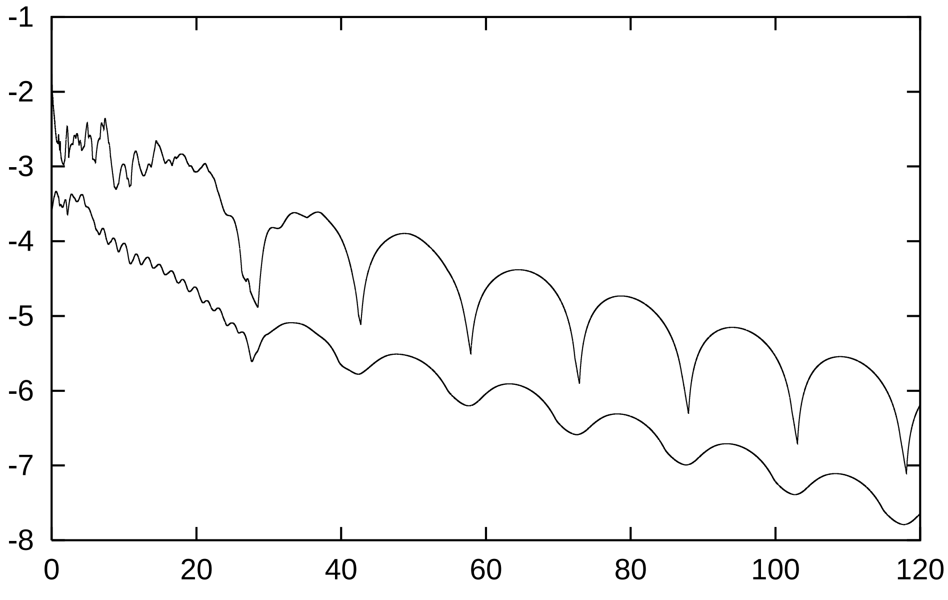

Fig.3.4.7 - Convergence histogram

3.4.2 Blade machine

The problem we will deal with in this subsection has an immediate industrial motivation – we will solve transonic flow through a very complicated blade machine.

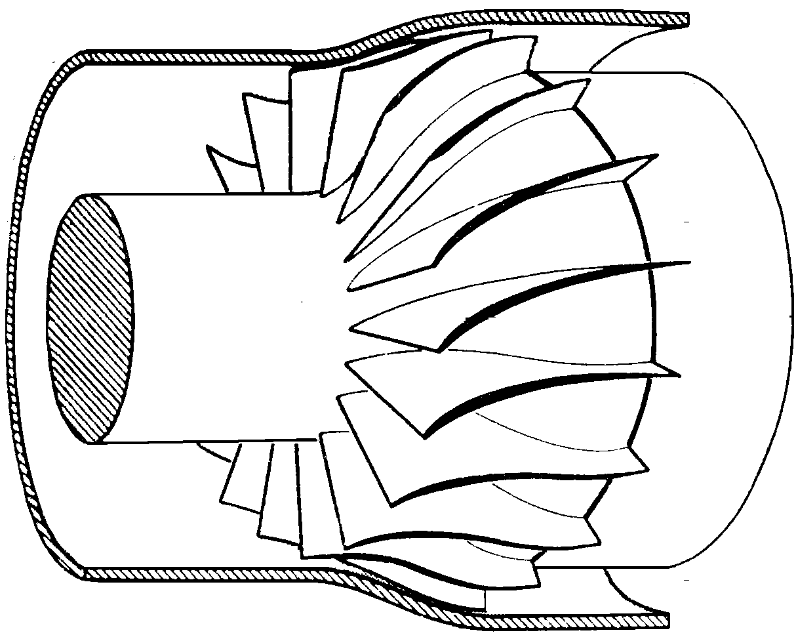

Fig.3.4.8 - A steam turbine

Unfortunately, nowadays our tools (mesh generators, computers etc.) are not able yet to solve it three-dimensionally, therefore we are forced to simplify it. We start from the assumption that we have already calculated an axially symmetric flow in the channel without blades and have obtained a family of axially symmetric stream surfaces. We choose a suitable one of them, transform it and its intersections with the blades into the (x, y) plane. So we obtain a 2D domain Ω shown in the Fig.3.4.9, so-called *cascade of profiles.* This infinite blade row is cut periodically and the computation is done in one period only using periodic boundary conditions. For more information about the cutting process and about the transformation see [12]. Once more, we construct its three-dimensional analogy by shifting it in the z-axis direction.

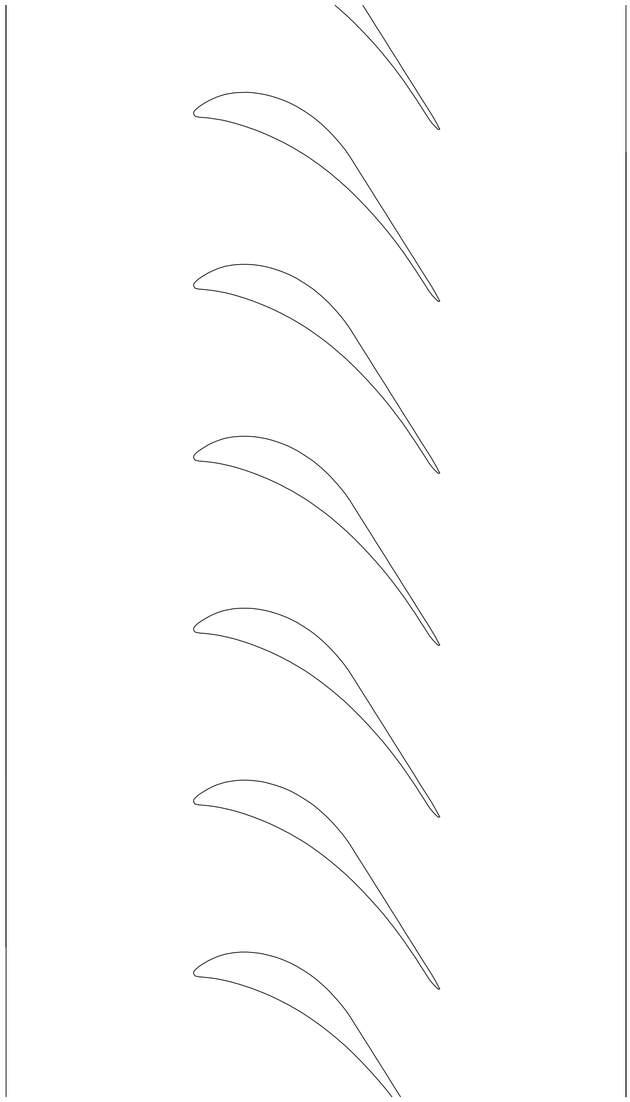

Fig.3.4.9 - Cascade of profiles

The prism-grid on it contains 16404 grid points and 25300 elements.

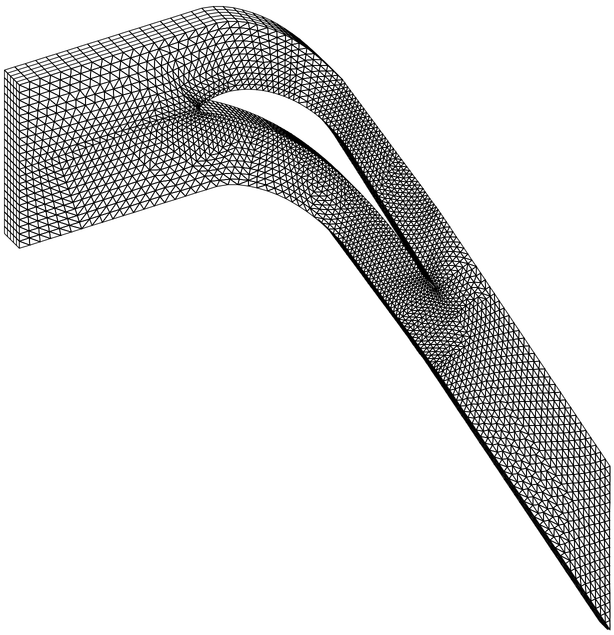

Fig.3.4.10 - Grid on one period of the cascade

At the inlet we do prescribe the following dimensionless boundary condition:

$$\tilde{\varrho_0} = 1, \ \tilde{u_0} = 0.94380095, \ \tilde{v_0} = 0.33051439, \ \tilde{w_0} = 0, \ \tilde{p_0} = 6.8762452$$

i.e. $M = 0.3223$. The dimensionless outlet boundary condition is

$$\tilde{\varrho_0} = 1, \ \tilde{u_0} = 0.94380095, \ \tilde{v_0} = -1.46289147, \ \tilde{w_0} = 0, \ \tilde{p_0} = 3.01044889 \ .$$

The dimensionless size of the row-period is then 0.05511679. The initial condition in the left part of the domain is identical with the inlet boundary condition and in the right part the outlet one was used. Results of our computation which are shown in Fig.3.4.11.-3.4.16. are in harmony with results published in [18], [9] and [17]. In spite of that, you see that the grid we are using is not fine enough, which documents clearly the entropy distribution shown in Fig.3.4.15. We add a recent result (Fig.3.4.17) obtained starting from the same grid by using an adaptive refinement scheme (see [15]). The difference, we hope, documents clearly the adaptive grid refinement is worth studying (see also [16], [21], [8], [36] and others).

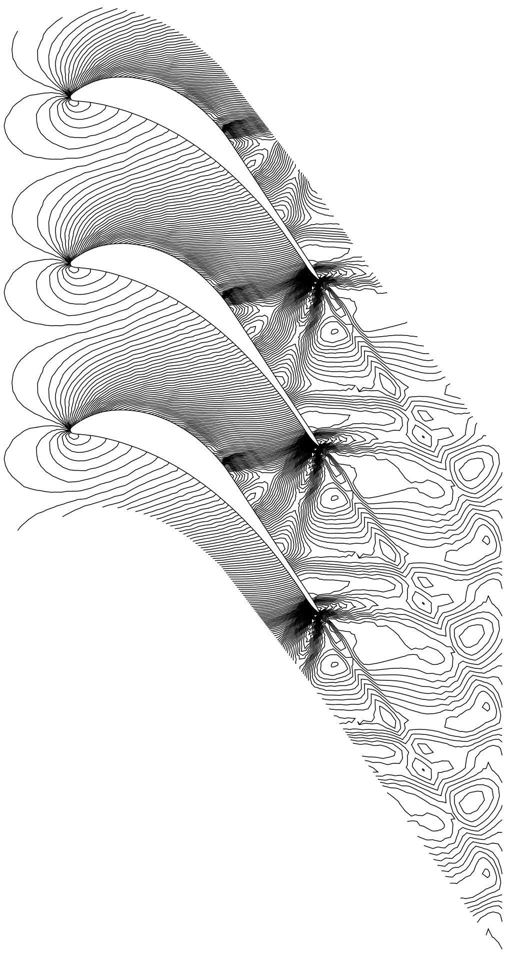

Fig.3.4.11 - Mach number isolines

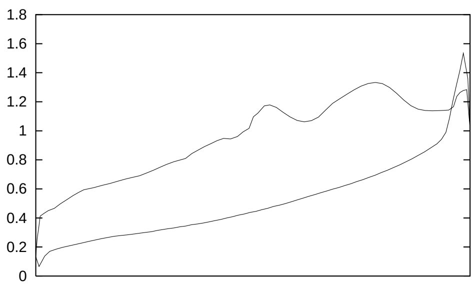

Fig.3.4.12 - Mach number at the profile

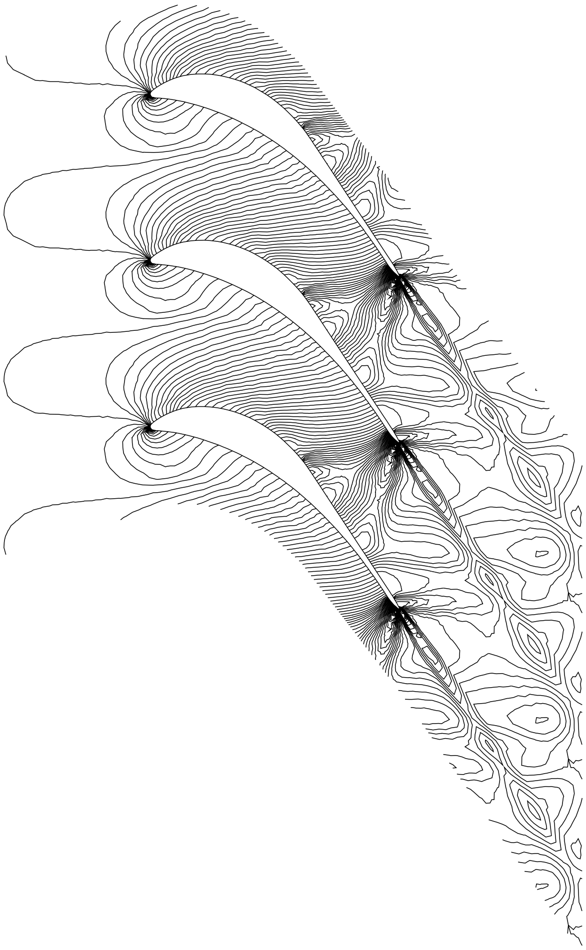

Fig.3.4.13 - Density isolines

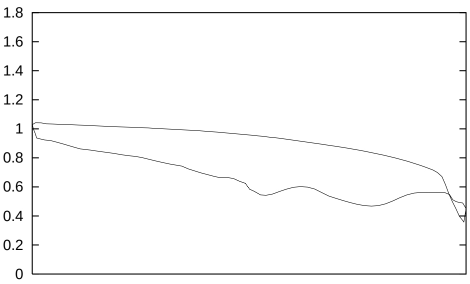

Fig.3.4.14 - Density at the profile

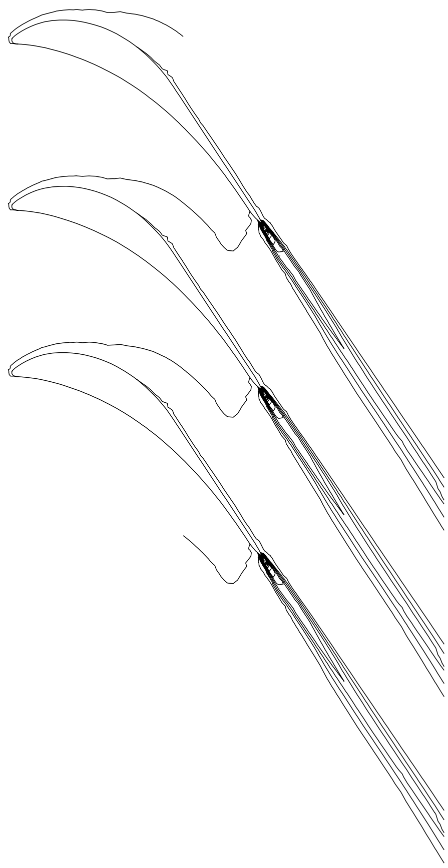

Fig.3.4.15 - Entropy distribution

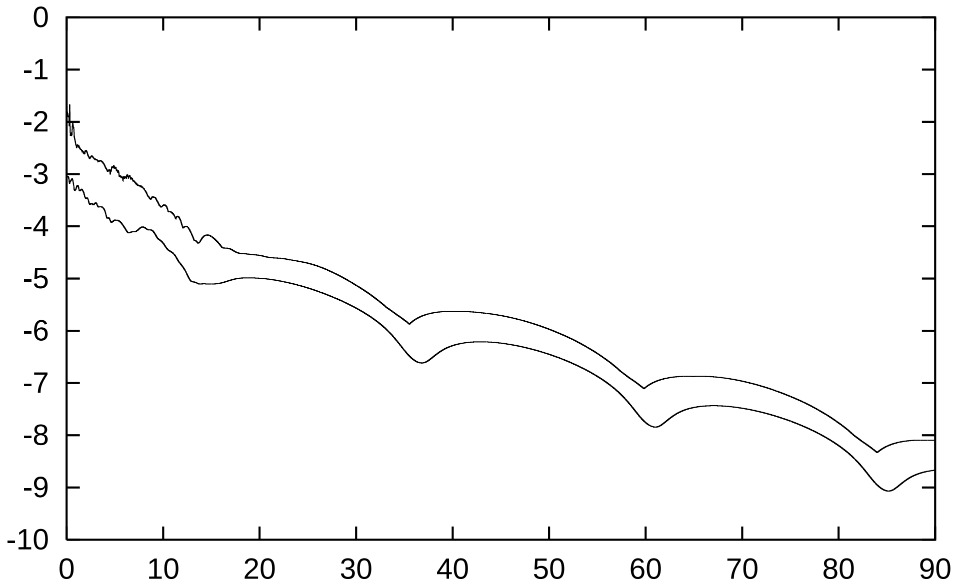

Fig.3.4.16 - Convergence histogram

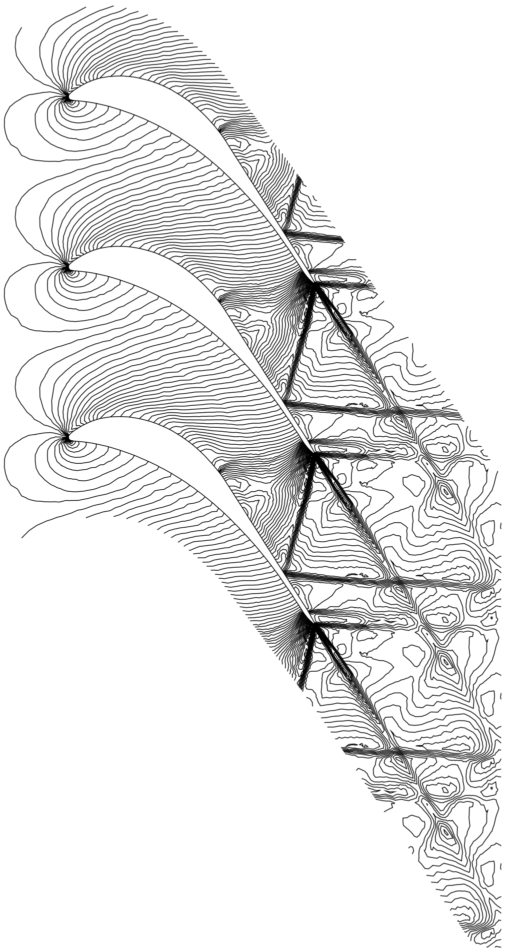

Fig.3.4.17 - Mach number isolines, adaptive grid refinement

3.4.3 Forward facing step

Finally, we proceed to our both last and most difficult computation mentioned in this contribution. It concerns the famous supersonic test channel with the forward facing step placed on its bottom. The domain itself is 1m high, 3m long and 25cm deep, the height of the step is 20 cm and there are 40cm left in front of it. We constructed a tetrahedron-grid (as shown in Fig.3.4.18)

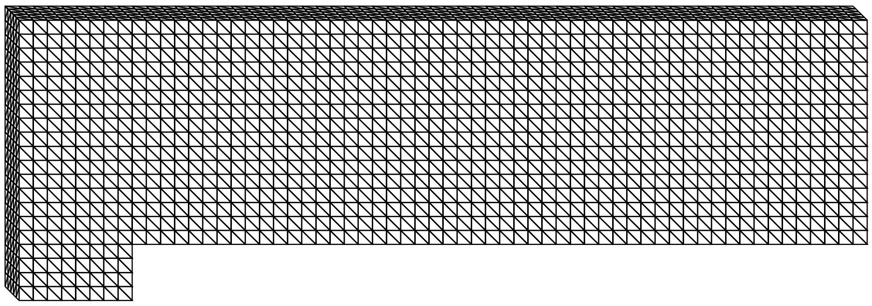

Fig.3.4.18 - Grid on the forward facing step

which contains 6438 grid points and 29760 elements. Dimensionless inlet boundary condition we prescribe in this case is

$$\begin{aligned}\tilde{\varrho}_0 &= 1.4\\ \tilde{u}_0 &= 3\\ \tilde{v}_0 &= 0\\ \tilde{w}_0 &= 0\\ \tilde{p}_0 &= 1\end{aligned}$$

i.e. $M = 3$. Results of this computation shown in Fig.3.4.19 - Fig.3.4.24 correspond to the chosen grid which is not very fine. For more numerical results concerning this test channel see e.g. [26], [23] and [25].

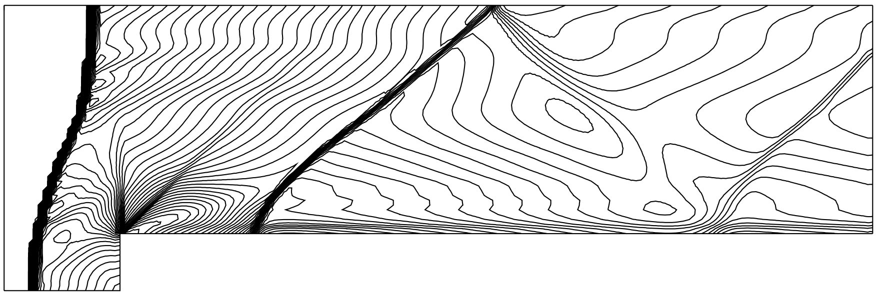

Fig.3.4.19 - Mach number isolines

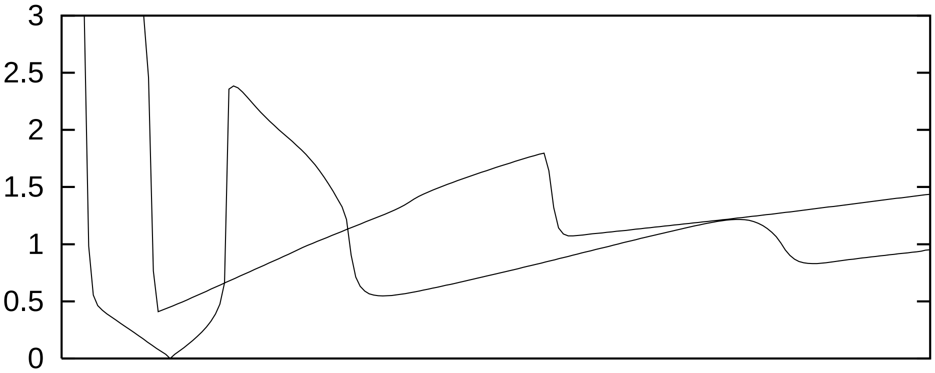

Fig.3.4.20 - Mach number at the solid walls

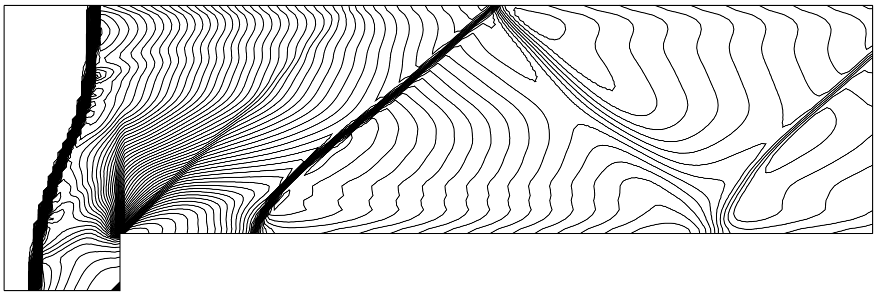

Fig.3.4.21 - Density isolines

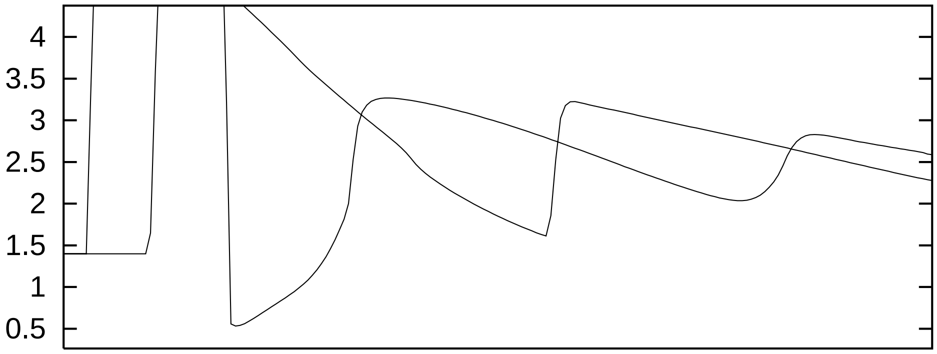

Fig.3.4.22 - Density at the solid walls

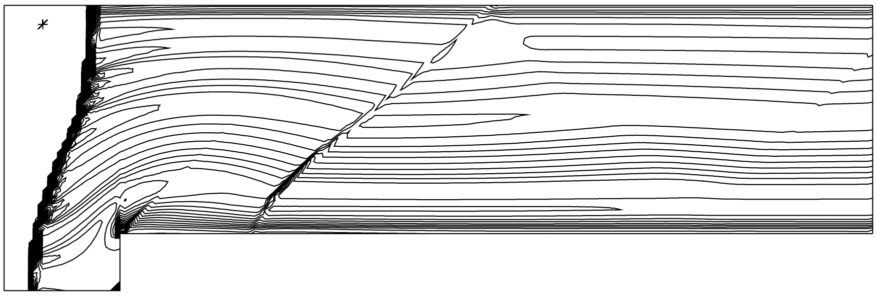

Fig.3.4.23 - Entropy distribution

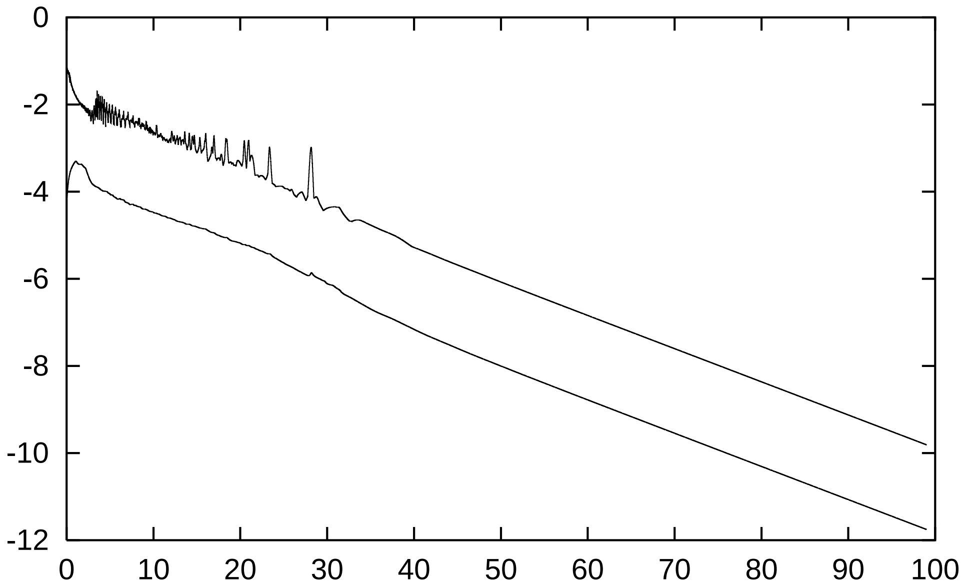

Fig.3.4.24 - Convergence histogram

4 Description of the program

The program *euler.cpp* is based on theoretical results of this work. It was written in the C++ programming language and works in the operation system Unix. It contains the three-dimensional schemes of Steger-Warming, Van Leer, Vijayasundaram and Osher-Solomon which can be used for two- or three-dimensional computations. There is certain variability concerning numerical treatment of boundary conditions – for inlet and outlet sides various fluxes (including the inside one) can be used. In every data file concerning the solver the symbol '$*$' starts a comment.

4.1 A short manual

Before you start a computation, you have to prepare two input files – a data file describing the grid (about its format later) and a configuration file which contains all the remaining necessary informations about the problem. The best way how to explain its format is to give an example:

```
*** This configuration file belongs to 'euler.cpp'
*** 1. The contact file:
** <name>
msg
*** 2. The data input file:
** <name>
gamm.grid
*** 3. The solution output file:
** <name>
gamm.sol
*** 4. Does the solution file contain the grid?
** <yes/no>
no
*** 5. Convergence:
** (used for computation-end test)
** <1>: L^1 norm
** <2>: L^infty norm
** <double>: computation-end density error limit
2
1e-16
*** 6. Output convergence to a special file?
** <yes/no>
yes
** ...<1>: L^1 norm output or
**    <2>: L^infty norm output or
**    <3>: both norms output,
**    <name> of the convergence file
3
gamm.conv
*** 7. The CFL-condition:
```

```
** (securing the computation stability)
** <1>: only current edge measure used
** <2>: whole element surface used
** <double>: the CFL-constant
1
0.85
*** 8. Number of iterations:
** <long>
100000
*** 9.Output interval:
** <int>
500
*** 10. Kappa:
** <double>
1.4
*** 11. Do you wish to compute a periodic problem?
** <yes/no>
no
** ...two periodic boundary indexes:
** <int> <int>

*** 12. Inlet:
** <int int ... int> index list
1
** corresponding 3D vector list
1.0   1.0   0.0   0.0   1.5911911657
*1.5   205.709277   0.0   0.0   101000
*** 13. Outlet:
** <int int ... int> index list
2
** corresponding 3D vector list
1.0   1.0   0.0   0.0   1.5911911657
*1.5   205.709277   0.0   0.0   101000
*** 14. Slip boundary
** <int>: length of the slip index list
** <int, int ... int> the slip index list
2
3 4
*** 15. Reflection boundary
** <int>: length of the reflection index list
** <int, int ... int> the reflection index list
0

*** 16. The initial condition:
** <1>: a constant vector
** <2>: a solution file
1
```

```
** a constant vector or a solution file:
** <vector> or <name>
** (must have form corresponding to point 4)
1.0   1.0   0.0   0.0   1.5911911657
*1.5   205.709277   0.0   0.0   101000
```

This configuration file was used for numerical solution of the flow through the GAMM channel. Let us give a short explanation to the points which could be not trivial to understand:

One: the contact file is a file which the running solver can be contacted by. The solver, having finished an iteration, looks into the current directory and in case there is a file of this name, the solver tries to open it, read commands and carry them out. After having finished, it joins '.read' at the end of the filename. At the moment, these commands are still few, we count on their development according to requirements. Let us give an example again:

```
* This contact file belongs to 'euler.cpp'
* comment
give_iter_made_num
* give_limits
give_L^infty
give_L^1
* give_nbound
* give_nelem
* give_npoin
* give_state
give_timestep
* no_comment
* no_wait
* stop
* wait
* write_solution
```

After having read this message, the solver wrote down number of iterations it had done, last relative density error in both norms and the last time-step.

Four: the solution file can but does not have to contain informations about the grid in the same format as read from the data file.

Five: when the relative density error in the chosen norm falls under the given value, the computation stops.

Six: into this file convergence histogram in the Gnuplot data format is put.

Eight: in case still running, the solver stops having finished this iteration.

Nine: with this frequency solution file on the hard disc is restored.

Twelve: length of this index list must be according to the prescribed 3D boundary conditions number. In case you have a 2D grid, set the fourth vector component to zero.

Sixteen: the solution process can be initialized by a constant 3D vector or by a solution file (in this case the format from point 4 must be respected).

4.2 Data formats

Both input and output data formats are as simple and clear as possible. It may help you viewing some example files because necessary comments are added. Let us introduce them:

4.2.1 input

number of points (%lu), number of elements (%lu), number of boundary data (%lu), list of points (in 2D case %f %f a line, in 3D case %f %f %f a line), list of elements (in 2D case %lu %lu %lu a line. in 3D case %lu %lu %lu %lu a line) and list of boundary data a member of which contains an edge (a side) and an integer index - in 2D case %lu %lu %d, in 3D case %lu %lu %lu %d.

4.2.2 output

In case your solution file has to contain the grid, it will be copied there from the data file, then the κ constant and the list of solution vectors in the form ϱ u v p (in 2D case) or ϱ u v w p (in 3D case) added. In the other case, only number of elements, the κ constant and the list will be written. Of course, solution vectors are ordered correspondingly to the elements. All these files contain comments.

5 What is to be done further

In subsection **2.6** we started analyzing inlet and outlet boundary conditions and we came to the conclusion, that various numbers of physical quantities at the boundary sides (edges) are determined by the solution inside – in case of subsonic inlet one, in case of subsonic outlet four of them. Do these quantities depend on current flow problem? Which quantities are determined? Developing the program, we made a temporary compromise considering at the subsonic inlet the pressure and at subsonic outlet density and the velocity vector being determined, which of course is not sufficient. Note that when $\kappa = 1.4$ (the most common value for numerical experiments, used in all our computations as well), the inequality (2.6.137) is satisfied by every $\varrho_b > 0.44$, i.e. density always could have been prescribed instead of pressure at the subsonic outlet.

Maybe there is a way in using Riemann invariants according to negative eigenvalues but I'm not sure. We had better ask physicists, who have much stronger feeling for the natural reality than mathematicians, about what is happening with the density and pressure informations inside of a subsonic flow, to get at least some hints.

There are many further problems (viscosity, heat conduction, adaptive grid refinement etc.) but they have little importance in comparison with the subsonic inlet and outlet boundary conditions one.

Part II
Grid generation

Introduction

To solve a flow problem in a one-, two- or three-dimensional domain efficiently means not only to have a good numerical scheme. Since we are not able to process infinite quantity of information, we must solve our problems as systems of finite number of unknowns in any way. The FVM is based on finite space (so-called *grid*) and time discretization. Grids can have many shapes – working in 1D we use abscissas, in 2D our theory requires convex polygons and in the 3D case convex polyhedra are used. In this contribution we will set up a method able to discretizate an arbitrary 2D bounded domain with continuous piecewise linear boundary by creating an unstructured homogeneous grid consisting of triangles and we will support it theoretically by proving its correctness.

Grid generation is a subject of world-wide interest. Published methods are mostly two-dimensional (see [19], [2], [30], [34], [20], [22], [39] e.g.) but there are some papers concerning the 3D mesh generation too (see [29], [1], [4]).

Let us remark that the idea of the following scheme does not depend on the dimension, we are restricted to 2D for technical reasons only.

1 Description of the scheme

Our scheme sticks on the solution of two independent tasks which we are going to introduce now.

Task one: let Ω be a generalized oriented polygon. We denote B the set of its boundary vertexes. Let $I \subset \Omega$ be a finite set of points. Our aim is to divide Ω in a finite number of triangles $\mathcal{T} = \{T_!, T_2, \ldots, T_k\}$ in order that
a) $\overline{\Omega} = \bigcup_{T \in \mathcal{T}} \overline{T}$
b) for every $p \in I$ there is a $T \in \mathcal{T}$ so that p is a vertex of T
c) for every $p \in B$ there is a $T \in \mathcal{T}$ so that p is a vertex of T
d) there is no $T \in \mathcal{T}$ a vertex of which does not lie in $B \cup I$
e) in case $T_!, T_2$ are two different members of $\mathcal{T}$, just one of the following options is valid:
i) $\overline{T_1}$ and $\overline{T_2}$ have an empty penetration
ii) the penetration of $\overline{T_1}$ and $\overline{T_2}$ is just one shared vertex
iii) the penetration of $\overline{T_1}$ and $\overline{T_2}$ is just one shared edge
Here the expression '$\overline{T_1}$ and $\overline{T_2}$ share a vertex' means the point is a vertex in $\overline{T_1}$ and it is a vertex in $\overline{T_2}$ etc. Definitions of 'generalized oriented polygon', 'boundary vertex' and 'triangle' come soon.

Task two: let Ω be a generalized oriented polygon the boundary vertex set B of which contains n_b members. Let n be an arbitrary natural number and $P : \mathbb{R}^2 \times \mathbb{R}^2 \to \mathbb{R}$ a strict falling function. We search for a $n-$member set $I \subset \overline{\Omega}$, $I \cap B = \emptyset$ in order that

$$\sum_{x \in I} \sum_{y \in I \cup B, x \neq y} P(x, y) \tag{1.1}$$

is minimal.

1.1 Task one

Definition 1.1.1

Let a, b be two different points in $\mathbb{R}^2$. By the symbol ab $(= ba)$ we will denote the set $\{x \in \mathbb{R}^2$ which a $t \in (0,1)$ exists to so that $x = a + t(b-a)$ $\}$. Points a, b are so-called *outside points* of ab.

Definition 1.1.2

Let ab be an abscissa. The arranged couple $[ab, \frac{b-a}{|b-a|}]$ is so-called *oriented abscissa ab*, point a its *start point* and point b its *end point*. We say that two oriented abscissas *cut* themselves if the corresponding abscissas have just one intersection point. The penetration of two oriented abscissas is not empty if the penetration of the corresponding abscissas is not empty.

Definition 1.1.3

By the concept *domain* we will call an open subset $\Omega \neq \emptyset$ of $\mathbb{R}^2$ two arbitrary points $x_1 \neq x_2$ of which it is possible to connect by a piecewise linear, continuous curve lying in Ω.

Definition 1.1.4

Let $\Omega \neq \emptyset$ be an open subset of $\mathbb{R}^2$. Its subset $K \neq \emptyset$ is its *component* if K is a domain and there is no other domain $\tilde{K} \subset \Omega$ that $K \subset \tilde{K}$ & $K \neq \tilde{K}$.

Definition 1.1.5

Let $\Gamma_1, \Gamma_2, \ldots, \Gamma_n$ be such oriented abscissas that the end point of Γ_i is identical with the start point of Γ_{i+1} for $i = 1, 2, \ldots, n-1$, the end point of Γ_n is identical with the start point of Γ_1 and in case $\Gamma_i \cap \Gamma_j \neq \emptyset$, $i \neq j$, $i, j \in \{1, 2, \ldots, n\}$, their direction is opposite. The unification $\bigcup_{i=1}^{n} \overline{\Gamma_i}$ is so-called *cycle* L if its complement to $\mathbb{R}^2$ has just two components. The bounded one of them is so-called *interior of* L, denoted by $\mathrm{int}(L)$. Two oriented abscissas of a cycle are *neighbours* if it is about Γ_i, Γ_{i+1} where $i \in \{1, 2, \ldots, n-1\}$ or it is about Γ_1, Γ_n. Outside points of $\Gamma_1, \Gamma_2, \ldots, \Gamma_n$ are so-called *vertexes* of the cycle. We say that two cycles $L, \tilde{L}$ *cut* themselves if $\mathrm{int}(L) \cap \mathrm{int}(\tilde{L}) \neq \emptyset$ & $\mathrm{int}(L) \not\subset \mathrm{int}(\tilde{L})$ & $\mathrm{int}(\tilde{L}) \not\subset \mathrm{int}(L)$.

Definition 1.1.6

An arbitrary set $\emptyset \neq \Omega \subset \mathbb{R}^2$ is so-called *generalized oriented polygon* if its boundary is positive oriented and it consists of a finite number of cycles which do not cut themselves. We call vertexes of these cycles vertexes of Ω. We say that there is convex angle by a vertex p of Ω if in a cycle of $\partial\Omega$ lie two neighbour oriented abscissas in order that p is end point of the first one and start point of the other one and the corresponding inside angle of Ω is convex (i.e. belongs to the interval $\langle 0, \pi))$.

Example 1.1.7 (generalized oriented polygon)

a) b) c)

Theorem 1.1.8

To every generalized oriented polygon belongs at least one vertex which there is a convex angle by.

Proof: Immediately from the inside angle sum $\pi(n-2)$ for an arbitrary polygon with n vertexes.

Definition 1.1.9

Let Ω be a generalized oriented polygon. An abscissa $\Gamma \subset \Omega$ the outside points of which are vertexes of Ω is so-called *diagonal* of Ω. Let us emphasize that no vertexes lie on a diagonal.

Definition 1.1.10

Generalized oriented polygon with just three vertexes is so-called *triangle*.

Theorem 1.1.11

Every generalized oriented polygon the at least one component of which is not a triangle, contains a diagonal.

Proof: We denote this generalized oriented polygon by the symbol T. Due to the theorem 1.1.8 we have a vertex which is a convex angle by. We denote by ab, bc couple of the corresponding neighbour abscissas from ∂T. In case the triangle $abc \subset T$, $ac \subset T$ and there is no vertex T on ac, the abscissa ac is a diagonal of T. Else, we denote by the symbol K the convex surface of the vertexes of T which lie in the triangle abc or on the abscissa ac. There is just one point d nearest to the point b. In case d is a vertex of ∂K, the convexity gives us that bd is a diagonal of T. Else, due to the convexity again, it suffices to take an outside point of the longest subabscissa of ∂K which contains the point d.

Theorem 1.1.12

Let Ω be a generalized oriented polygon and let Γ be its diagonal. The complement of Γ to Ω is a generalized oriented polygon again.

Proof: Immediately from the definition 1.1.6.

Theorem 1.1.13 (visibility theorem)
Let Ω be a generalized oriented polygon and a, b its vertexes in order that the oriented abscissa ab belongs to a cycle of $\partial\Omega$. Then another vertex $c \in \partial\Omega$ exists so that the triangle $abc \subset \Omega$ and the abscissas ac, bc do not contain any vertex of Ω.

Proof: Immediately from theorems 1.1.11 and 1.1.12 by the mathematical induction.

Remark 1.1.14
The complement of $\overline{abc}$ to Ω is a generalized oriented polygon again.

Definition 1.1.15
By the concept *triangulation criterion* we call a function $\Phi : \mathbb{R}^2 \times \mathbb{R}^2 \times \mathbb{R}^2 \to \mathbb{R}$ satisfying the following condition: in case a, b, c, d are four different points in $\mathbb{R}^2$ meeting $(b_1 - a_1)(c_2 - a_2) - (b_2 - a_2)(c_1 - a_1) > 0$ & $(b_1 - a_1)(d_2 - a_2) - (b_2 - a_2)(d_1 - a_1) > 0$, the function Φ is defined and in case $\Phi(a, b, c) < \Phi(a, b, d)$ the point d does not lie in $\overline{abc}$.

Remark 1.1.16
The first two inequalities from the previous definition secure that points c, d lie 'on the left' to the oriented abscissa ab – they are connected with the positive boundary orientation. The next condition secures that the triangulation algorithm 1.1.18 won't fail.

Example 1.1.17
A very satisfactory triangulation criterion is the following one:

$$\Phi(a, b, c) = \frac{ca.cb}{|ac||bc|} \tag{1.2}$$

which is connected with the angle acb cosine. You may easily verify its correctness.

Algorithm 1.1.18
Consider $k = 0$, $\Omega_0 = \Omega$ and $\mathcal{T} = \emptyset$. Choose an arbitrary triangulation criterion Φ.

1. Choose an arbitrary oriented abscissa ab from any cycle of $\partial\Omega_k$.

2. Define the set $M_{ab} = \{\ c \in \mathbb{R}^2,\ c$ is a vertex of Ω_k, $c \neq a$, $c \neq b$ so that abc is a triangle lying in Ω_k and the abscissas ac, bc do not contain any vertex of $\Omega_k\}$. Theorem 1.1.13 implies $M_{ab} \neq \emptyset$. Due to the positive boundary orientation $(b_1 - a_1)(c_2 - a_2) - (b_2 - a_2)(c_1 - a_1) > 0$ for every point $c \in M_{ab}$.

3. Define the set $S_{ab} = \left(\bigcup_{c \in M_{ab}} \overline{abc} \cap I\right) \cup M_{ab}$ and denote c its point which $\Phi(a, b, c)$ is minimal at.

4. Add the triangle abc into $\mathcal{T}$ and define a new domain Ω_{k+1} as the complement of $\overline{abc}$ to Ω_k. Due to the theorem 1.1.13 Ω_{k+1} is a generalized oriented polygon again.

5. Set $k := k + 1$ and repeat this five-points-loop until Ω_k is empty.

This algorithm stops after a finite number of cycles and it is not difficult to verify that the triangulation is correct (see definition of the first task). Thus, our Task one has always at least one solution.

1.2 Task two

The reader may imagine that members of the sets B and I are bounded and free microscopic particles with charge, respectively, which repulse themselves inside of a two-dimensional vessel $\overline{\Omega}$ by forces characterized by a potential P. The idea is very simple – when the system comes to its equilibrium state (i.e. particles are not moving), the particles will be placed in Ω uniformly (their density will be constant approximately). Hence, the set I obtained in this way could lead to a good triangulation of the domain. There is a physical requirement for emergence of this equilibrium state – existence of frictional forces (i.e. there is no vacuum) in the vessel $\overline{\Omega}$. The free particles (the set I members) number estimate

$$n \approx \frac{2|\Omega|}{\sqrt{3}h^2} - \frac{n_b}{2},$$

where $|\Omega|$ is the domain area size and h the medium distance of neighbour boundary vertexes comes from the aim to obtain a grid the triangles of which are mostly regular.

The rest is a business of the computer simulation. The problem is discretized in time, free particles are moved in harmony with the Coulomb law and in every step we decrease their kinetic energy (because of the friction). After the system has found its equilibrium (i.e. free particles are moving around their equilibrium positions), we apply the algorithm 1.1.18.

2 Examples

In the Unix X-Window system a graphic application of this algorithm was written some simple example grids created by which we are going to introduce now. We think that looking at these figures, you will understand the idea of the moving particles much better.

The grid shown in Fig.1 was constructed at the same moment the generator placed random points into Ω (in this case a square). The random point set is quite wild, in spite of that our algorithm could not fail. Further, in Fig.2 and Fig.3 are shown two equilibrium states obtained by putting different numbers of free particles into the domain. The 'triangular' number we mentioned already (see the relation (1.2)) and the 'quadrangular' one is also easy to be estimated. Of course, the triangulation from the Fig.2 is much better – we want to indicate only that a similar algorithm for creating quadrangle-grids could be written. Figures 4 and 5 show that with the domain becoming more difficult the triangulation becomes highly unstructured. In the last two figures, there are two simple grids put onto our test domains introduced in Part I of this thesis.

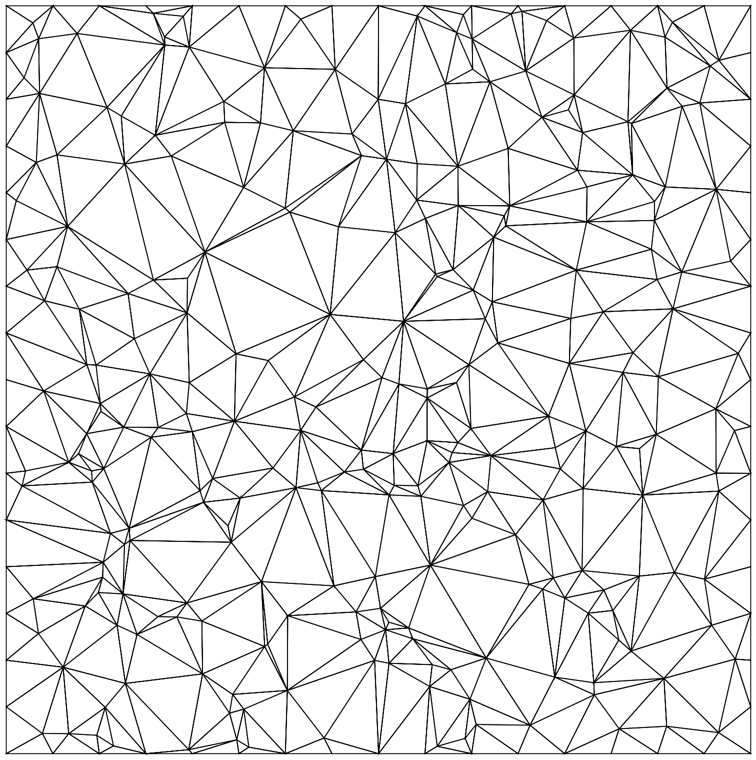

Fig.1 - 'Random' point set in a square

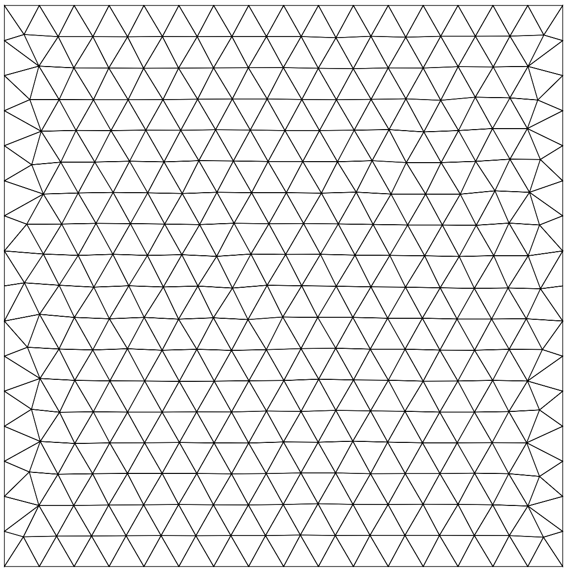

Fig.2 - 'Triangular' point set in a square

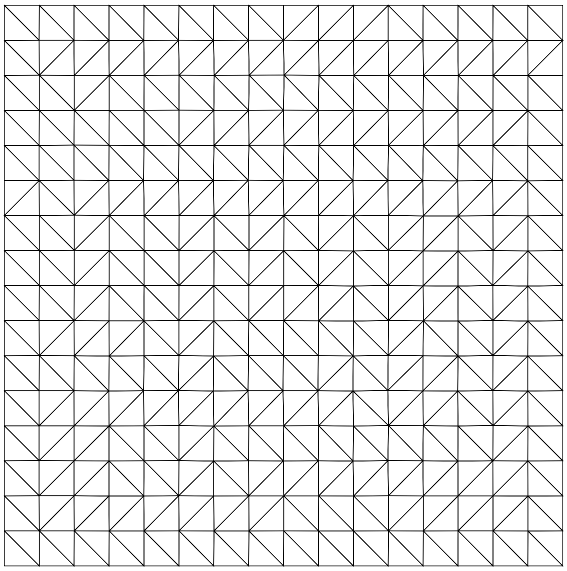

Fig.3 - 'Quadrangular' point set in a square

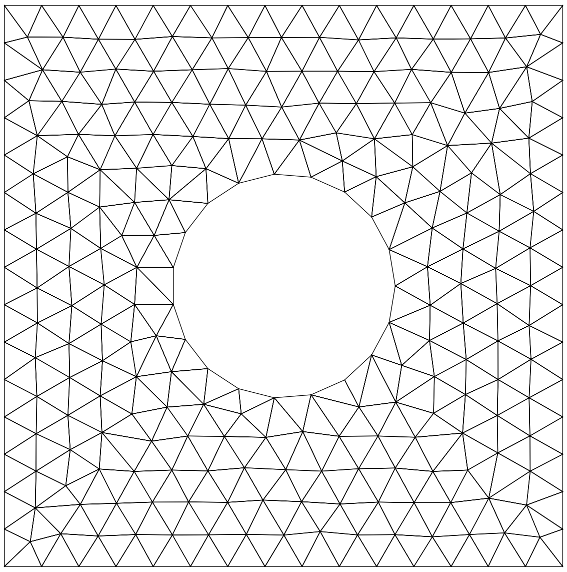

Fig.4 - Domain with a circular hole 1

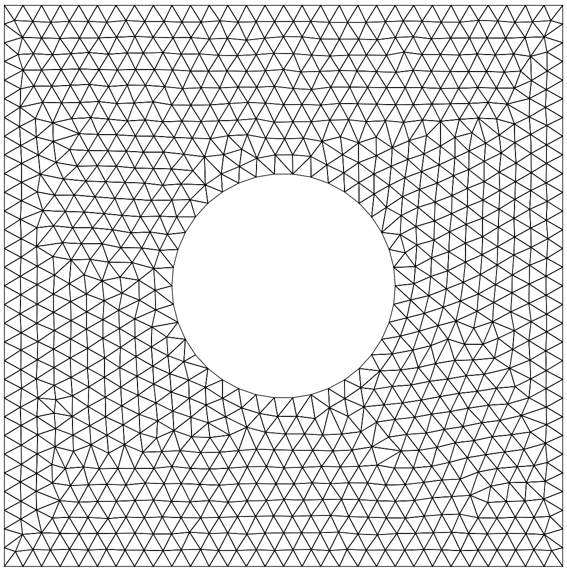

Fig.5 - Domain with a circular hole 2

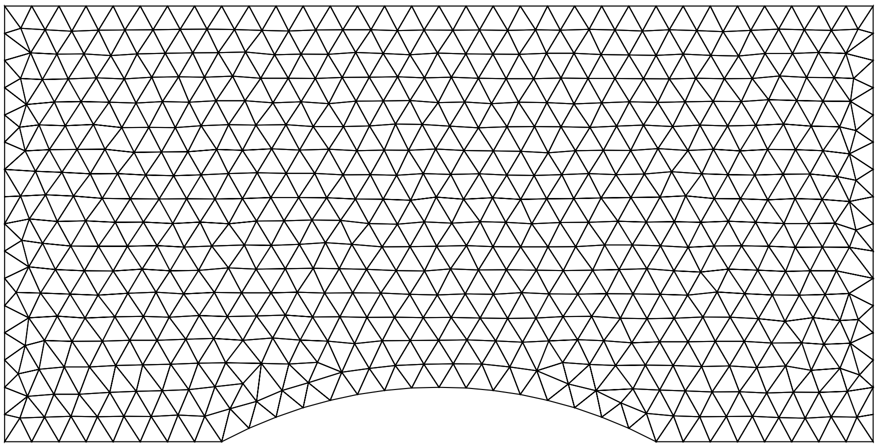

Fig.6 - Triangulation on the GAMM channel

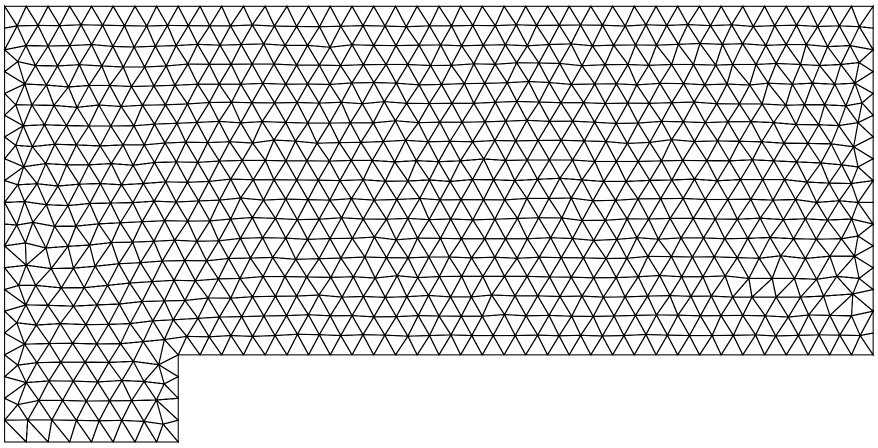

Fig.7 - Triangulation on a forward facing step

References

[1] J. C. Cavendish, D. A. Field, and W. H. Frey. An approach to automatic finite element mesh generation. *International Journal for Numerical Methods in Engineering*, 21:329 – 347, 1985.

[2] James C. Cavendish. Automatic triangulation of arbitrary planar domains for the finite element method. *International Journal for Numerical Methods in Engineering*, 8:679 – 696, 1991.

[3] B. Cockburn, F. Coquel, Ph. Le Floch, and C. W. Shu. Convergence of finite volume methods. Preprint, Centre de Mathematique Appliquée, Ecole Polytechnique, Palaiseau, 1991.

[4] W. A. Cook. Body oriented coordinates for generating 3-dimensional meshes. *International Journal for Numerical Methods in Engineering*, 8:27 – 43, 1974.

[5] F. Coquel and Ph. Le Floch. Convergence of finite difference schemes for conservation laws in several space dimensions. Preprint, Centre de Mathematique Appliquée, Ecole Polytechnique, Palaiseau, 1989.

[6] F. Coquel and Ph. Le Floch. Convergence of finite difference schemes for conservation laws in several space dimensions: the corrected antidiffusive flux approach. *Math. Comp.*, 57:169 – 210, 1989.

[7] J. W. Van der Burg. *Numerical Techniques for Transonic Flow Computations.* PhD thesis, University of Twente, 1992.

[8] L. J. Durlofsky, B. Enquist, and S. Osher. Triangle based adaptive stencils for the solution of hyperbolic conservation laws. *Journal of computational physics*, 98:64 – 73, 1992.

[9] M. Feistauer, J. Felcman, and V. Dolejší. Numerical simulation of compressible viscous flow through cascade of profiles. *ZAMM*, to appear.

[10] M. Feistauer and P. Knobloch. Operator splitting method for compressible Euler and Navier-Stokes equations. Preprint, Charles University, Prague, 1994.

[11] M. Feistauer, M. Medviďová, and P. Knobloch. Finite element-finite volume operator splitting method for compressible Euler and Navier-Stokes equations. Proceedings of Colloqium Dynamics, Prague, 1993.

[12] Miloslav Feistauer. On irrotational flows through cascades of profiles in a layer of variable thickness. *Aplikace matematiky*, 29, 1983.

[13] Miloslav Feistauer. *Mathematical methods in fluid dynamics.* Longman Scientific & Technical,Harlow, 1993.

[14] J. Felcman. Finite volume solution of the inviscid compressible fluid flow. *ZAMM*, 72:513 – 516, 1992.

[15] J. Felcman and V. Dolejší. Adaptive methods for the solution of the Euler equations in elements of blade machines. *ZAMM*, to appear.

[16] J. Felcman, V. Dolejší, and M. Feistauer. Adaptive finite volume method for numerical solution of the Euler equations. pages 894 – 901. Computational Fluid Dynamics-94 (S. Wagner, E. H. Hirschel, J. Périaux, and R. Piva – Eds), Wiley, 1994.

[17] J. Fořt, M. Huněk, K. Kozel, and M. Vavřincová. Numerical simulation of steady and unsteady flow through plane cascades. Numerical Modelling in Continuous Mechanics-II (M. Feistauer, K. Kozel, and R. Rannacher – Eds), Charles University, Prague, 1995.

[18] J. Fořt, K. Kozel, and M. Vavřincová. Numerical simulation of transonic flows through cascades using cell centered and cell vertex type schemes. *Acta Technica*, 33:37 – 59, 1993.

[19] Oliver Friedrich. A new method for generating inner points of triangulations in two dimensions. Preprint no. 92-04 DLR, Göttingen, 1992.

[20] P. L. George. Automatic mesh generation. John Wiley & Sons Ltd., 1991.

[21] U. Goehner and G.Warnecke. A second order difference error indicator for adaptive transonic flow computation. Preprint, University Stuttgart, 1993.

[22] W. J. Gordon and C. A. Hall. Construction of curvilinear coordinate systems and applications to mesh generation. *International Journal for Numerical Methods in Engineering*, 7:461 – 477, 1973.

[23] P. Hansbo. Explicit streamline diffusion finite element methods for the compressible Euler equations. Preprint no. 1991 - 31/ISSN 0347-2809, Chalmers University of Technology, Göteborg, 1991.

[24] M. Huněk, K. Kozel, and M. Vavřincová. Numerical solution of transonic potential flow in a 2D compressor using multi-grid techniques. Proceedings of IV. GAMM Seminar, Kiel, 1988.

[25] C. Johnson, A. Szepessy, and P. Hansbo. On the convergence of shockcapturing streamline diffusion finite element method for hyperbolic conservation laws. Preprint no. 1987 - 21/ISSN 0347-2809, Chalmers University of Technology, Göteborg, 1987.

[26] Petr Knobloch. Numerical solution of compressible flow. Master's thesis, Charles University, Prague, 1993 (in Czech).

[27] K. Kozel and M. Vavřincová. Finite volume method for the Euler equations. Proceedings of Second ISNA Conference, Prague, 1987.

[28] D. Kröner and M. Rokyta. Convergence of upwind finite volume schemes for scalar conservation laws. Preprint no. 208, SFB 256, Univ. Bonn, 1992.

[29] Radovan Krejčí. Preprocessing and postprocessing of static and dynamic tasks. Master's thesis, Charles University, Prague, 1995 (in Czech).

[30] S. H. Lo. A new mesh generation scheme for arbitrary planar domains. *International Journal for Numerical Methods in Engineering*, 21:1403 – 1426, 1991.

[31] Mária Medviďová. *Numerical solution of compressible flow.* PhD thesis, Charles University, Prague, 1995.

[32] J. Peraire, J. Peiro, L.Formaggia, K.Morgan, and O. C. Zienkiewitz. Finite element Euler computations in three dimensions. *International Journal for Numerical Methods in Engineering*, 26:2135 – 2159, 1988.

[33] Mirko Rokyta. *Euler Equations and Their Numerical Solution by the Finite Volume Method.* PhD thesis, Charles University, Prague, 1992.

[34] Arno Ronzheimer. Zweidimensionale Netzgenerierung durch Delaunay Triangulation. Studienarbeit Nr. 86/02, Braunschweig, 1986.

[35] Th. Sonar. *Nichtlineare Dissipationsmodelle und Entropie - Production in finiten Differenzverfahren.* PhD thesis, Univ. Stuttgart, 1991.

[36] Th. Sonar. Strong and weak error indicator based on the finite element residuum for compressible flow computations. Preprint DLR,Göttingen, 1992.

[37] Th. Sonar. On the design of an upwind scheme for compressible flow on general triangulations. Preprint DLR,Göttingen, 1993.

[38] G. Vijayasundaram. Transonic flow simulation using upstream centered scheme of Godunov type in finite elements. *J. Comp. Phys.*, 63:416 – 433, 1986.

[39] M. M. F. Yuen, S. T. Tan, and K. Y. Yung. A hierarchical approach to automatic finite element mesh generation. *International Journal for Numerical Methods in Engineering*, 32:501 – 525, 1991.

Remarks